2009

Epigenetic Control Mechanisms In Somatic Cells Mediated By Dna Methyltransferase 1

Bongyong Lee
University of Central Florida

EPIGENETIC CONTROL MECHANISMS IN SOMATIC CELLS MEDIATED BY DNA METHYLTRANSFERASE 1.

by

BONGYONG LEE
B.S. Yonsei University, 1992
M.S. Yonsei University, 1996

A dissertation submitted in partial fulfillment of the requirements
for the degree of Doctor of Philosophy in Biomedical Sciences
in the Burnett School of Biomedical Sciences
in the College of Medicine
at the University of Central Florida
Orlando, Florida

Fall Term
2009

Major Professor: Mark T. Muller

ABSTRACT

DNA methylation regulates gene expression through a complex network of protein/protein and protein/DNA interactions in chromatin. The maintenance methylase, DNA methyltransferase 1 (DNMT1), is a prominent enzyme in the process that is linked to DNA replication and drives the heritable nature of epigenetic modifications in somatic cells. The mechanistic details that explain how DNMT1 catalytic action is directed in a chromatin setting are not well understood. We hypothesize that post translational modifications and a variety of protein-protein interactions processes are key regulatory elements that set the methylation of CpG elements essential for normal growth behavior in somatic cells. These fundamental processes can be disrupted by DNA damage leading to inappropriate gene silencing and loss of growth control in somatic cells.

First, we show that DNMT1 is post-translationally modified by sumoylation and we have mapped these sumoylation sites by defined mutations. Sumoylated DNMT1 is catalytically active on genomic DNA *in vivo* and substantially increases the enzymatic activity of DNMT1 both *in vitro* and in chromatin. These data establish that sumoylation modulates the endogenous activity of a prominent epigenetic maintenance pathway in cells.

Second, we investigated novel mechanisms whereby somatic cells can erase then reset DNA methylation events in somatic cells. In this study, the relationship between DNA damage and gene silencing was explored. To this end, we generated a HeLa cell line containing a specialized GFP reporter cassette (DRGFP) containing two mutated GFP genes and a unique I-SceI restriction endonuclease site. These cells do not express GFP. A unique double strand break is then delivered by transfecting in the gene for I-SceI. About 4% of the cells produced a functional GFP by gene conversion and homologous recombination (HR); however roughly half

of the GFP recombinants expressed the gene poorly and this was attributed to gene silencing. Silencing of the GFP expressing cell clones was due to DNA methylation and could be reversed using a drug that inhibits global methylation (5-aza-2'-deoxycytidine). Approximately half of the repaired genes were heavily methylated, and half were hypomethylated. That is, a key intermediate methylation state after HR repair is hemimethylated DNA, defined as methylation limited to one strand. Evidence is given that DNMT1 is acting as a de novo methylase at the HR repair patches in cells. Moreover, the DNA damage inducible protein, GADD45α, interacts specifically with the catalytic domain of DNMT1 and GADD45α binds with extremely high affinity to hemimethylated DNA sites. Thus, GADD45α is a key regulatory element in silencing of HR repaired DNA segments and appears to inhibit the activity of DNMT1. Consistent with these results, we found that GADD45α increased the expression of recombinant GFP following HR repair, further suggesting its role in orchestrating strand specific DNA methylation by DNMT1. Since these experiments were performed in live cells, there is strong physiological relevance.

We propose that DS DNA damage and the resulting HR process involves precise, strand selected DNA methylation mediated by the prominent methylase enzyme, DNMT1. Moreover, DS DNA break repair through HR and gene conversion, may potentially erase and reset DNA methylation patterns and therefore alter the expression of repaired genes. The overall process is tightly regulated by the DNA damage inducible protein GADD45α, which may coordinate strand specific methylation by recruiting DNMT1 to HR repair templates. The ability of GADD45α to modulate DNMT1 catalytic activity may explain its role as a passive mediator of demethylation that has been reported by other groups. The overall process of silencing post DNA repair is a strong evolutionary force that may predispose cells to malignant transformation.

ACKNOWLEDGMENTS

I would like to thank Dr. Mark Muller for all your guidance, help and support. I would also like to thank my committee members for all of your insightful comments and suggestions. And last, but not least, I would like to thank my parents and family for always supporting me in every endeavor, and for allowing me to follow my dreams.

TABLE OF CONTENTS

LIST OF FIGURES

GENERAL INTRODUCTION

The human genome contains two layers of information: genetic and epigenetic. The genetic information provides the blueprint for producing all gene products while the epigenetic information guides how the genetic plan becomes actuated. It is vitally important that genes are turned on and off at proper times and in the correct order and tissue. The major form of epigenetic information in mammals is DNA methylation, in which a methyl group from *S*-adenosyl-L-methionine is added covalently to the 5-position of cytosine, mostly within the CpG dinucleotide repeats. DNA methylation has a significant and potentially long term impact on gene expression and genome stability (1-3)

The enzymatic machinery that establishes and maintains DNA methylation involves a number of DNA (cytosine-5) methyltransferases (DNMT) isoforms including DNMT1, DNMT2, DNMT3a and DNMT3b. DNMT1 was the first methyltransferase discovered. It has a strong preference for hemimethylated DNA and is generally the most abundant methyltransferase in somatic cells (4). DNMT1 localizes to replication foci during S phase (5) and interacts with a proliferating cell nuclear antigen (PCNA) and many other proteins (6). The major role of DNMT1 is to maintain the methylation patterning during DNA replication by methylating newly synthesized daughter strands. It is often called a "maintenance methylase". DNMT3a and -3b can methylate the CpG cytosine residue in a background of unmethylated DNA and function as *de novo* methyltransferases. They have no preference for hemi- versus non-methylated DNA (7). DNMT3a and -3b are thought to be required for *de novo* methylation of the genome (for example, following embryo implantation) as well as methylation of newly integrated retroviral sequences (8). The third member of methyltransferase is DNMT2. It has a catalytic domain, which shows clear homology to prokaryotic DNA methyltransferase (9). Although it has been controversial

whether DNMT2 has a functional role in mammalian cells, recent reports show that it binds to DNA *in vivo* and has a methyltransferase activity (10,11).

While the majority of CpGs are methylated in the mammalian genome, the overall DNA methylation patterns are non-randomly distributed. Heterochromatin regions tend to be hypermethylated and transcriptionally inactive (12,13). In contrast, gene promoters having dense concentrations of CpG dinucleotides tend to be hypomethylated (14); however, in tumor cells, this normal pattern is often altered. The repetitive and parasitic DNA elements are hypomethylated causing genomic instability and CpG island promoter regions are hypermethylated resulting in gene silencing (12,13). For example, in retinoblastoma and renal cancers, the promoter region of the retinoblastoma (pRb) gene and von Hippel Lindau (VHL) gene is hypermethylated (15,16). As a result, these regulatory genes are silenced resulting in loss-of-function. Clearly, DNA methylation patterns in cancer cells are distorted. Through the effects of both hypo- and hyper-methylation, DNA methylation significantly affects the genomic landscape of cancer cells. Several recent genome wide-scale methylation studies have confirmed methylation pattern changes in cancer cells and generated significant novel information about DNA methylation. For example, approximately 1% to 10% of CpG islands in individual tumors are aberrantly hypermethylated (17,18). Contrary to previous ideas, some cancer cells showed hypomethylation in CpG islands causing active transcription of associated genes. About 5% of gene-associated CpG islands are methylated in normal peripheral blood leukocytes and a fraction of these normally methylated CpG islands are hypomethylated in cancer cells (19). Genome-wide studies also showed that the aberrant methylation of CpG islands is not limited in promoter-associated CpG islands. Some CpG islands within the 3' end of genes and in intergenic regions are also hypermethylated in cancer cells (20,21). Thus, the DNA methylation patterns in cancer

cells are more complicated than previous thought and may have as yet unanticipated effects on gene regulation.

The mechanism of aberrant DNA methylation in cancer remains unclear what contributes to both genome-wide hypomethylation and regional hypermethylation. Two mechanisms have been proposed: selective advantage and selective targeting. The selective advantage hypothesis assumes that abnormal DNA methylation starts with random seeding of methylation throughout the genome. Then, those methylation events occurring within the promoter regions of genes that are important for cell survival and proliferation, like tumor suppressor genes are selected during tumorigenesis. Supporting this idea, recent mouse model for cancer showed that Myc overexpression was coupled with inactivation of phosphatase and tensin homolog (Pten), transformation related protein 53 (Trp53), or E2F transcription factor 2 (E2f2) (22). However, since not all hypermethylated genes confer a growth advantage, the selective advantage is not the only mechanism. The second hypothesis suggests that the aberrant targeting of DNMTs to certain regions causes hypermethylation. Those regions include intrinsic, *cis*-acting elements that make them more susceptible to de novo DNA methylation. This hypothesis is supported by several findings that hypermethylated genes tend to cluster in the genome (23,24), and show common sequence signatures (24-26). Although several sequences showing increased susceptibility to DNA methylation have been identified, the specific function of these patterns remains unknown. Also, an example of a trans-acting factor supporting this hypothesis is the oncogenic fusion protein PML-RAR. PML-RAR is known to induce de novo DNA methylation on its target genes (27).

In mammalian cells, DNMT1 is the major and ubiquitously expressed methylase and plays an important role in controlling gene expression in development and disease. The

importance of DNMT1 is underlined by several studies with *dnmt1* homozygous null mutations. Dnmt1 null mice die prior to the 8-somite stage (28) and somatic cells with conditional *dnmt1* null mutations display genomic hypomethylation and die by apoptosis (29). Given the fact that alterations of DNA methylation patterns are general features of tumor and cancer cells, DNMT1 is an obvious candidate for a role in this epigenetic deregulation. Indeed, the overexpression of DNMT1 increased CpG island methylation in human fibroblasts (30) resulted in elevated global methylation and transformation of NIH3T3 cells (31). In addition, the expression levels of DNMT1 are often elevated in tumors and cancer cell lines (32-34) and associated with the progression of pancreatic carcinoma (35). Also, several studies showed that reduced levels of DNMT1 contribute to oncogenic transformation. Mice expressing low levels of DNMT1 have substantially decreased genomic methylation levels, develop aggressive T-cell lymphomas and show chromosomal instability (36,37). Thus, model studies with changing the expression level of DNMT1 clearly showed that DNMT1 levels are correlated with alterations of DNA methylation patterns; however, this correlation does not seem to be consistent for a given tumor cell and changes in DNMT1 levels often do not reflect variations in DNA methylation levels (33,38). This suggests that failure to regulate DNMT1 may contribute to tumorigenesis.

Hypothesis and Specific Objectives

DNA methylation plays an essential role in the control of gene expression, chromatin condensation, and genome stability. In mammals, the establishment and maintenance of DNA methylation requires precise regulation of DNA methyltransferases, 1, 3a, and 3b. Although hypo- and hypermethylation has been linked to the cancer, very little is known about regulation of DNA methylation during disease. The findings that alterations in DNA methylation patterns

may have severe consequences for human health have led us to carefully examine the regulation of major DNA methyltransferase, DNMT1.

Overall objective of this dissertation is to examine the regulatory features of the most prominent methylation pathway in somatic cells. The activity of DNMT1 is critical in coordinating epigenetic changes and must be tightly regulated to maintain normal growth controls in somatic cells. We hypothesized that post translational modifications and a variety of protein-protein interaction processes are key regulatory elements that set methylation of CpG elements essential for normal growth behavior in somatic cells. The fundamental process can be disrupted by DNA damage leading to inappropriate gene silencing and loss of growth control in somatic cells.

In assessing the regulation of DNMT1, we found that its activity as a maintenance methyltransferase is regulated by its sumoylation. The sumoylation of DNMT1 was rigorously assessed by in vivo and in vitro sumoylation assays. Using various deletion mutants, we further investigated the interaction domain of DNMT1 with Ubc9, a SUMO1 conjugating enzyme, and its sumoylation sites. In vivo complex of methylase (ICM) assay revealed that sumoylated DNMT1 is catalytically active on genomic DNA and its sumoylation significantly enhances its methyltransferase activity. In addition, in vitro methyltransferase assays further confirmed that the sumoylation of DNMT1 significantly enhanced the methyltransferase activity of DNMT1. Together our data indicate that the sumoylation of DNMT1 is biologically relevant and represents new pathway for modulating maintenance methylation in somatic cells.

To explore the link between DNA damage repair and DNA methylation, we induced double strand breaks (DSBs) and monitored recombination and methylation at repaired sites.

Using DRGFP reporter plasmid, containing two nonfunctional tandem GFP genes, we were successfully able to analyze the homology-directed recombination (HR) event induced by DSBs. The recombination outcome was monitored by functional GFP expression using FACS analysis and recombinant DNA was examined by PCR. We showed that many recombinant GFP genes are silenced by DNA methylation. The expression of recombinant GFP was increased by treating cells with a hypomethylation agent, aza-dC. Moreover, stimulation of recombinant GFP expression was readily observed in *dnmt1*$^{-/-}$ genetic backgrounds (HCT116 *dnmt1*$^{-/-}$ and ES *dnmt1*$^{-/-}$) suggesting that DNMT1 introduced DNA methylation at repaired sites. The involvement of DNMT1 in HR repair was further confirmed its association with recombinant chromatin using a chromatin immunoprecipitation (Chip) analysis. Together, we found that HR repair of DSBs is a source generator of methylation "reset" in somatic cells and DNMT1 is responsible or establishing the epigenetic outcome.

Interestingly, we noticed that the expression pattern of the repaired GFP was bimodal, that is, there were two populations of cells expressing GFP, high expressors and low expressor, in a 1:1 ratio. The examination of methylation status of individual DNA molecules revealed that the recombination site was heavily methylated in low expressors, while hypomethylated in high expressors. This finding suggests that only one strand of repaired DNA is methylated and subsequent replication and maintenance DNA methylation generates hypermethylated and hypomethylated double strand DNAs. As a regulation mechanism of this strand-specific DNA methylation during HR, we propose that a protein-protein interaction plays an important role in the regulation DNA methylation followed by damage repair. Specifically, the interaction of DNMT1 with growth arrest and DNA-damage-inducible alpha (GADD45α) is important for the regulation of DNMT1 activity during repair. In an effort to understand a role of GADD45α in

the regulation of DNMT1, we characterized GADD45α protein itself with respect to its DNA binding ability and inhibitory function in DNA methylation. We showed the first evidence that GADD45α directly binds to DNA; moreover, it has a strong (>100 fold) preference for hemimethylated DNA. In addition, GADD45α directly interacts with DNMT1, specifically with the catalytic domain of DNMT1 and strongly inhibits the methyltransferase activity of DNMT1 in vitro and in vivo. We found that co-expression of GADD45α during HR significantly increased the expression of recombinant GFP gene. Taken together, these data suggest that GADD45α indeed has some role in coordinating the DNA methylation during HR.

In order to understand how DNMT1 is regulated to maintain the epigenetic information in somatic cells, we hypothesized that:

(1) The epigenetic state of somatic cell methylation is mediated by sumoylation of DNMT1.

(2) Alterations in DNA methylation of growth regulatory genes following double strand DNA damage are mediated by DNMT1 leading to inappropriate gene silencing antecedent to malignant transformation.

(3) DNA repair-induced methylation is mediated by protein-protein interactions through a class of DNA damage responsive factors that bind DNMT1.

CHAPTER 1: THE SUMOYLATION OF DNMT1 AND ITS BIOLOGICAL FUNCTION

1.1 Introduction

DNMT1 was the first well characterized eukaryotic DNA methyltransferase (39) and it is thought to play an important role in S-phase associated DNA methylation. It localizes to replication foci through several independent domains (5) and methylates newly synthesized daughter strands. It comprises a large N-terminal domain and a highly conserved C-terminal catalytic domain. The N-terminal region interacts with many chromatin-associated proteins. For example, the far N terminus of DNMT1 interacts with DNMT1 associated protein 1 (DMAP1) for transcriptional repression (40). It contains a nuclear localization signal, a PCNA interacting domain (6), a replication targeting region (5), and a cysteine–rich Zn^{2+} binding domain. DNMT1 also contains a domain showing homology to the polybromo-1 protein from chicken (41). This domain contains two bromo adjacent homology (BAH) domains that may drive protein-protein interactions (Fig. 1).

The N-terminal part of DNMT1 interacts with the retinoblastoma (Rb) protein to repress the E2F1 responsive genes (42). Also, DNMT1 directly interacts with a histone methyltransferase SUV39H1 (43), histone deacetylases HDAC1 and HDAC2 (40,42), methyl CpG binding proteins (MBD) (44,45), a heterochromatin binding protein (HP1) (43). All these interactions are involved in transcriptional repression. Finally, DNMT1 interacts directly with DNMT3a and DNMT3b (46). Clearly, DNMT1 forms multiple, complex networks with other proteins involved in gene regulation and epigenetic signaling.

DNMT1 is also post-translationally modified. Glickman et al. reported that murine Dnmt1 is phosphorylated at serine 514 with unknown biological consequences (47) In addition, it is also ubiquitylated. Ubiquitin is a 76-amino acid polypeptide and can be attached to the

lysine residue of a target protein. The major role of ubiquitylation is to direct proteins to be degraded by the 26S proteasome (48). Ubiquitylation occurs as a result of the sequential action of three classes of enzymes including E1 activating enzyme, E2 conjugating enzyme, and E3 ligase. Substrate specificity is determined by E3 ligase. The ubiquitin-mediated protein degradation is evidently essential in growth control and cell cycle regulation (48). Two recent reports show that DNMT1 is degraded through a proteasomal pathway (49,50). DNMT1 interacts with E3 ubiquitin ligase Cdh1, which is a component of anaphase promoting complex and is involved in late mitotic or early G1 degradation of cell cycle regulatory proteins (49). Its degradation is dependent on an N-terminal 120 amino acid domain and is markedly reduced upon treatment of a proteasome inhibitor (MG132) (50). Ubiquitylation can be regulated by the phosphorylation of the target protein. The phosphorylation creates binding sites for E3 ligases (51) or stabilizes proteins via the inhibition of E3 ligase interactions (52). The relationship between phosphorylation and ubiquitylation of DNMT1 is not known. DNMT1 phosphorylation levels are not significantly altered under conditions of aza-dC induced degradation (49), suggesting that phosphorylation may actually facilitate DNMT1 ubiquitylation.

A small ubiquitin-related modifier (SUMO) modification, sumoylation, is a newly identified post-translational modification. It was discovered in studies on the nuclear import system (53). SUMO1 is 18% identical to ubiquitin and has a similar protein structure (54). SUMO is also attached to the lysine residue of the target protein. This reaction is ATP-dependent and requires the E1 activating enzyme Aos1/Uba2, as well as the E2 conjugating enzyme Ubc9 (55). Compared to the ubiquitin-conjugating system (where E3 ligases recognize targets) in the sumoylation pathway, an E2 enzyme (Ubc9 in this case), mediates partial recognition of target proteins. Ubc9 recognizes a sumoylation consensus sequence (ψKXE/D; ψ

is a hydrophobic residue) (56). Although sumoylation is quite similar to the ubiquitylation, the biological role and consequences of the modification are very different. It modulates several important functions of target proteins, such as protein-protein, protein-DNA interactions, subcellular localization, in addition to protein stability (55). One distinct function of the sumoylation is its ability to antagonize ubiquitin-mediated degradation. For example, a lysine residue 21 in IκBα can be modified by both SUMO1 and ubiquitin (57). The sumoylation of this residue inhibits the proteolysis of IκBα. Among mammalian DNA methyltransferases, mouse Dnmt3a and -3b have been reported to be sumoylated which modulates protein/protein interactions leading to transcriptional repression (58,59).

While investigating post-translational modification of DNMT1, we found that human DNMT1 is also sumoylated like Dnmt3a and -3b. DNMT1 is a 1616 amino acid residue protein and has more than 10 putative sumoylation sites. The putative sumoylation sites are distributed throughout its primary amino acid sequences. In this work, we show that DNMT1 is modified by SUMO1 and the sumoylation occurs when DNMT1 is actively methylating genomic DNA in situ. Specifically, DNMT1 sumoylation enhances its methyltransferase activity. The data suggest that DNMT1 sumoylation affects interaction of DNMT1 with other proteins that regulate catalytic action of DNMT1 in a chromosomal setting.

1.2 Material and Methods

1.2.1 Plasmids

DNMT1-V5, DNMT3a-V5, HA-SUMO1, HA-SUMO1-AA, and Myc-Ubc9 were PCR amplified from cDNA plasmids (kindly provided by Keith D. Robertson) using Accuprime *Pfx* DNA polymerase (Invitrogen) according to the manufacturer's instruction. Restriction enzyme sites were incorporated into the PCR primers. Briefly, DNMT1 and DNMT3a PCR products were digested with EcoRI and NotI (or XhoI for DNMT3a) and cloned into pcDNA3.1/V5-HisA plasmid (Invitrogen) using the same restriction enzyme sites. SUMO1 was digested with BglII and XhoI and cloned into pCMV-HA (Clontech). To clone the Myc-Ubc9, first, a pCMV-Myc1 plasmid was constructed by inserting a Myc linker containing one copy of epitope into pcDNA3.1(+) (Invitrogen) using the HindIII and BamHI sites (the HindIII site was mutated by inserting Myc linker). Ubc9 PCR products were digested with EcoRI and XhoI and cloned into pCMV-Myc1 plasmid. Deletion mutants used for immunoprecipitation were created by PCR using DNMT1-V5 as a template, except for 1114-1616 mutant. The 1114-1616 mutant was PCR amplified from a CAT plasmid (kindly provided by Moshe Szyf). All PCR products were cut with EcoRI and NotI and cloned into pcDNA3.1/V5-HisA plasmid (Invitrogen) using the same restriction enzyme sites. For deletion mutants used for in vivo complex of methylase (ICM) assay, a PCR amplified catalytic domain from DNMT1-V5 was cloned into above deletion mutants using NotI site. The orientation of cloned catalytic domain was determined by restriction mapping analysis. Mutation of the active site cysteine (C1226A) of DNMT1 and replacement of two glycine residues of SUMO1 with alanine residues were generated by PCR using a site-directed mutagenesis kit (Stratagene). HA-PIASy and HA-SENP1 was kindly provided by Dr. Hongtao Yu.

1.2.2 Cell Culture and Transfection Assays

Wild type HCT116, *dnmt1*$^{-/-}$ cells (a generous gift from Dr. Bert Vogelstein), and HEK293FT cells purchased from Invitrogen were grown in Dulbecco's modified Eagle's medium (Gibco) with 10% fetal bovine serum. HeLa cells were grown in RPMI 1640 (Gibco) with 10% fetal bovine serum. Cells were transfected in six-well plates with Lipofectamine2000 reagent (Invitrogen) according to the manufacturer's instructions.

1.2.3 Co-immunoprecipitation and Western Blotting

Whole cell extracts were prepared by lysing cells in RIPA buffer (1X PBS pH 7.5, 1% NP-40, 0.5% deoxycholate, 0.1% SDS, 10% glycerol) containing 1X protease inhibitor cocktail (Roche), 1 mM DTT, 1 mM $MgCl_2$, 2 mM PMSF, and 100 mM N-ethylmaleimide (NEM). For immunoprecipitation, the whole cell extracts was diluted 5 fold with 0.5X PBS containing 1X protease inhibitor cocktail, 1 mM DTT, 1 mM EDTA, and 2 mM PMSF. Antibody (1 μg) was added to samples for 3 h, followed by 30 μl of protein A Sepharose 4B beads (Zymed) overnight. Beads were washed three times with 1X PBS, 0.5% NP-40 or RIPA buffer (for sumo modification detection). Bound proteins were eluted with sample buffer and analyzed by western blotting. Antibodies used are as follows: anti-V5 (Invitrogen), anti-DNMT1 (NEB), anti-HA11 (Covance), anti-SUMO1 (Zymed), anti-SUMO1 sc-5308 (Santa Cruz), anti-Topo1 (TopoGEN), and anti-Myc (Upstate).

To examine sumoylation of endogenous DNMT1, nuclear extracts were prepared by resuspending cells in a buffer A (10 mM HEPES/KOH, pH 8.0, 1.5 mM $MgCl_2$, 10 mM KCl, and 1 mM DTT). The cells were incubated on ice for 15 min and disrupted in a type S Dounce homogenizer. Nuclei were collected by centrifugation at 10,000g for 1 min and washed twice

with buffer A. The nuclei were then resuspended in buffer B (20 mM Tris/HCl, pH 7.5, 1.5 mM $MgCl_2$, 10% glycerol, 500 mM NaCl, 0.2 mM EDTA, 1 mM DTT, 0.5 mM PMSF, and 1X protease inhibitor cocktail (Roche)) and kept on ice for 30 min. Nuclear extracts were prepared by centrifugation at 20,000g for 20 min. The supernatants were used for immunoprecipitation experiments. To immunoprecipitate the endogenous DNMT1 or SUMO1 conjugates, nuclear extracts (1 mg protein) were diluted twofold with buffer B without NaCl. DNMT1 antibody (5 μg, Santa Cruz, N-16) or SUMO1 antibody (10 μg, Santa Cruz, D-11) was added to samples for 3 h, followed by 50 μl of protein A Sepharose 4B beads (Zymed) at 4 ℃ for 18 h. Beads were washed three times with buffer C (20 mM Tris/HCl, pH 7.5, 300 mM NaCl, 0.5 mM EDTA, 1 mM PMSF, and 0.25% NP-40). The bound proteins were eluted and analyzed by western blotting.

1.2.4 In Vivo Complex of Methylase Assay

In vivo complex of methylase (ICM) assay was performed as described in Liu et al. (11). Briefly, Cells treated with aza-dC were lysed with 1% sarkosyl in TE (10 mM Tris/HCl, pH 7.5, 1 mM EDTA) and lysates layered onto a step CsCl gradient followed by ultracentrifugation (35000 rpm, SW50.1 rotor for 20 h, at 22 ℃). The gradient was fractionated (0.4 ml aliquots) and DNA fractions were pooled. The concentrations were measured by UV spectroscopy. Different amounts of DNA were slot blotted onto a membrane and probed with proper antibody. The immune complex was detected with Amersham's enhanced chemiluminescence kit. Signals were quantified using a GeneTools program (SynGene, Cambridge, UK).

1.2.5 In Vitro Sumoylation

Recombinant DNMT1 (500 ng) purified from insect cell lines was used as substrate for the in vitro sumoylation reaction. Reactions contained 900 ng of SAE1/SAE2, 620 ng of Ubc9, and 1.25 μg of SUMO1. All components of sumoylation were purified from *E.coli* BL21 (DE3) Codon Plus cells (Stratagene). Reactions were carried out at 30 ℃ for 2 h in the presence of 5 mM ATP, 50 mM HEPES-KOH (pH 7.5), 50 mM NaCl, and 10 mM $MgCl_2$ in a 60 μl reaction volume. The reaction was stopped by adding 100% trichloroacetic acid and precipitated. Pellets were washed with cold acetone and re-dissolved in laemmli buffer (0.125 M Tris/HCl, pH 6.8, 4% SDS, 20% glycerol, 0.01% bromophenol blue, and 10% β-mercaptoethanol). The samples were separated on a SDS-PAGE gel, followed by western blotting.

1.2.6 In Vivo Sumoylation using a Baculovirus Expression System

Production of sumoylated DNMT1 using a reconstituted sumoylation system in Sf9 cells was performed as described in Langereis et al. (60). Viral stocks for SUMO1 and Ubc9 were kindly provided by Dr. Wilson. Viral stocks for DNMT1 were provided by Dr. Robertson. Topo1 viral stock was provided by TopoGEN. Sf9 cells were seeded in six-well plates at a density of 10^6 cells per well. High titer viral stocks were added to obtain the desired multiplicity of infection (MOI). The infected cells were collected after 72 h post-infection and whole cells extracts were prepared for immunoprecipitation with anti-SUMO1 antibody (Santa Cruz sc-5308). Immunoprecipitation was performed as described above followed by western blotting using anti-DNMT1 (NEB) or anti-Topo1 (TopoGEN) antibody.

1.2.7 In Situ Fractionation and Immunofluorescence Staining

HeLa cells grown on cover slips were transfected with DNMT1-V5, HA-SUMO1, and Myc-Ubc9. After 24 h post-transfection, cells were treated 5 μM aza-dC for 24 h. The cells on cover slips were fixed directly or in situ fractionated before fixation according to the protocol of Fey et al. (61) with some modification. Briefly, cover slips were immersed in 0.2% TritonX-100 in cytoskeleton (CSK) buffer (10 mM PIPES, pH 6.8, 100 mM KCl, 300 mM sucrose, 3 mM $MgCl_2$, 1 mM EGTA, and 1.2 mM PMSF) and incubated at 4 ℃ for 5 min. Then the cover slips were treated with extraction buffer (42.5 mM Tris/HCl, pH 8.3, 8.5 mM NaCl, 2.6 mM $MgCl_2$, 1.2 mM PMSF, 1.0% Tween 40, and 0.5% deoxycholic acid) for 5 min at 4 ℃. After this extraction, cells were further treated with 2 M NaCl in CSK buffer for 5 min at 4 ℃. After each extraction, cells were fixed with 2% paraformaldehyde in PBS for 15 min at room temperature. Fixed cells were incubated with anti-V5 antibody and anti-SUMO1 antibody (Abcam, Y199) for overnight, rinsed with 1X PBS, and incubated with Alexa-fluor 488 goat anti-mouse IgG and Alexa-fluor 568 goat anti-rabbit IgG (Molecular probes). Nuclei were stained using Topro3 iodide (Molecular probes) and the cover slips were mounted onto glass slides using Vectashield mounting media (Vector laboratories, CA, USA). Confocal images were obtained on a Zeiss LSM510 confocal microscope.

1.2.8 In Vitro DNA Methyltransferase Assay

DNA methylation activity of the in vitro sumoylated DNMT1 was measured by the incorporation of tritiated methyl group from labeled SAM (S-adenosyl-L-[methyl-^{3}H] methionine, 10 Ci/mmole (PerkinElmer)) into an oligonucleotide substrate containing a single CpG site in hemimethylated form (D1subHMF: 5'- GAA GCT GGG ACT TCM GGC AGG

AGA GTG CAA-3', D1subUMR: 5'- TTG CAC TCT CCT GCC GGA AGT CCC AGC TTC-3', where M denotes 5-methylcytosine). Oligonucleotides were purchased from Integrated DNA Technologies. Double-stranded oligonucleotides were annealed by mixing equal amounts of complimentary oligonucleotides, heating to 95 ℃ for 5 min, 65 ℃ for 10 min, and cooling down to 20 ℃. The methylation reaction was carried out at concentration of 0.5 μM DNA, 0.05 nmole SAM, and 100 ng of in vitro sumoylated DNMT1 in methylation buffer (20 mM Tris/HCl, pH 7.5, 5 mM EDTA, 5 mM DTT, 1 mM PMSF, and 10% glycerol) at 37 ℃. At defined times, the reactions were stopped by adding phenol/chloroform and DNA was precipitated by adding same volume of isopropyl alcohol. The DNA pellet was dissolved in TE buffer and transferred to Whatman filter paper. Radioactivity was determined using LS6500 scintillation counter (Beckman Coulter).

1.3 Results

1.3.1 DNMT1 is Sumoylated both In Vivo and In Vitro.

To examine DNMT1 sumoylation in vivo, we co-transfected a plasmid expressing DNMT1-V5 along with expression vectors for HA-SUMO1 and Myc-Ubc9. Whole cell extracts were prepared in the presence of an inhibitor of the SUMO hydrolase, NEM (N-ethylmaleimide) (62). Since the size of V5 epitope tagged-DNMT1 is relatively large (187 kDa) and the level of sumoylation appears to be relatively low, the SUMO1-specific band shift of DNMT1-V5 was not readily observable in the whole cell extracts or immunoprecipitates by western blotting using anti-V5 antibody (Fig. 2A right panel); however, when the immunoprecipitates were probed with anti-HA11 antibody, the sumoylated form of DNMT1-V5 was clearly seen (Fig. 2A and Fig. 12). The bands seen in the left panel (Fig. 2A lane1) were not seen in the negative controls (omitting DNMT1-V5 or HA-SUMO1), which reveals dependence on all three expression components. The signals seen in blots probed with anti-V5 antibody (Fig. 2A lane 4 and 6) clearly migrated faster than the modified DNMT1-V5 (compare left and right panels). Examination of the sumoylated DNMT1 revealed two or more HA-SUMO1 specific bands of DNMT1-V5 in vivo.

To confirm the sumoylation of DNMT1, we employed recombinant SAE1/SAE2, Ubc9, and SUMO1 to show that purified recombinant DNMT1 was modified by SUMO1 in vitro. As shown in Fig. 2B (lane 1), two bands were observed in western blots probed with anti-SUMO1 antibody. The signal seen in lane 1 was clearly dependent on co-incubation of DNMT1 and SUMO1 (Fig. 2B compare lanes 1, 2 and 3).

In vivo sumoylation was also evaluated using Sf9 cells and a reconstituted mammalian sumoylation system. It has been reported that Sf9 cells possess an active endogenous

sumoylation system (60). Langereis et al. (60) showed that this system sumoylates an exogenous target protein efficiently by co-expression of mammalian Ubc9 and SUMO1. Figures 3A and 3B show sumoylation of DNMT1 or a positive control protein (topo1) in this cell system. Sf9 cells were infected with recombinant baculoviruses expressing Ubc9, SUMO1, and DNMT1 or topo1. After 72 h post-infection, cells were collected and whole cell extracts were prepared for immunoprecipitation. We immunoprecipitated all SUMO1-conjugated proteins using anti-SUMO1 antibody, then probed the subsequent western blot with a DNMT1 antibody to determine whether DNMT1 exists in the immunoprecipitated proteins. We were able to detect a weak, but significant and reproducible signal of DNMT1 (Fig. 3A, lane 2). DNMT1 sumoylation clearly requires the co-expression of Ubc9 and SUMO1 (compare lane 2 with 1 and 3 in Fig. 3A). As a positive control for validating this system, we variefied sumoylation of the known SUMO1 target protein, topo1 (63). Topo1 is robustly sumoylated in Sf9 cells with co-expression of Ubc9 and SUMO1 (Fig. 3B).

To verify that sumoylation occurs on endogenous DNMT1, we performed immunoprecipitation experiments. First, we immunoprecipitated endogenous DNMT1 using highly specific DNMT1 antibody and probed membrane with anti-SUMO1 antibody. As a negative control, we used nuclear extracts from HCT116 *dnmt1*$^{-/-}$ cells. Fig. 4A demonstrates that endogenous DNMT1 was sumoylated. The bands shown in Fig. 4A lane 2 were not observed in HCT116 *dnmt1*$^{-/-}$ nuclear extracts (lane 3) or negative antibody controls (lane 1). The SUMO1 antibody specific bands that appear with anti-DNMT1 antibody immunoprecipitation show that endogenous DNMT1 is modified by SUMO1. To confirm this result, we immunoprecipitated total SUMO1 conjugates from nuclear extracts (using anti-SUMO1 antibody) and checked for the presence of DNMT1 (Fig. 4B). The band shown in Fig.

4B lane 2 was slightly larger than the unmodified form of DNMT1, as expected (input lane 4) and was not detected in control lanes (1 and 3). Detecting DNMT1 in the SUMO1 immunoprecipitates is consistent with Fig. 4A; therefore the collective data strongly support the idea that endogenous DNMT1 is subject to SUMO1 modification.

1.3.2 DNMT1 Interacts with Ubc9.

The E2 conjugating enzyme, Ubc9, has been shown to interact with a large number of proteins, and many of them have been targets for sumoylation (55). To support the notion that DNMT1 is sumoylated, we performed co-immunoprecipitation using cells transiently transfected with tagged versions of each protein. Myc tagged Ubc9 co-immunoprecipitated with DNMT1-V5 when co-transfected into HEK293FT cells, and vice versa (Fig. 5A).

To define the domains responsible for the interaction, we constructed a series of V5 tagged DNMT1 deletion mutants (Fig. 5B). These were co-transfected into HEK293FT cells with Myc-Ubc9, and their ability to interact was assessed using co-immunoprecipitation experiments as shown in Fig. 5C. The lysates of co-transfected cells were immunoprecipitated with anti-V5 antibody and the immunoprecipitates were analyzed by western blotting. All deletion mutants of DNMT1 showed some degree of interaction with Ubc9, except for the 1-419 mutant. Since the recovery and yield of the mutant proteins was variable, we normalized the co-immunoprecipitated Ubc9 band intensity with the amount of precipitated each deletion mutant (lower blot Fig. 5C). This experiment was repeated three times. As shown in Fig. 5C right panel, 412-1113 mutant showed the strongest interaction with Ubc9 and the domain could be narrowed down to amino acids between 645 and 1113 containing the two contiguous bromo adjacent

homology (BAH) domains. The BAH domain is often found in proteins involved in transcriptional regulation and is thought to be a protein-protein interaction module, especially in gene silencing (64). Also, a 1114-1616 mutant, which contains only a catalytic domain, showed weak interaction with Ubc9; however, we could not determine whether the catalytic domain interacts with Ubc9 independently or if it merely contains a domain required for full interaction with Ubc9. From these results, we conclude that the BAH domains in DNMT1 (amino acids 645-1113) are primarily responsible for the interaction with Ubc9.

1.3.3 Sumoylation of DNMT1 Deletion Mutants.

As shown in Fig. 2A, multiple high molecular weight (MW) bands were detected in the DNMT1 sumoylation analysis, suggesting that the methylase is modified at multiple sites (more than two high-molecular-mass bands were detected by anti-HA antibody). We additionally found several potential sites (similar to the consensus for SUMO modification) in DNMT1 (55). We mutated several lysine residues to arginine (residues 148, 194, 675, 739, 957, 1135, and 1609) and checked for sumoylation; however, we failed to detect any impairment of sumoylation from those mutants (data not shown). In order to determine the location of sumoylation sites, we co-expressed deletion mutants with HA-SUMO1 and Myc-Ubc9 in HEK293FT cells and analyzed their sumoylation status (Fig. 6). The mutant proteins were immunoprecipitated and beads were extensively washed with the modified 0.5X or 1X RIPA buffer to detect specific and nonspecific bands. Three mutant proteins displayed sumoylation (Fig. 6). The deletion mutant harboring amino acids 1-419 did not interact with Ubc9 and also was not sumoylated. Thus, we could not rule out the sumoylation of this mutant since it did not interact with Ubc9. Notably, 412-1113 mutant protein, which strongly binds to Ubc9 (Fig. 5), appears to have three sumoylated forms, but the 645-1113 protein has only one, indicating that two sumoylation sites reside between

amino acids 412 and 644. Interestingly, the mutant protein 1114-1616, consisting of only the catalytic domain, also showed two sumoylated products. Sumoylation of this particular mutant suggests that it indeed interacts with Ubc9, but is weak (Fig. 5C). In summary, there appears to be five sumoylation sites, however, new sumoylation sites might be revealed in some deletion mutants when secondary SUMO1 consensus elements become available.

1.3.4 Sumoylated DNMT1 is Covalently Bound on Genomic DNA In Vivo.

Previously, we reported an in vivo methylase assay (ICM or In vivo Complex of Methylase) that quantifies DNA methyltransferases (DNMTs) trapped on the genome at large using aza-dC to arrest covalent complexes (11). The ICM assay is an antibody based method to detect and quantify endogenous catalytic action of specific DNMTs. This assay reflects the catalytic action of methylase in cells that treated with the DNA hypomethylating agent, aza-dC (which is incorporated into genomic DNA). Subsequent action of methylase leads to a stable, covalent methylase/DNA complex that can be quantified by western blotting with purified genomic DNA (Fig. 7).

In this analysis, the ICM assay was used to determine whether DNMT1 trapped on genomic DNA is modified by SUMO1. The results (Fig. 8A, B) clearly show that a SUMO1 signal was detected in the DNA peak. This signal is only detected in the WT HCT116 cell line and not in the *dnmt1*$^{-/-}$ cell line. To normalize the data on a per genome basis, we recovered genomic DNA from the gradient and spotted fixed amounts of DNA on a slot blot over a range of 0.3 to 0.9 μg total DNA (Fig. 8B). The SUMO1 signals appear to be roughly 2 fold less than the DNMT1 signals (compare fractions 2, 3 in Fig. 8A); however, quantitative comparisons with different antibody probes cannot be compared and may be misleading. These data strongly

support the notion that DNMT1 trapped on genomic DNA following aza-dC treatment is modified by sumoylation (either before or after trapping). A potential problem with this sort of methodology is that the readout is a blot signal without providing molecular weight identity, as one would see in a conventional western blot. In other words, is the DNA associated signal we detect with the SUMO1 probe due to SUMO1 or to simple background binding of the SUMO1 antibody to DNMT1 that resides in the DNA fraction? Note that the knock out cell line (HCT116 *dnmt1*$^{-/-}$) does not clarify the picture since there will be no full length DNMT1 protein in the DNA peak; thus, we would expect a negative result when probed with both DNMT1 and SUMO1. To validate our results, transient transfection experiments were carried out in HCT116 *dnmt1*$^{-/-}$ cells with plasmids harboring V5 epitope tagged DNMT1 (DNMT1-V5), HA epitope tagged SUMO1 (HA-SUMO1), and Myc epitope tagged Ubc9 (Myc-Ubc9) in aza-dC treated cells. As shown in Fig. 9, the SUMO1 signal was detected only in cells expressing DNMT1-V5 in an aza-dC dependent manner. In addition, there was no detectable SUMO1 signal from the cells expressing SUMO1 mutants (HA-SUMO1-AA), which cannot modify its target (65). These data show clearly that it is possible to trap endogenous DNMT1 onto the genome under conditions where sumoylation has been neutralized by mutation. Probing with anti HA antibody confirms that no SUMO1 modified DNMT1 is present. The data also indicate that any SUMO1 signal in the DNA peak is in a form attached to the target protein (as opposed to free or unbound). An additional control, the active site mutant of DNMT1 (C1226A), shows that neither DNMT1 nor SUMO1 signals were detected as covalent intermediates with DNA (Fig. 9). Failure to detect a signal with C1226A mutant further supports the notion that the SUMO1 signal depends on DNMT1. Also, we show that DNMT3a is sumoylated when it is bound to DNA using ICM

assay (Fig. 9). These data confirm the veracity of the ICM for examining post-translational modification by sumoylation with DNA methylation enzymes.

Recently, Spada et al. reported that HCT116 *dnmt1*$^{-/-}$ cells express a truncated form of DNMT1, which is responsible for maintaining the global methylation in the knockout cell line (66). The truncated form of DNMT1 (DNMT1$^{\Delta E3-6}$), lacks the amino acids between 40 and 200, including the part of DMAP binding domain (40) and PCNA binding domain (6). The ICM experiment shown in Fig. 8A did not detect the truncated mutant because our antibody probe maps within the deletion; therefore, its presence cannot be evaluated with this particular probe. In theory, the endogenous SUMO1 modified DNMT1$^{\Delta E3-6}$ should be present in the DNA peak in this experiment; however we did not detect any signal as shown in Fig. 8A (bottom row). This could be due to low levels of expression of the truncated mutant (as reported by Spada et al. (66)) combined with the fact that the endogenous SUMO1 signals tend to be rather weak (Fig. 8A, SUMO1 probe compare to DNMT1 probe). Alternatively, the truncated mutant may lack key domains for SUMO1 modification (e.g. PCNA, DMAP). To examine these possibilities, we evaluated a series of deletion mutants for SUMO1 modification in complexes with genomic DNA, using the ICM method.

1.3.5 Analysis of Sumoylation of DNMT1 Mutants Trapped on Genomic DNA.

A series of deletion mutants in DNMT1, including the internal deletion (DNMT1$^{\Delta E3-6}$) were tested for their ability to form arrested covalent complexes with genomic DNA using transient expression assays. Expression levels for the various mutants were normalized (based on western blots), allowing comparison in different experiments. The data show the truncated mutant (DNMT1$^{\Delta E3-6}$) retained catalytic activity in a chromatin setting (Fig 10B), consistent with

prior data that methylation activity can be mediated by this mutant in the DNMT1 knock out cell line (66). A closer look at the data reveals that the mutant lacking the PCNA domain ($DNMT1^{\Delta E3-6}$) is marginally less active (by about 40%) than WT DNMT1 based on global genomic DNA methylation. SUMO1 modification was evaluated by probing with anti-HA11 (Fig. 10B, right blot). Sumoylation appears to be similar in $DNMT1^{\Delta E3-6}$ compared to WT DNMT1 (Fig. 10B).

The same analysis was carried out with the various mutants listed in Fig. 11A. The catalytic domain deletion mutant (1114-1616) was incapable of methylating the genome and its sumoylation status could not be evaluated in this experiment. The N-terminal mutants (412-1616 and 645-1616) were much less active than WT DNMT1 in terms of DNA binding efficiency upon treatment with aza-dC (Fig. 11B, left panel). Finally, sumoylation levels are reduced as more of the N-terminus is deleted (Fig. 11B, right panel).

To examine how sumoylation of the internal deletion mutant ($DNMT1^{\Delta E3-6}$) relates to sumoylation of the catalytically active form (detected by the ICM assay), we compared SUMO1 modifications by immunoprecipitation experiments using nuclear extracts (Fig. 12). These data reveal that the overall level of SUMO1 was similar between WT and mutant, although the distribution of SUMO1 sites was very different in $DNMT1^{\Delta E3-6}$ (compare lanes 1 and 2). Notably, deleting the PCNA domain appears to promote SUMO1 modification at a single prominent site, while the WT DNMT1 is modified at two major sites (Fig. 12, lanes 1,2).

1.3.6 SUMO1 Co-localizes with DNMT1 on Aza-dC Genomic DNA.

We designed a cytolocalization approach as a complementary method to evaluate SUMO1 modified DNMT1 in cells. This experiment is possible because both SUMO1 and DNA binding involve covalent modifications; thus, SUMO1 and the aza-dC DNA/DNMT1 adduct both are stable, detergent and salt resistant complexes, whereas other DNA binding proteins (histones and other weakly bound non-histone chromosomal proteins) are removed under these harsh ionic conditions (2 M NaCl). Cells were transfected with DNMT1-V5, Myc-Ubc9 and HA-SUMO1 and the distribution of the SUMO1 modified methylase evaluated before and after detergent (0.2% TritonX-100) and ionic (2.0 M NaCl) extraction by immunofluorescence staining of treated cells. Sequential extractions were imaged in control cells (no aza-dC) and in cells treated with aza-dC which traps DNMT1 on genomic DNA in situ (Fig. 13). As expected, in control cells (no aza-dC), the bulk of DNMT1 and SUMO1 target proteins are removed by detergent and NaCl extraction. In aza-dC treated cells, essentially all of the SUMO1-DNMT1 was retained after high NaCl extraction (Fig. 13, column D). This result reveals that 24 hr of aza-dC treatment is sufficient to trap virtually all of the ectopically expressed DNMT1 onto the genome; thus, we conclude that the hypomethylating drug is a remarkably efficient way to bind nuclear DNMT1 to the genome. In contrast, only about 40-50% of the SUMO1 signal was retained after 2M NaCl extraction. Presumably, SUMO1 modifications occur on target proteins that are not covalently attached to genomic DNA (non-histone and histone proteins for example). These proteins would be removed by the extraction methods used and any remaining SUMO1 (anti-HA IgG) signal represents a subset of sumoylated protein that is specifically trapped on the genome through the action of a methylase. This result suggests that a rather large fraction (40-50%) of the total cellular SUMO1 modification is directed at DNMT1 which is covalently bound

on genomic DNA. The imaging analysis also confirms that DNMT1 and SUMO1 signals co-localize in extracted nuclei.

1.3.7 Sumoylation of DNMT1 Increases the Activity of DNMT1 In Vitro.

Sumoylation affects various aspects of target protein function. To investigate the role of DNMT1 sumoylation, we examined whether the enzymatic activity of DNMT1 is affected by sumoylation. Purified DNMT1 was sumoylated in vitro and its catalytic activity was measured using S-[methyl-^{3}H]adenosyl methionine as a methyl donor with a hemimethylated oligonucleotide substrate. As a control, DNMT1 was also mock sumoylated with an inactive mutant, SUMO1-AA, in which C-terminal diglycine residues of SUMO1 are mutated to two alanine residues; therefore, these two reactions contained identical sets of purified proteins except that in one reaction was SUMO1 negative (compare two lanes in Fig. 14A). As shown in Fig. 14B, sumoylation of DNMT1 increased the catalytic activity of DNMT1 by as much as 10 fold (range of 4-10 fold). Thus, sumoylation strongly stimulated DNMT1 activity on hemimethylated substrates.

1.3.8 Sumoylation of DNMT1 Enhances its Ability to Bind DNA.

The sumoylation of target proteins is a dynamic process. A target protein may be modified by SUMO proteins and desumoylated by deconjugating enzymes. The cycle between sumoylation and desumoylation seems to be in a rapid equilibrium resulting in very low level of steady state sumoylated form of target proteins in the cell. To investigate the role of DNMT1 sumoylation, we performed ICM assays under condition known to be favorable or unfavorable for sumoylation. We overexpressed the SUMO E3 ligase, PIASy (protein inhibitor of activated STAT), a deconjugating enzyme, SENP1 (SUMO/sentrin-specific protease), along with

DNMT1-V5, HA-SUMO1, and Myc-Ubc9 in HEK293FT cells. Transfected cells were treated with 10 μM aza-dC for 1 h to measure global methylation activity using the ICM. As shown in Fig. 15, DNMT1 binding was decreased with SENP1 and increased with PIASy. SENP1 reduced bound DNMT1 by 0.64 or 0.58 fold and PIASy increased DNMT1 levels by 1.15 or 1.36 fold (Fig. 15 right panel). The fold increase or decrease was dependent of the expression levels of each protein. In addition, SENP1 decreased the level of DNMT1 sumoylation, whereas PIASy increased. Surprisingly, PIASy robustly stimulated the sumoylation of DNMT1 (ca. 20 fold). Since PIASy increased both DNA binding and sumoylation, we conclude that sumoylation of DNMT1 might occur prior to genomic DNA binding. If DNMT1 has been modified by SUMO1 after DNA binding, we would predict an increased level of sumoylation, but no change in the amount of DNMT1 bound on genomic DNA. This was not the case for DNMT1; therefore, sumoylation of DNMT1 facilitates the access of DNMT1 to DNA, in a chromatin setting.

We carried out co-immunoprecipitation experiments to examine the interaction of DNMT1 with SENP1 or PIASy. HEK 293FT cells were co-transfected with DNMT1-V5, HA-SUMO1, Myc-Ubc9, and HA-SENP1 or HA-PIASy. Whole cell extracts were immunoprecipitated with anti-V5 antibody and precipitated proteins were analyzed by western blotting with anti-HA11. Note that SUMO1, SENP1, and PIASy are all tagged with HA epitope allowing us to check co-immunoprecipitated SENP1 or PIASy and the sumoylated form of DNMT1 on the same membrane. As shown in Fig. 16, both SENP1 and PIASy were co-immunoprecipitated with DNMT1-V5. As expected, co-expression of SENP1 decreased the level of sumoylated DNMT1 (Fig. 16A compare lane 2 and 3) and PIASy increased the amount of sumoylated DNMT1 (Fig. 16B compare lane 2 and 3). However, the increase in DNMT1 sumoylation by PIASy was not as robust as the ICM assay (Fig. 15). This suggests that DNMT1

sumoylation is regulated spatially and temporally in the cell. That is, DNMT1 might be sumoylated more efficiently as it approaches to the target DNA.

Taken together, these data suggest that DNMT1 is sumoylated before its DNA binding and the sumoylation enhances the DNA binding efficiency of DNMT1.

1.4 Discussion

In this study, we show that human DNMT1 is modified by SUMO1 in vivo and in vitro. Consistent with this modification, DNMT1 interacts with an E2 conjugating enzyme, Ubc9. The major interaction domain has been mapped to two bromo adjacent homology domains of DNMT1. The sumoylation sites of DNMT1 are distributed throughout its primary sequence and we have shown that each deletion mutant of DNMT1 has two or three sumoylation sites. Sumoylation of DNMT1 increased its DNA methyltransferase activity in vitro and in vivo.

The modification of proteins by the reversible covalent attachment of SUMO protein is a flexible, yet powerful method of regulation. Large numbers of proteins have been identified as sumoylation substrates. Proteomic experiments show that more than 300 proteins are sumoylation targets in budding yeast (67). Among the major DNA methyltransferases in mammals, sumoylation of Dnmt3a and Dnmt3b has been reported (58,59,68). The sumoylation of Dnmt3a disrupts its ability to interact with HDACs and impairs its capacity to repress transcription (59). The role of sumoylation of Dnmt3b is not known (58). DNMT1 has many putative sumoylation sites fitted in a consensus ψKXE/D motif, which prompted us to investigate the sumoylation of DNMT1. Since the level of sumoylation of target proteins is extremely low in general, we over-expressed SUMO1, Ubc9, and DNMT1 with hope of observing this process. Overexpression of each protein allowed us to detect the sumoylated forms of DNMT1 in HEK293FT cells. Sumoylation was further confirmed through an in vitro sumoylation assays and a reconstituted sumoylation system in Sf9 cells. Relative to the in vivo situation, the efficiency of the Sf9 cell system was low, implying that certain endogenous factors are required in regulating this modification. Most likely, such factors might be E3 ligases, which determine substrate specificity and increase sumoylation efficiency. Currently, three classes of E3 ligases,

PIASs (protein inhibitors of activated STAT), RanBP2 (RAN binding protein 2), and Pc2 (polycomb protein 2), have been reported. Dnmt3 enzymes interact with PIAS1 and PIASx, which are members of PIAS protein family; however, DNMT1 does not (59). Neither PIAS1 nor PIASx stimulate the Dnmt3a sumoylation, but Pc2 has been shown to possess E3 ligase activity directed at Dnmt3a (68).

Ubc9 is the sole conjugating enzyme for sumoylation. We have shown that DNMT1 interacts with Ubc9 and interaction region mapped to residues 645-1113. This region contains two BAH domains (64). Proteins containing BAH domains are mainly involved in replication, methylation, and transcriptional regulation. For example, a yeast Orc1p (origin recognition complex subunit 1) is part of the origin replication complex, which directs DNA replication (69) and transcriptional silencing at the mating-type locus with another BAH domain containing protein Sir3p (silent information regulator 3) (70). The BAH domain of Drosophila Orc1 binds to HP1 (heterochromatin-associated protein 1) suggesting a role in the packaging chromatin fiber resulting in transcriptionally inactive (71). Also other methyltransferases, such as CMT1 (chromomethylase1) in *Arabidopsis thaliana* (72) and *Ascolbus immerses* DNA methyltransferase, masc2 (73) have BAH domains. Sumo modification of those proteins has not been reported. Our data showed for the first time that BAH domains are involved in the interaction with Ubc9. In addition, the BAH domain of DNMT1 is also involved in targeting DNMT1 to replication sites. Our ICM result showed that a mutant with residues 645 to 1616 was catalytically active in vivo, whereas deletions having only the catalytic domain were not. The activity of the 645-1616 mutant was less than wild type since we needed to treat cells with aza-dC for 24 h (usually only 1 h required with wild type). Since the 645-1616 mutant lacks a PCNA binding domain, we conclude that its heterochromatin targeting ability is impaired.

Considering the role of BAH domain in other proteins and our data together, it is possible that the sumoylation of DNMT1 might be associated with late-replicating events for several reasons. First, the replication of heterochromatin or repressed chromatin is a late S phase event (74). Second, the heterochromatin protein HP1 family interacts with DNMT1 and increases DNA methylation activity (75). Third, the BAH domain is clearly able to target the 645-1616 mutant to DNA and interact with Ubc9. Thus, sumoylation of DNMT1 is most likely involved when DNMT1 methylates DNA at heterochromatin regions. Supporting this idea, a recent study showed a high abundance of SUMOs in heterochromatin (76). Future study will be focused on dissecting the contribution of the BAH domain on sumoylation of DNMT1.

We have shown that all DNMT1 deletion mutants were sumoylation targets except for the 1-419 mutant; however, the 1-419 mutant lacks the Ubc9 interaction domain, which may explain the results. In addition, the DNMT1$^{\Delta E3\text{-}6}$ mutant had fewer SUMO1 modified bands compared to full length protein (Fig. 12) implying that there is at least one sumoylation site between residue 40 and 200. Interestingly, the DNMT1$^{\Delta E3\text{-}6}$ mutant contained one very robust SUMO1 site (Fig. 12 lane 2, marked as an asterisk). It is not clear whether the 40 to 200 deletion in DNMT1$^{\Delta E3\text{-}6}$ mutant caused the exposure of new sumoylation site or allows sumoylation machinery to access to target lysine residue more easily resulting in efficient sumoylation. Clearly, wild type DNMT1 and DNMT1$^{\Delta E3\text{-}6}$ mutant showed different sumoylation pattern. Spada et al. (66) reported that DNMT1$^{\Delta E3\text{-}6}$ mutant was trapped by aza-dC with two fold lower efficiency relative to wild type. Thus, it is possible that the sumoylation at a given lysine residue may facilitate DNA binding or enhance DNMT1 affinity for DNA.

Sumoylation regulates numerous biological functions, such as protein-protein interaction, enzyme activity, and subcellular localization (77). DNMT1 has a large N-terminal regulatory domain that can be further subdivided into two domains (78). The regulatory domain interacts with various proteins, like PCNA (6), DMAP1 (40), HDAC1 (79), and HDAC2 (40). It seems that N-terminal part of DNMT1 serves as a platform for the assembly of various proteins involved in chromatin condensation and gene regulation. We have shown that the sumoylation sites are distributed throughout DNMT1. Analysis of sumoylation in various deletion mutant s revealed three sites in the middle domain 412-1113, and 2 sites in the C-terminal catalytic domain (1114-1616). In addition, comparison of full length protein with $DNMT1^{\Delta E3-6}$ mutant implied that there might be one site in 1-419 mutant. Although we counted total six sumoylation sites in DNMT1, we could not rule out the possibility of additional secondary sites that appear only in the deletion mutants. Actually, four distinct slower migrating bands were detected with full length protein (Fig. 2A and Fig. 12). Interestingly, the catalytic domain showed weak interaction with Ubc9 and two sumoylated bands. However, the catalytic domain has no enzymatic activity as judged by ICM analysis. This result is in agreement with data published by other groups (78,80,81). Thus, it is not clear whether there are sumoylation sites in a catalytic domain of full length DNMT1 or its sumoylation is biologically relevant.

We and other groups have shown that DNMT1 can form a covalent complex with aza-dC incorporated DNA in vivo (11,66,82). Since aza-dC is a mechanism based inhibitor, trapping DNMT1 is a direct measure of methyltransferase activity. This property of aza-dC and purification of DNMT-DNA complex using CsCl gradient followed by antibody based detection, allowed us to quantify the post-translational modification and activity of DNMTs in cells (11). In the ICM assay, the separation of DNA bound protein from free proteins by CsCl gradient

centrifugation gives us highly purified DNMT-DNA complexes free of bulk nuclear proteins. The detection of a SUMO signal in the ICM assay measures the post-translational modification status of DNMT1 when it methylates its target, cytosine residue. We also showed that the SUMO1 signal as well as DNMT1 signal is very resistant to detergent and salt after aza-dC treatment by indirect immunostaining. Before fixation, cells were sequentially extracted by various detergents and salts. Most of DNMT1 is extracted by 0.47 M NaCl, but DNA bound DNMT1 still remained even after 2 M NaCl treatment. Also, SUMO1 immunostaining was dependent on the presence of DNMT1. These results are consistent with ICM data, in which an ionic detergent, sarkosyl, is used for cell lysis and disrupts the electrostatic protein-DNA and protein-protein complexes (11). DNA bound DNMT1 is not dissociated from the DNA even in high concentration of CsCl (5.8 M).

The ICM analysis of deletion mutants showed that a series of N-terminal deletion affect the targeting of DNMT1 and the minimum regulatory region for its localization to the target was mapped to two BAH domains. Previously, the BAH domain was shown to target DNMT1 to replication sites in a PCNA independent manner (5). In our study, we show that the BAH domain is needed to recruit the DNMT1 to its target site in cells.

Although SUMO E3 ligases are not required for sumoylation in vitro, SUMO E3 ligase may be important in regulating substrate specificity in vivo, particularly for substrates that lack consensus SUMO motifs. Indeed, we tested several SUMO consensus lysine residues, by mutating to arginine (including 148, 194, 675, 739, 957, 1135, and 1609), but we could not identify sumoylation sites of DNMT1. From this, we conclude that the sumoylation sites of DNMT1 reside in non-consensus SUMO motifs. We also showed that an E3 ligase (PIASy) specifically enhanced sumoylation of DNMT1. Co-expression of DNMT1 and PIASy along

with SUMO1 and Ubc9 further increased the level of DNMT1 sumoylation; however, sumoylation levels of immunoprecipitated DNMT1 were much less than that of bound DNMT1 in ICM assay. Since sumoylation is tightly regulated in temporal and spatial manner, target proteins are more likely to be modified when they are properly localized at correct time. Although overexpressed proteins may not be properly regulated in the cell, at least some should encounter favorable conditions. For DNMT1, it seems to be robustly sumoylated just prior to DNA binding with help from PIASy. In addition, DNA bound DNMT1 may retain its sumoylation status longer on DNA if desumoylation occurs after release from DNA. In agreement with idea, we observed a decreased level of DNA bound DNMT1 in the presence of a deconjugating enzyme (SENP1). Overexpression of SENP1 decreased the overall sumoylation level in whole cell extracts suggesting activity against other sumoylated proteins. Although it is not clear whether SENP1 is a specific SUMO protease for sumoylated DNMT1, overexpressed SENP1 clearly reduced the DNMT1 sumoylation and decreased the level of DNA bound DNMT1.

DNMT1 is the major DNA methyltransferase and plays a central role in the establishment of the epigenetic networks in mammalian cells. DNMT1 expression and its enzyme activity may be regulated at transcriptional and translational level. To establish epigenetic patterns, DNA methylation must be carefully controlled in any given situation. The regulation of DNA methylation by DNMT1 also requires interaction with many cellular proteins. Given the fact that DNMT1 interacts with numerous proteins, our understanding how DNMT1 is fine tuned is limited. In this regard, sumoylation of DNMT1 gives new insights.

DNA methylation patterns are often altered in cancer cells. Typically, cancer cells display a global reduction of overall methylation levels and local hypermethylation of certain

CpG islands. Perturbation of normal epigenetic regulatory patterns may contribute to tumorigenesis and DNMT1 is a good candidate for a role in this epigenetic change. Actually, DNMT1 levels are often elevated in cancer; however, this does not necessarily correlate with variations in DNA methylation. That is, it is not clear how changes in DNMT1 levels could cause global and regional hypomethylation. Thus, it is important to understand all aspects of DNMT1 regulation. A failure in sumoylation or desumoylation of the maintenance enzyme, DNMT1 could change its function and impact gene silencing profiles. It is also possible that the defects in sumoylation itself could alter tumorigenesis. Contrary to ubiquitylation, only one type of E1 and E2 enzyme is used in sumoylation. Thus, a defect or misregulation of E3 ligase enzyme and desumoylation enzyme are more likely involved in tumorigenesis. Supporting this idea, recently Cheng et al. (83) reported that one of the desumoylating enzyme, SENP1, plays a key role in the regulation of the hypoxic response through regulation of HIF1alpha stability. Thus, it is important to investigate the cellular components of sumoylation as well as DNMT1 in order to understand roles in maintaining the epigenetic patterns. Future studies will be aimed at finding the regulator of DNMT1 sumoylation and testing this idea.

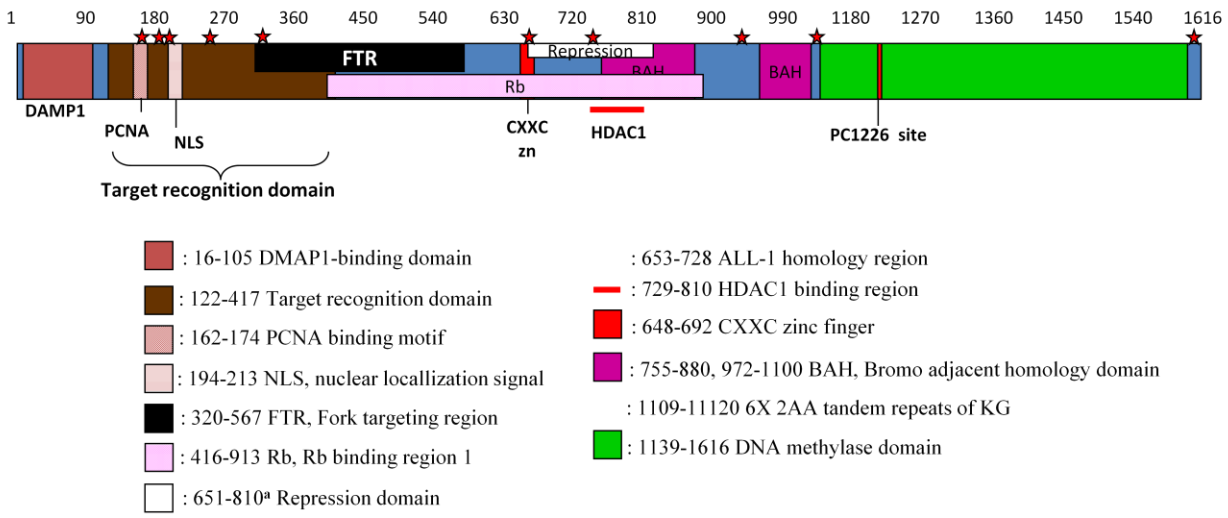

Figure 1 Domain structure of human DNA methyltransferase 1.

Figure 2 DNMT1 is sumoylated in vivo and in vitro.

In vivo analysis of DNMT1 sumoylation is shown in Panel A. V5 epitope tagged DNMT1 was co-transfected with HA-SUMO1 and Myc-Ubc9 expression vectors into HEK293FT cells. DNMT1-V5 was immunoprecipitated (IP) from the transfected whole cell extracts (WCE) using anti-V5 antibody, as described in the "Material and Methods". Bound proteins are resolved on a SDS-PAGE gel, then subjected to western blotting with anti-HA11 antibody to detect HA-SUMO1. The in vitro sumoylation of DNMT1 is shown in Panel B. In vitro sumoylation reactions were carried out in the presence of 500 ng purified DNMT1, 900 ng SAE1/SAE2, 620 ng Ubc9, 5 mM ATP, and 1.25 μg of SUMO1. The reactions were loaded onto a SDS-PAGE, transferred to membrane and stained with a PonceuS dye (right panel) or probed with anti-SUMO1 antibody (left panel).

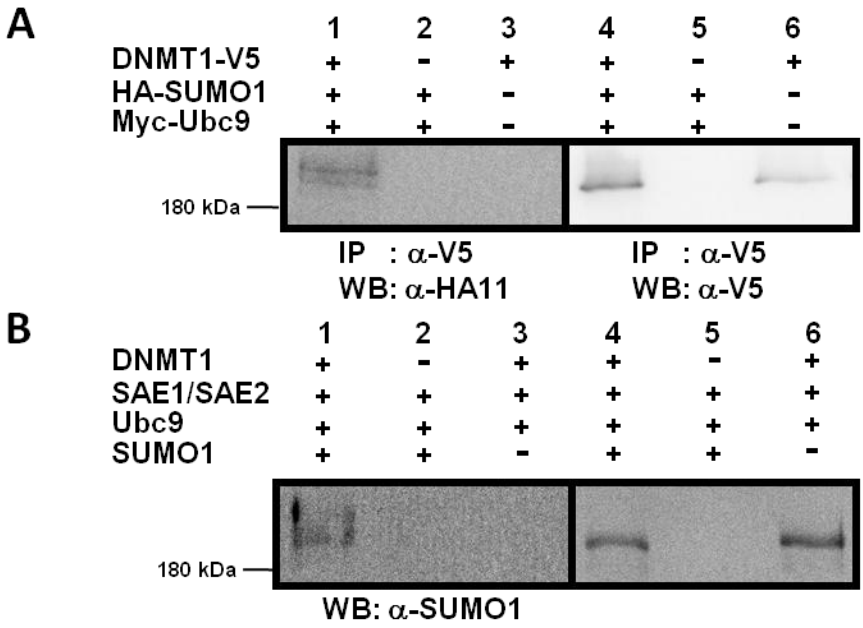

Figure 2 DNMT1 is sumoylated in vivo and in vitro.

Figure 3 DNMT1 is sumoylated in the Sf9 cells.

Panels A and B show the in vivo sumoylation of DNMT1 or topo1 in Sf9 cells with a reconstituted sumoylation system. Approximately 10^6 cells were infected with recombinant baculoviruses expressing SUMO1 (input multiplicity of infection (MOI) of 3), Ubc9 (MOI of 3), and DNMT1 (MOI of 1) or topo1 (MOI of 2). At 72 h post-infection, the whole cell extracts were prepared. SUMO conjugated proteins were immunoprecipitated with anti-SUMO1 antibody (Santa Cruz) and recovered polypeptides were analyzed by western blotting with anti-DNMT1 antibody to monitor the formation of sumoylated DNMT1 (Panel A) or topo1 (Panel B).

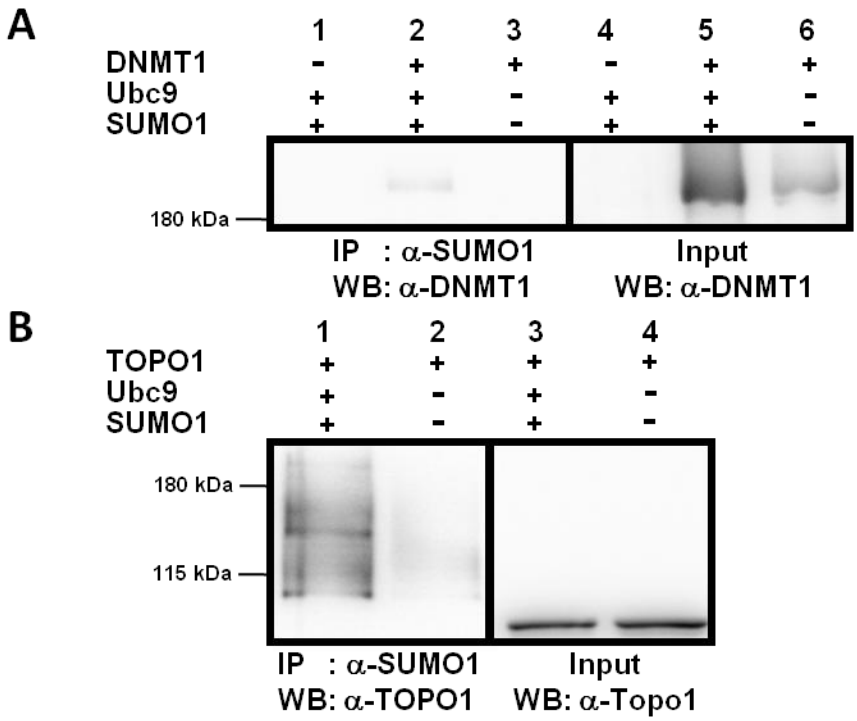

Figure 3 DNMT1 is sumoylated in the Sf9 cells.

Figure 4 Sumoylation of endogenous DNMT1.

Sumoylation of endogenous DNMT1 is shown. DNMT1 (A) or all SUMO1 conjugates (B) were immunoprecipitated from the nuclear extracts of HCT116 WT or *dnmt1*$^{-/-}$ cells. Bound proteins were analyzed by western blotting using anti-SUMO1 (A) or anti-DNMT1 (B) antibody.

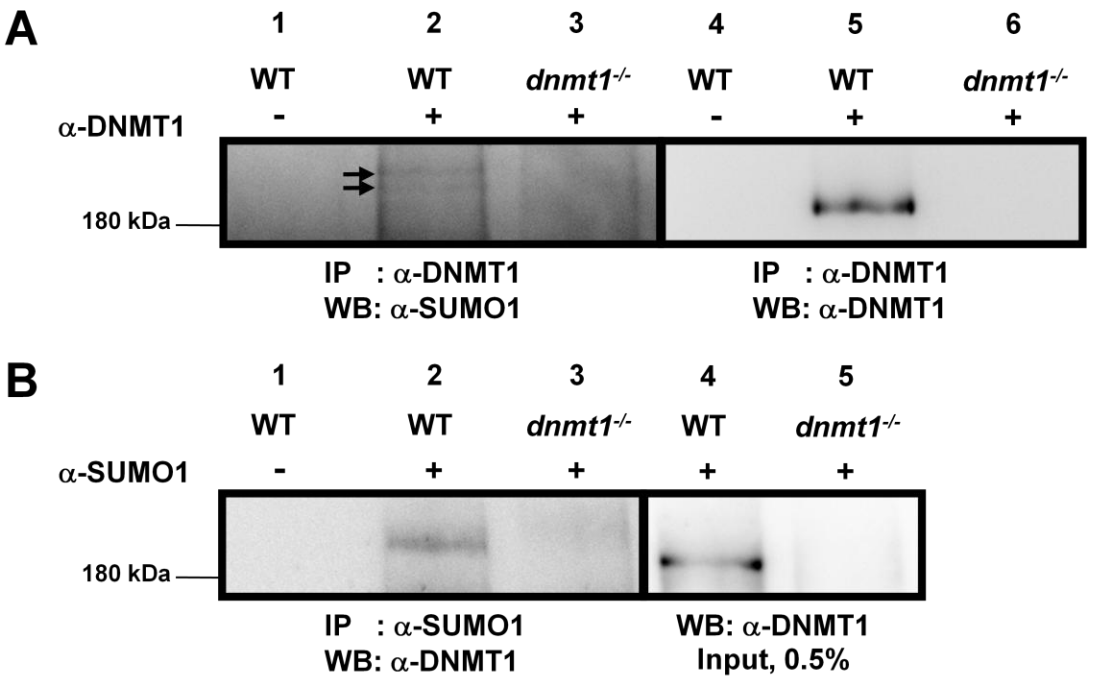

Figure 4 Sumoylation of endogenous DNMT1.

Figure 5 DNMT1 interacts with Ubc9.

DNMT1-V5 was co-transfected with Myc-Ubc9 into HEK293FT cells (Panel A). Myc-Ubc9 was immunoprecipitated from the transfected whole cell extracts with anti-Myc antibody. The immunoprecipitates was analyzed by western blotting using anti-V5 antibody (left panel). DNMT1-V5 was immunoprecipitated and bound proteins were analyzed (right panel). Panel B depicts a schematic representation of V5 epitope tagged DNMT1 deletion mutants. Panel C tests for interactions of each DNMT1 deletion mutant with Ubc9. Each of the DNMT1 deletion mutants was co-transfected with Myc-Ubc9 into HEK293FT cells. Whole cell extracts were immunoprecipitated with anti-V5 antibody and precipitated proteins analyzed by western blotting with anti-Myc antibody to probe co-immunoprecipitated Ubc9 or with anti-V5 antibody to measure the total recovery of each deletion mutant (left panel). Band intensities were quantified using the GeneTools program (SynGene, Cambridge, UK). The amount of co-immunoprecipitated Ubc9 was normalized by the amount of immunoprecipitated deletion mutant and plotted (right panel). The statistical data are based on three independent experiments.

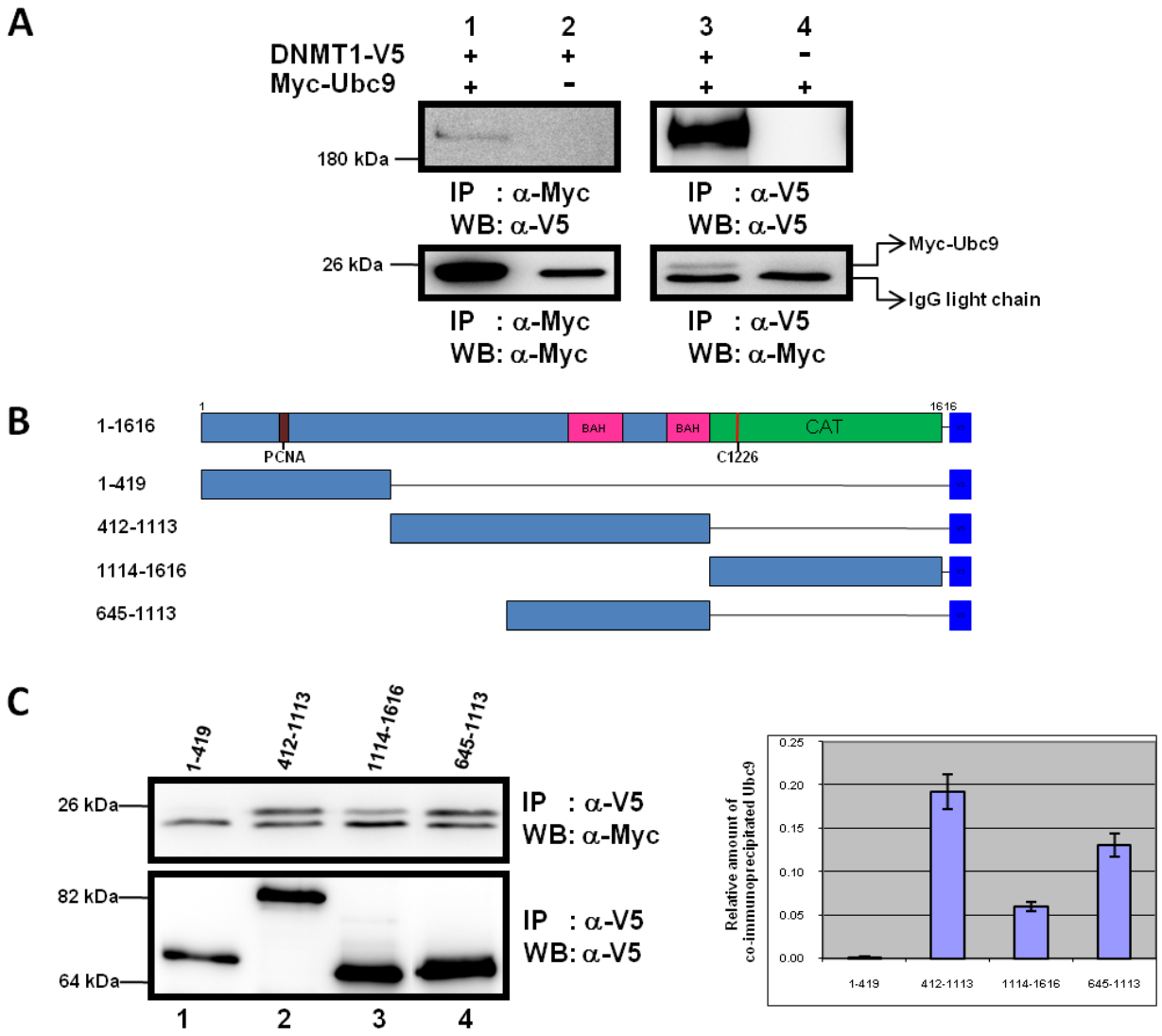

Figure 5 DNMT1 interacts with Ubc9.

Figure 6 Sumoylation of each DNMT1 deletion mutants in vivo.

Each V5 epitope tagged DNMT1 deletion mutants was co-transfected with HA-SUMO1 and Myc-Ubc9 into HEK293FT cells. DNMT1 deletion mutants were immunoprecipitated with anti-V5 antibody. The equal amounts of beads were aliquoted into two tubes and washed extensively with 0.5X or 1X RIPA buffer. Washing with 1X RIPA buffer is more stringent condition, allowing us to distinguish the non-specific bands. Immunoprecipitates were resolved on a SDS-PAGE gel, then subjected to western blotting with anti-HA11 antibody to detect HA-SUMO1. Arrow heads indicate the sumoylated form of each mutant and asterisks indicate non-specific bands.

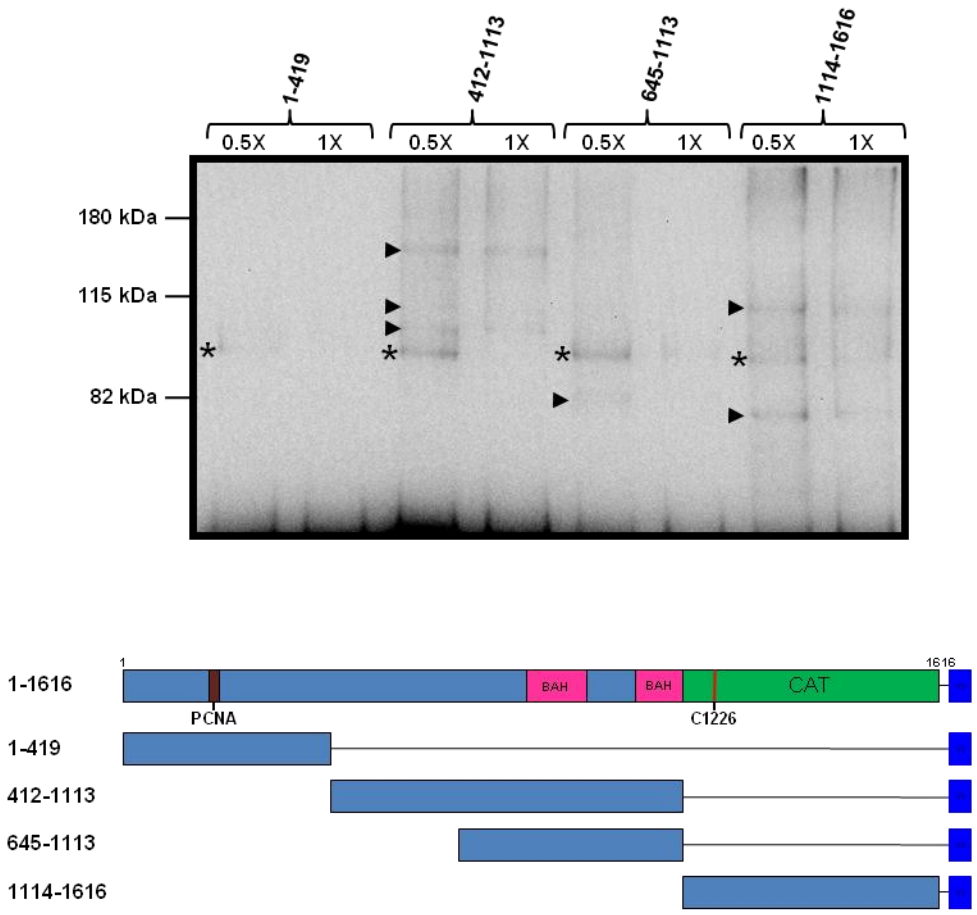

Figure 6 Sumoylation of each DNMT1 deletion mutants in vivo.

Figure 7 Schematic representation of DNA methylation.

(A) A covalent intermediate is formed between cytosine and the enzyme during the catalytic reaction. Then a methyl group is transferred from S-adenosyl-L-methionine (AdoMet) followed by the release of DNMT. (B) Proposed mechanism when 2'-deoxycytidine is replaced by the 5-aza-2'-deoxycytidine (aza-dC). The absence of proton at the N5 position of the aza-dC base ring prevents β elimination resulting in trapped DNMT.

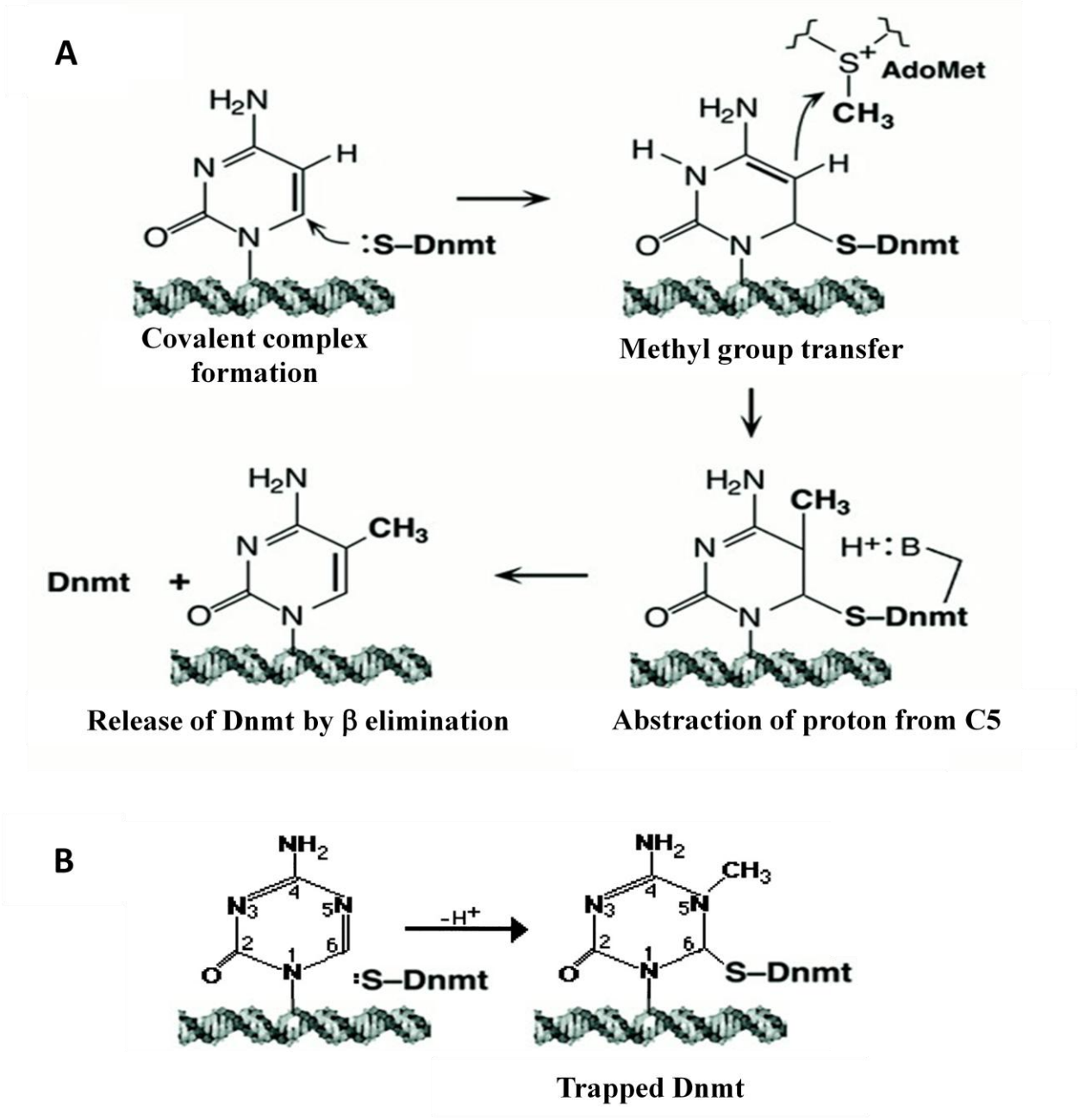

Figure 7 Schematic representation of DNA methylation

Figure 8 ICM assay for the sumoylation of DNMT1 in HCT116 and HCT116 *dnmt1*$^{-/-}$ cells.

Panel A shows the ICM assay results with wild type and mutant cell lines. Approximately 4 X 10^6 cells were treated or untreated with 10 μM aza-dC for 1 h. DNA was banded in CsCl density buoyant gradient and the gradient was fractionated as described in "Material and Methods". Individual fractions were slot blotted onto membranes and probed with proper antibody. (B) Slot blot of DNA pools. DNA fractions were pooled and its concentration was measured. Either 0.3, 0.6, or 0.9 μg of DNA was slot blotted onto a membrane, which was probed with DNMT1 antibody or SUMO1 antibody.

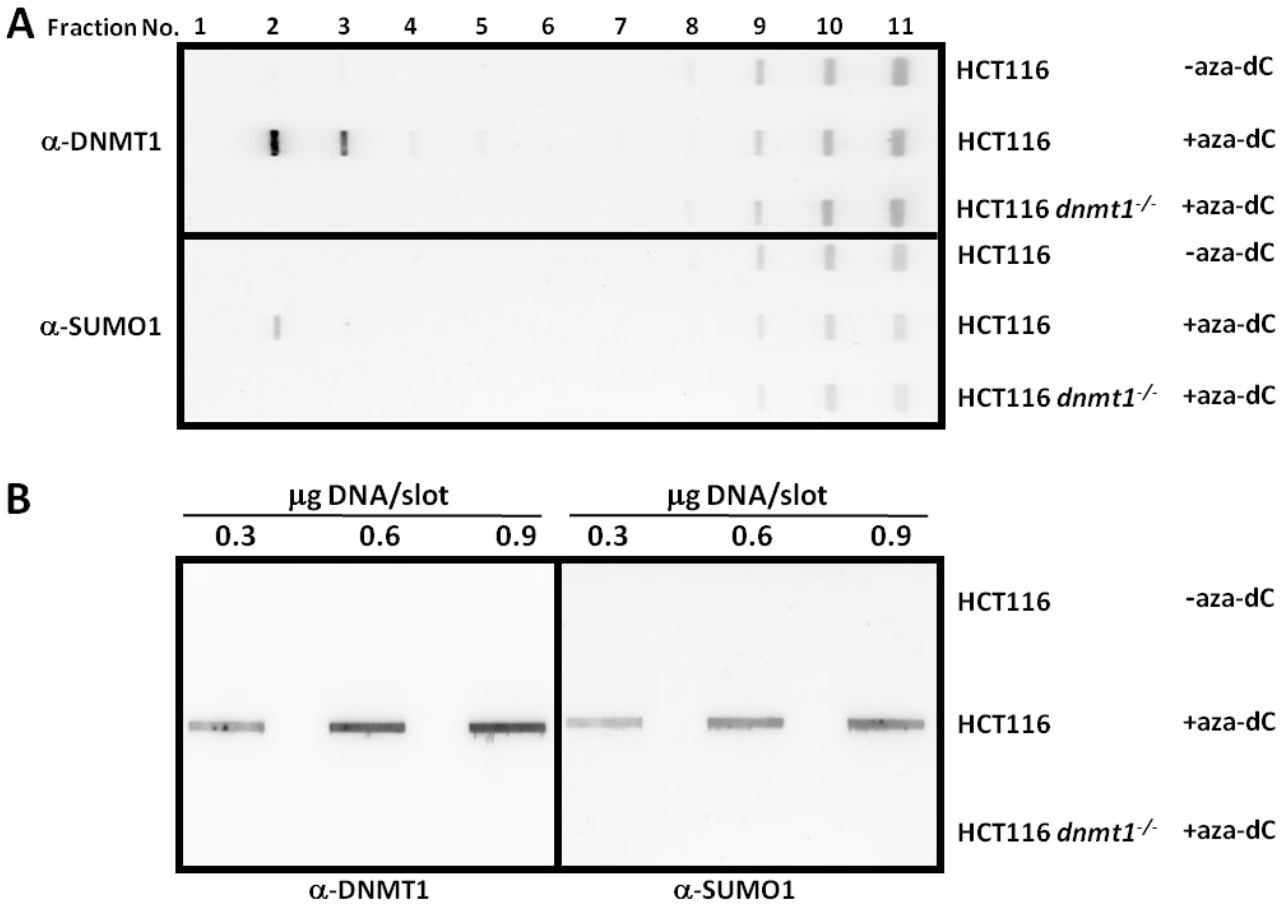

Figure 8 ICM assay for the sumoylation of DNMT1 in HCT116 and HCT116 *dnmt1*$^{-/-}$ cells.

Figure 9 ICM assay with transiently transfected HCT116 *dnmt1*$^{-/-}$ cells.

HCT116 *dnmt1*$^{-/-}$ cells were transfected with DNMT1-V5, HA-SUMO1, and Myc-Ubc9 and treated or untreated with 10 μM aza-dC for 1 h. Some of cells were transfected with DNMT1-V5 C1226A, DNMT3a-V5, or HA-SUMO1-AA. DNA fractions were pooled and either 0.3, 0.6, or 0.9 μg of DNA was slot blotted onto a membrane. The membrane was probed with anti-V5 antibody to detect DNA bound DNMTs or with anti-HA11 antibody to detect HA-SUMO1.

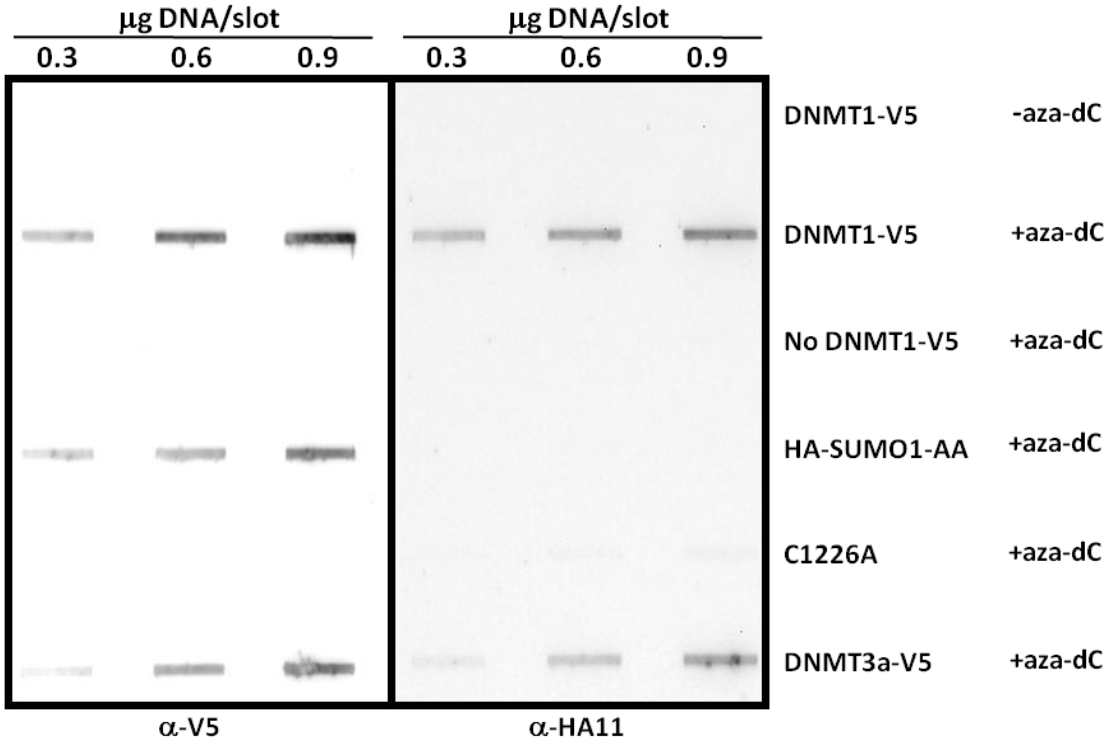

Figure 9 ICM assay with transiently transfected HCT116 *dnmt1*$^{-/-}$ cells.

Figure 10 ICM assays of DNMT1 and DNMT1$^{\Delta E3\text{-}6}$ in HCT116 *dnmt1*$^{-/-}$ cells.

(A) Schematic representation of V5 epitope tagged DNMT1 and DNMT1$^{\Delta E3\text{-}6}$.

(B) ICM assay results. HCT116 *dnmt1*$^{-/-}$ cells were transiently transfected with V5 tagged DNMT1 or DNMT1$^{\Delta E3\text{-}6}$, along with HA-SUMO1 and Myc-Ubc9. After 24 h post-transfection, cells were treated with 5 μM aza-dC for 24 h or treated with 10 μM aza-dC for 1 h after 47 h post-transfection. DNA fractions of CsCl gradient were pooled and slot blotted onto membranes and probed with anti-V5 antibody or anti-HA11 antibody.

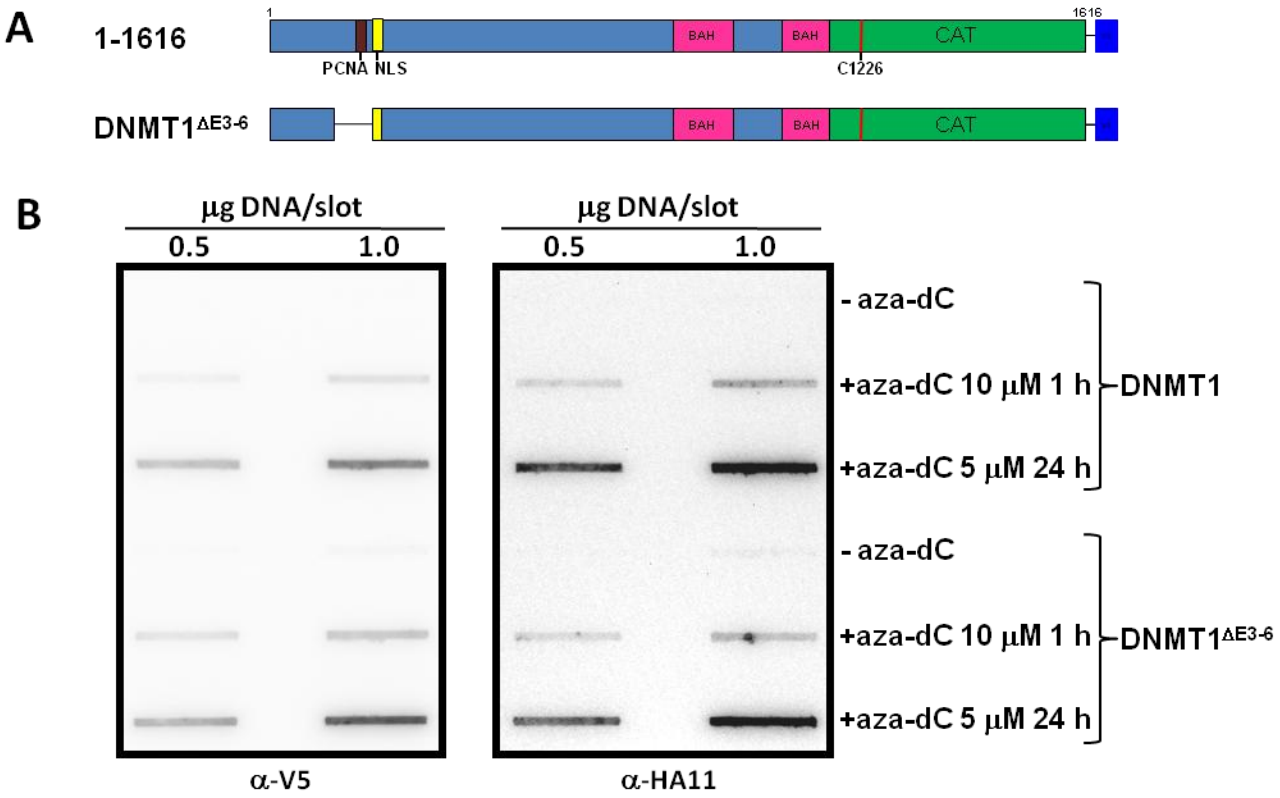

Figure 10 ICM assay of DNMT1 and DNMT1$^{\Delta E3-6}$ in HCT116 *dnmt1*$^{-/-}$ cells.

Figuer 11 ICM assay of DNMT1 deletion mutants in HCT116 *dnmt1*$^{-/-}$ cells.

(A) Schematic representation of V5 epitope tagged DNMT1 deletion mutants for ICM assay.

(B) ICM assay results. HCT116 *dnmt1*$^{-/-}$ cells were transiently transfected with V5 tagged each deletion mutants, HA-SUMO1, and Myc-Ubc9. After 24 h post-transfection, cells were treated with 5 μM aza-dC for 24 h. DNA fractions of CsCl gradient were pooled and slot blotted onto membranes and probed with anti-V5 antibody or anti-HA11 antibody.

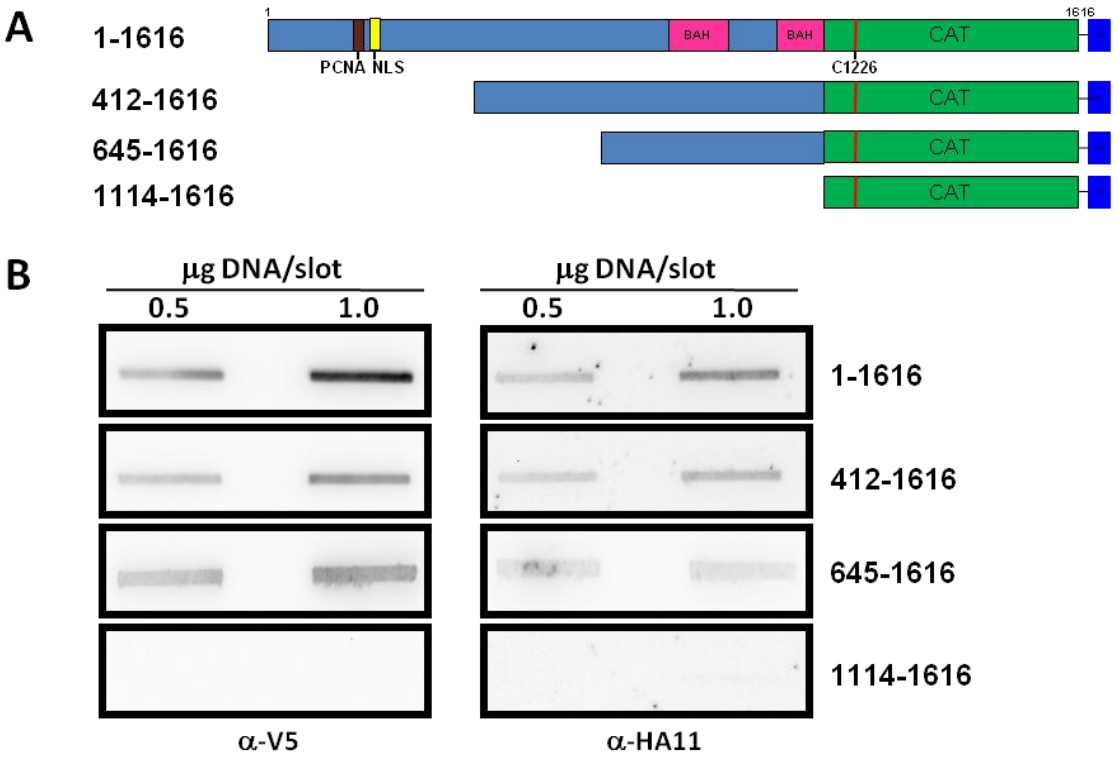

Figure 11 ICM assay of DNMT1 deletion mutants in HCT116 *dnmt1*$^{-/-}$ cells.

Figure 12 DNMT1 and DNMT1$^{\Delta E3-6}$ are sumoylated in vivo.

V5 epitope tagged DNMT1 or DNMT1$^{\Delta E3-6}$ was co-transfected with HA-SUMO1 and Myc-Ubc9 expression vector into HEK293FT cells. DNMT1-V5 or DNMT1$^{\Delta E3-6}$-V5 was immunoprecipitated from the transfected whole cell extracts with anti-V5 antibody. The bound proteins are resolved on a SDS-PAGE gel, then subjected to western blotting with anti-HA11 antibody to detect HA-SUMO1.

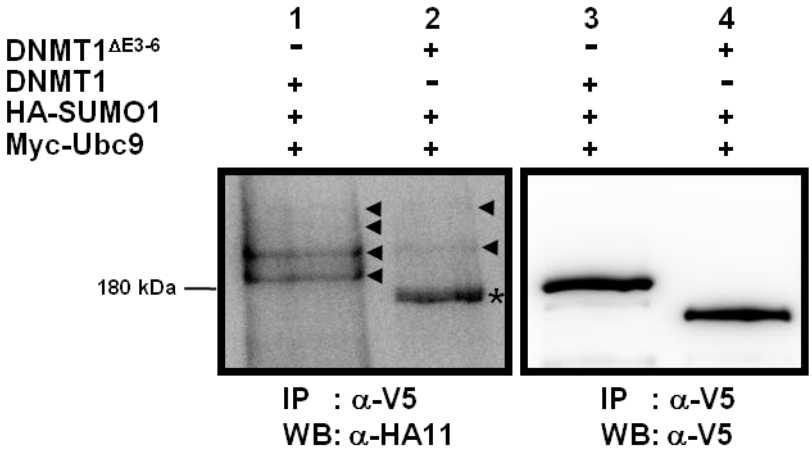

Figure 12 DNMT1 and DNMT1$^{\Delta E3\text{-}6}$ are sumoylated in vivo.

Figure 13 DNMT1 and SUMO1 are resistant to various extractions in aza-dC treated cells.

HeLa cells were transfected with DNMT1-V5, HA-SUMO1, and Myc-Ubc9. Cells were grown on the cover slip with or without 5 μM aza-dC for 24 h and cells were treated with detergents and salts sequentially before fixation. Transfected HeLa cells were stained with anti-V5 antibody to detect DNMT1-V5 and anti-SUMO1 antibody (Abcam, Y199) to detect HA-SUMO1 as well as endogenous SUMO1. The nuclei were stained with Topro3. Column A shows images from directly fixed cells and B, C, D show images from after extraction with 0.2% TritonX-100, extraction buffer, and 2 M NaCl, respectively. Merge image was generated with all three images and a differential interference contrast (DIC) image. Images were obtained on a Zeiss LSM510 confocal microscope.

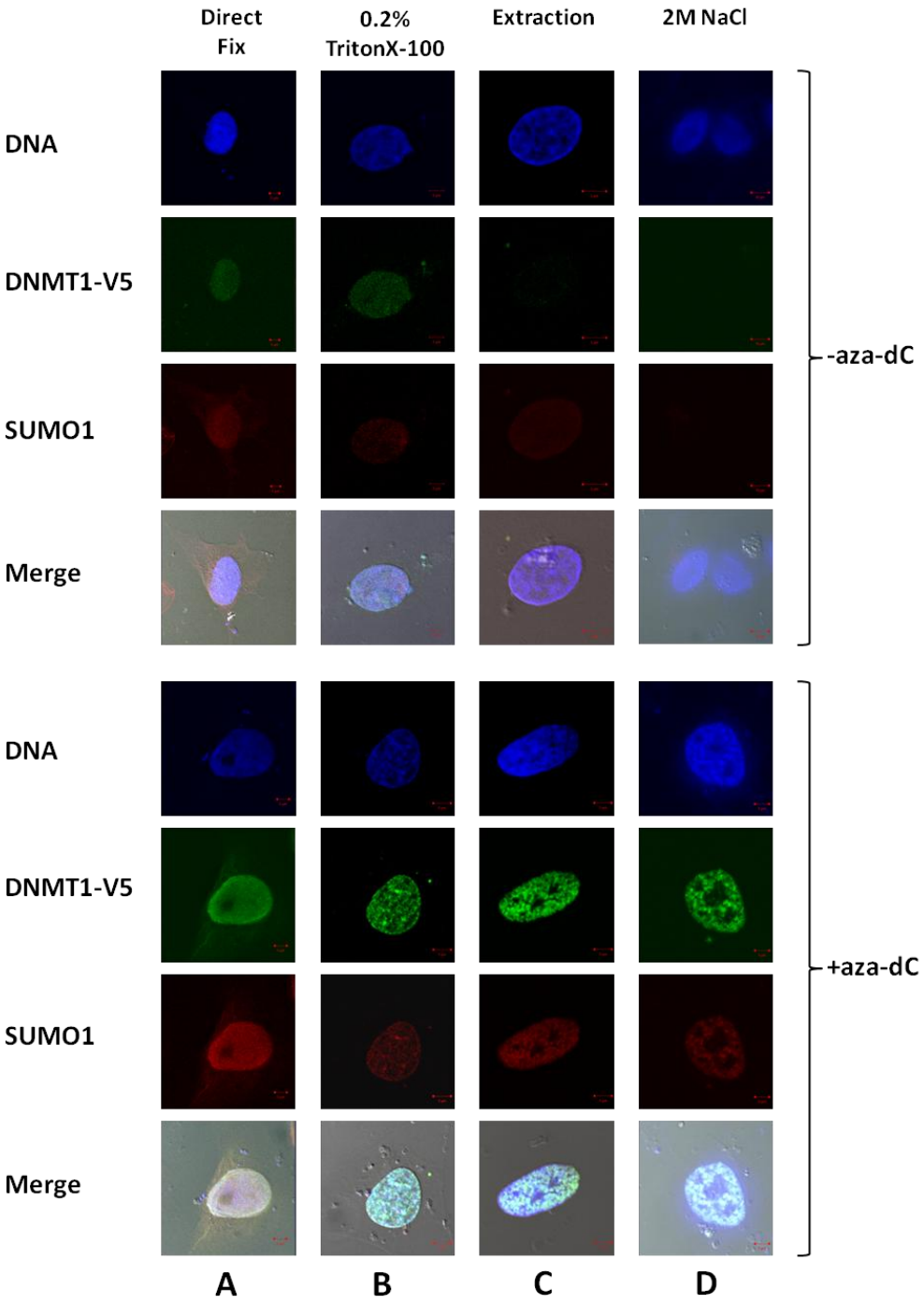

Figure 13 DNMT1 and SUMO1 are resistant to various extractions in aza-dC treated cells.

Figure 14 DNA methyltransferase activity of sumoylated DNMT1.

(A) In vitro sumoylation of DNMT1 with SUMO1 or its mutant SUMO1-AA. Reaction mixture was resolved on SDS-PAGE and subjected to western blotting using anti-SUMO1 antibody. The arrows indicate sumoylated DNMT1.

(B) DNA methyltransferase activity of sumoylated (black bars) or non-sumoylated (gray bars) DNMT1. Values are average ± SD of three independent experiments. Reactions contained identical concentrations of various proteins (DNMT1, SAE1/2, Ubc9, SUMO1 or SUMO1-AA mutant) as described in "Material and Methods". Methyl group (CH_3) incorporation was corrected for background (in reactions lacking DNMT1) and radioactive incorporation was converted into pmoles of the methyl group ([methyl-^{3}H]-SAM of 10 Ci/mmol). Control reactions with WT SUMO1 demonstrate that approximately 5% of the total DNMT1 is SUMO1 modified under the conditions of the in vitro reaction. To determine the influence of SUMO1 on methylase activity, we assume that non-SUMO1 modified DNMT1 is methylating the substrate in both reactions and that any difference between these two reactions is a direct result of sumoylation. This difference was adjusted for the efficiency of the sumoylation reaction. Statistical analysis was carried out using t-test (*: $P<0.005$, **: $P<0.0001$, and ***: $P<0.05$).

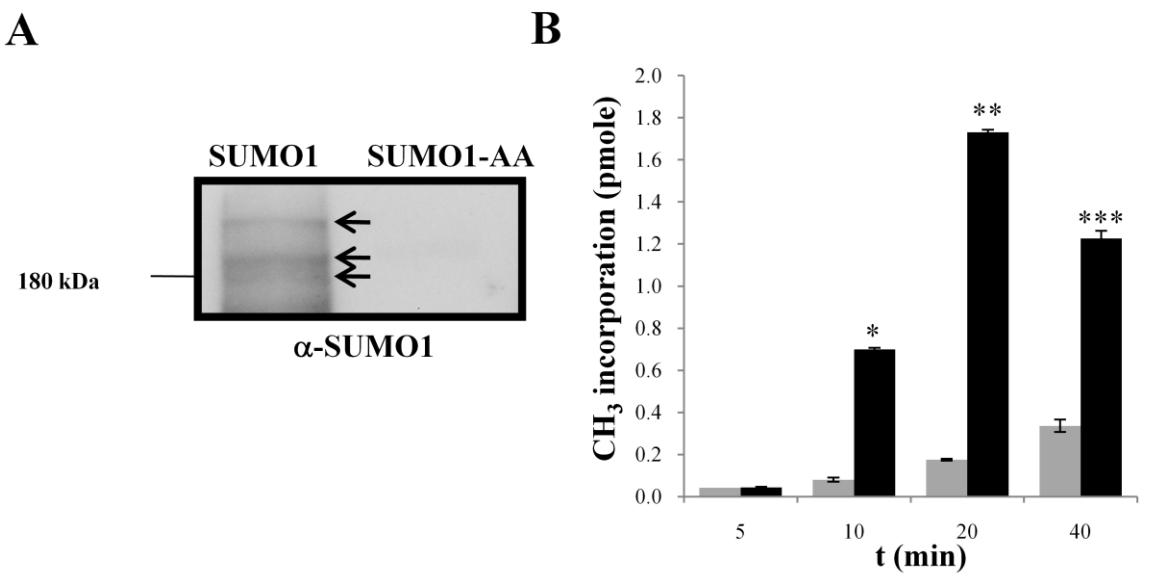

Figure 14 DNA methyltransferase activity of sumoylated DNMT1.

Figure 15 Sumoylation of DNMT1 increases the DNA binding efficiency of DNMT1 in vivo.

ICM assay with transiently transfected HEK293FT cells. Cells were transfected with DNMT1-V5, HA-SUMO1, Myc-Ubc-9, and HA-SENP1 or HA-PIASy. After 24 h transfection, cells were treated with 10 μM aza-dC for 1 h. DNA fractions (0.5 μg) were slot blotted onto membrane and probed with anti-DNMT1 or anti-HA11 antibody. Band intensities were quantified using the GeneTools program (SynGene, Cambridge, UK) and right panel shows the relative level of each band from slot blot. The statistical data are based on three independent experiments.

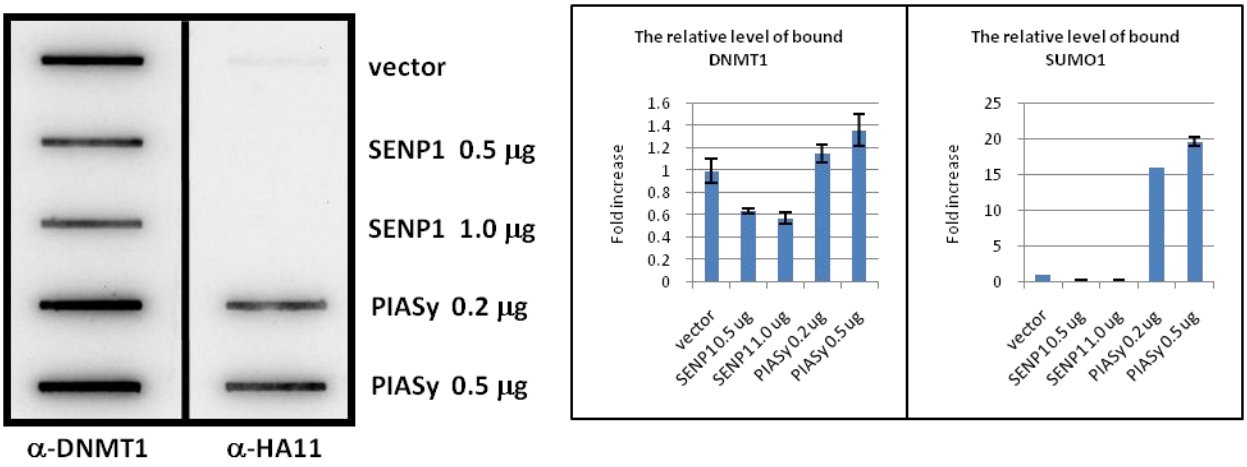

Figure 15 Sumoylation of DNMT1 increases the DNA binding efficiency of DNMT1 in vivo.

Figure 16 DNMT1 interacts with SENP1 and PIASy.

HEK293FT cells were transfected with DNMT1-V5, HA-SUMO1, Myc-Ubc-9, and HA-SENP1 (A) or HA-PIASy (B). DNMT1-V5 was immunoprecipitated from the transfected whole cell extracts using anti-V5 antibody. Bound proteins are resolved on a SDS-PAGE gel, then subjected to western blotting with anti-HA11 antibody to detect co-immunoprecipitated HA-SENP1 or HA-PIASy along with HA-SUMO1 modified DNMT1-V5 (bracketed). Arrow heads indicate the co-immunoprecipitated HA-SENP1 and HA-PIASy, respectively.

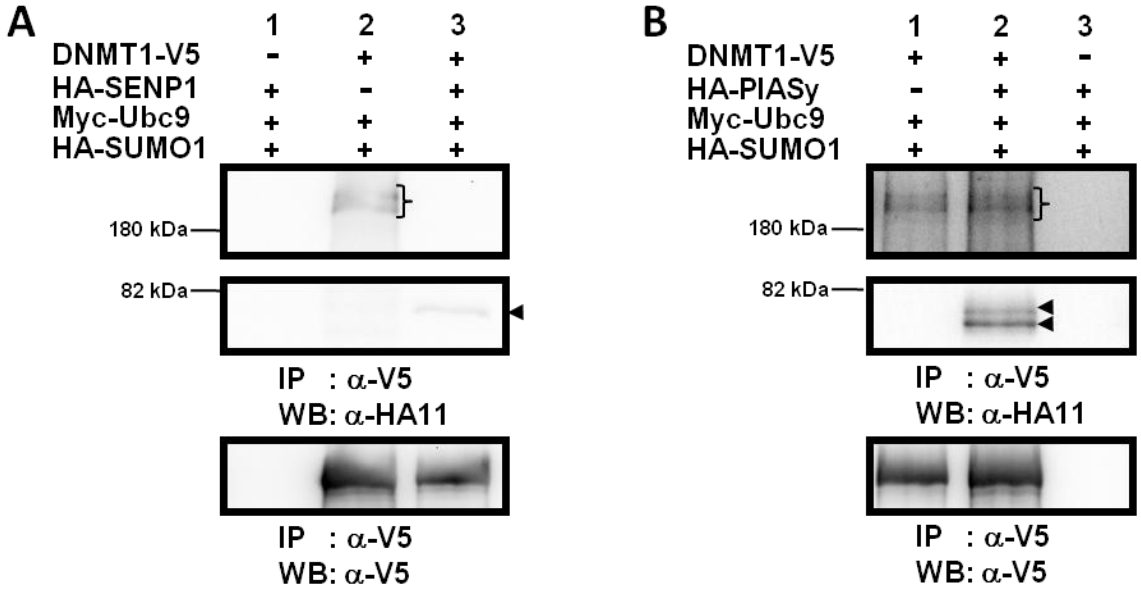

Figure 16 DNMT1 interacts with SENP1 and PIASy.

CHAPTER 2: THE ROLE OF DNMT1 IN HOMOLOGY DIRECTED DNA REPAIR

2.1 Introduction

The DNA within our cells is continually being exposed to cellular metabolites and exogenous DNA-damaging agents. Such damages could cause cell death or degenerative changes in the cells. Of the various forms of DNA damage, the most dangerous are DNA double-strand breaks (DSBs). DSBs are generated when each of the two strands of the DNA double helix are broken simultaneously at the sites that are sufficiently close enough to one another. Therefore, the two DNA ends become physically separated from one another. This dissociation may create serious problems arising from inappropriate recombination, thereby leading to chromosomal translocations (84).

To deal with the threats posed by DSBs, cells have developed multiple mechanisms to detect, signal, and repair the regions. Two main pathways, homologous recombination (HR) and non-homologous end-joining (NHEJ), are involved in the repair of DSBs. In prokaryotes, HR has been known to be a major pathway for the repair of DSBs, while in mammals, NHEJ was thought to be preferred; however, more recently, HR has also been shown to be a major pathway in mammals (85). These pathways are largely distinct from one another and function in complementary ways (86-88). NHEJ involves the ligation of two DNA ends without homology and is error prone because no undamaged DNA is templated. In contrast, HR uses an intact DNA as a template for DSB repair and it is more or less error free. Thus, the second DNA molecule having a sequence homology to the damaged region should be available in HR. In this process, often called gene conversion, a donor DNA sequence with homology to both sides of the DSB supplies genetic information to repair the DSB (89,90). The homologous sequence is copied into the broken locus, making the repaired locus an exact copy of donor sequence,

without altering the donor sequence. Cancer cells often defective in HR exhibit aneuploidy, chromosomal rearrangements, and chromosomal instability. For example, cell lines having defects in HR show high rates of spontaneous chromosomal abnormalities (91,92). In addition, NHEJ suppresses chromosomal aberrations, as well as malignant transformation (93,94). Thus, it has been proposed that failure to repair of DSB may cause a cell's malignant transformation.

Several reports implicate DNA methylation in DNA damage repair. 1) DNMT1 and proliferating cell nuclear antigen (PCNA) form a complex and DNMT1 is recruited to DNA repair sites by PCNA (6,95). 2) Mouse embryonic stem cells lacking Dnmt1 are genetically unstable due to mitotic recombination or chromosomal loss accompanied by duplication (96). 3) DNA damage induced by oxidative stress is accompanied by gene silencing (97). DNA methylation is a covalent modification of genomic DNA. In mammals, methylation occurs mostly on the cytosine residues of CpG dinucleotides, in which a methyl group is added to C5 position of cytosine ring by DNA methyltransferases. DNA methylation often induces a transcriptionally silent state of methylated regions (98). DNA methylation interferes transcription by preventing binding of basal transcription machinery or other transcription factors that require contact with cytosine residues. There are two types of DNA methylation, stable and metastable methylation. Stable methylation is inherited through generations in a male- or female-specific fashion. In contrast, metastable methylation is variable and generates different methylation patterns among individual cells and cell types. It is modified by environment and changes during the lifetime of individual cells.

Here in this study, we investigate the metastable methylation caused by DNA damage. Several reports support an association between DNA methylation and DNA repair. We investigated this association using the mammalian system designed by M. Jasin (92). In this

system, recombination between two defective GFP genes is induced by a double strand break (DSB) (Fig. 17). The recombination products can be analyzed by direct analysis of repaired genes using PCR, or by the presence of a functional green fluorescent protein (GFP). We show that homologous recombination often induces methylation of the repaired DNA resulting in silences of the recombined gene. This induced methylation is accomplished by the de novo methyltransferase activity of DNMT1.

We propose that methylation accompanied by homology-directed repair marks the repaired DNA region and protects cells against unregulated gene expression.

2.2 Material And Methods

2.2.1 Cell Culture

HeLa-DRGFP stable lines were cultured in RPMI medium supplemented with 10% fetal bovine serum (Invitrogen). HCT116-DRGFP and HCT116 *dnmt1*$^{-/-}$-DRGFP stable lines were cultured in DMEM medium with 10% fetal bovine serum (Invitrogen). The cell lines were grown at 37 ℃ in 5% CO_2.

2.2.2 Stable and Transient Transfection

HeLa-DRGFP or HCT116 based stable lines were transfected with lipofectamine2000 as recommended by the manufacturer (Invitrogen) with 2 μg of circular pDR-GFP plasmid and selected in the presence of puromycin (2 μg/ml). Puromycin-resistant colonies were seeded at 3 X 10^5 cells per 60 mm plate and transfected with 2 μg I-SceI plasmid DNA on the following day by lipofectamine transfection (Invitrogen). Cells were harvested 2 or 4 days after transfection.

2.2.3 Drug Treatments

DRGFP stable cells were transfected with control vector or I-SceI plasmid and 24 h later, Plates with low confluency were incubated with 1 μM or 5 μM of 5-aza-2'deoxycytidine (aza-dC) for 2 or 3 days. Every 24 h, the medium containing aza-dC was changed.

2.2.4 Genomic DNA Extraction

Genomic DNA was purified using QIAamp DNA mini kit (QIAGEN) according to the protocol provided by the manufacturer. DNA concentration was measured by UV spectroscopy.

2.2.5 PCR for Screening a Clone of Stable Cell Line

PCR was performed in a 20 µl reaction mixture containing 500 ng of genomic DNA, 2 µl of 10X PCR buffer, 1.5 mM $MgCl_2$, 0.3 mM dNTP, 1 unit of HotStarTaq polymerase (QIAGEN) and 5 µM of each primer. The following primers were used. UnRec, GCTAGGGATAACAGG GTAAT, Rec GAGGGCGAGGGCGATGCC, 3'-common, TGCACGCTGCCGTCCTCG (443 bp amplified fragment); β-actin/R AAAGCCATGCCAATCTCATC, β-actin/L GATCATTGCT CCTCCTGAGC (250 bp amplified fragment). Amplifications were performed in a Mastercycler (Eppendorf) using the following program: 95 ℃ /5 min x 1 cycle, 95 ℃ /45 sec, 52.5 ℃ (for Unrec) or 65.1 ℃ (for Rec) /30 sec, 72 ℃ /1 min, x 40 cycles; 72 ℃/10 min x 1 cycle. 4-8 µl of the PCR products were applied to a 2.0% agarose gel and visualized by ethidium bromide staining.

2.2.6 Flow Cytometry Analysis for GFP Positive Cells

DRGFP stable cells were transfected with I-SceI or control plasmid and after 2 or 4 days were treated with trypsin and collected. After two washes with PBS, cells were resuspended in 500 µl of PBS 1X. $6x10^4$ cells were analyzed using FACSCalibur (BD Biosciences).

2.2.7 Western Blotting

Whole cell extracts were prepared by lysing cells in RIPA buffer (1X PBS pH 7.5, 1% NP-40, 0.5% deoxycholate, 0.1% SDS, 10% glycerol) containing 1X protease inhibitor cocktail (Roche). Protein concentration was measured using Protein assay kit (Bio-Rad). Whole cell extracts were resolved on SDS-PAGE followed by western blotting. Antibodies used were as follows: anti-GFP (Santa Cruz), and anti-HA11 (Covance).

2.2.8 Chromatin Immunoprecipitation

HeLa-DRGFP cells (typically $7X10^5$ cells) were seeded in a 6-well plate one day before transfection. Cells were transfected with 2 μg of I-SceI plasmids using lipofectamine2000 (Invitrogen). Cells were plated in a 150 mm plate after 24 h and incubated further with 1 μM of aza-dC (sigma) for 24 h, or 48 h. The medium and aza-dC were changed every 24 h. Cells were harvested and GFP positive cells were scored by fluorescence-activated cell sorting (FACS). Remaining cells were stored at -80 ℃ for further usage.

Chip-IT Express kit (Active motif, CA USA) was used for Chip experiment. Since cells were treated with aza-dC for making DNA-DNMT complex, formaldehyde cross linking and reverse cross linking steps were omitted. Cells (~1 X 10^7) were resuspended in 0.5 ml ice-cold lysis buffer supplemented with 2.5 μl protease inhibitor cocktail (PIC, kit provided) and 2.5 μl of 100 mM PMSF. After 30 min incubation on ice, cells were homogenized with dounce homogenizer (10 strokes) and nuclei were collected. The nuclei were resuspended in 0.5 ml of digestion buffer (kit provided) and incubated at 37 ℃ for 10 min with 25 μl of enzymatic shearing cocktail (200 U/ml, kit provided). The reaction was stopped by adding 10 μl of 0.5 M EDTA. The sheared chromatin was stored at -80 ℃. An aliquot of sheared chromatin was further treated with proteinase K, extracted with a phenol/chloroform, and precipitated to determine DNA concentration and shearing efficiency (input DNA).

Chip reaction was set up according to manufacturer's guide (Active motif, CA USA). Briefly, the sheared chromatin (corresponding to 18 μg of DNA) was mixed with Protein G magnetic beads and 2 μl of anti-DNMT1 antibody (NEB) or 0.8 μg of normal rabbit IgG (Santa

Cruz). The reaction mixture was incubated at 4 ℃ for 48 h. Beads were washed with wash buffer (kit provided) and immunoprecipitated DNA was recovered.

PCR for Rec was performed in a 20 μl reaction mixture containing 5 μl (for Rec) or 1 μl (for Unrec) of recovered DNA, 0.2 mM dNTP, 1.25 unit of HotStarTaq polymerase (QAIGEN), and 5 μM of each primer. Amplifications were performed using a following program: 95 ℃ /15 min X 1 cycle, 95 ℃ /45 sec, 65.1 ℃ (for Rec) or 52.5 ℃ (for Unrec)/30 sec, 72 ℃/1 min X 40 cycles, 72 ℃ 10 min X 1 cycle. PCR for input DNA was performed in a 20 μl reaction mixture containing 100 ng of input DNA. Amplifications were performed for 30 cycles.

To verify the Chip results, the following primers were used for PCR; hMGMT-F, GAGTCAGGCTCTGGCAGTGT, hMGMT-R, GAGCTCCGCACTCTTCCGG (813 bp, amplified fragment), p16-F, GCAGTCCGACTCTCCAAAAG, p16-R, AGCCAGTCAGCCGA

AGGC (778 bp amplified fragment). Amplifications were performed using a following program: 95 ℃ /5 min X 1 cycle, 95 ℃ /45 sec, 50 ℃ /30 sec, 72 ℃ /1 min X 40 cycles, 72 ℃ 10 min X 1 cycle.

2.2.9 Bisulfite DNA preparation and PCR

Sodium bisulfite analysis was carried out essentially as described by Frommer et al. (99). Total DNA (8 μg) was digested with EcoRI restriction enzyme (NEB), and denatured in 0.3M NaOH for 15 min at 37 ℃ in a volume of 100 μl. Hydroquinone (60 μl of 10 mM) and $NaHS_3$ (1.04 ml of 3.6 M pH 5.0) were then added. Reaction mixtures were incubated at 50 ℃ for 16 h in the dark. The DNA was desalted and concentrated using Geneclean (Bio101), denatured with 0.3M NaOH for 15 min at 37 ℃, neutralized with 3M NH_4OAc (pH 7.0), and ethanol-

precipitated. An aliquot of DNA was amplified with the following modified primers: E01-F 5'-GTGTGATTGGTGGTTTTAGAGT-3', E02-R 5'-CCATCCTCAATATTATAACAAAT-3', E2-F 5'-GGAGTTGTTTATTGGGGTGGTGTTTATTTTGGT-3', E2-NF 5'-TGGATGGTGATGTAAATGGTTATAAGTTT-3', E2-R 5'-GTTTGTGTTTTAGGATGTTGTTG-3', E4-R 5'-ACTTATACAACTCATCCATACCAAAAATAATCC-3', E5-R 5'-ACTTATA CAACTCATC CATACCGAAAATAATCC-3', E6-F 5'-GGTTGTTATGAATAAAGGTGGTTATAAGA-3', E7-R 5'-CTCACTCATTAAACACCCCAAACTTTACAC-3', E8-F 5'-GAAGATTTTTPyG ATTTGTAGTTTAAGTTTTAGG-3', E9-R 5'-GAAGATTTTTPyGATTTGTAGTTTAAGTTT TAGG -3'. All PCR reactions were carried out in 100 μl reaction mixtures containing 5 μl bisulfite-treated genomic DNA, 200 μM dNTPs, 10 pmol of each primer, 1 mM $MgCl_2$, 50 mM KCl, 10 mM Tris, 5% dimethyl sulfoxide, 2 U of Taq polymerase (Stratagene), in a Primus thermocycler (MWG -Biotech) under the following conditions: 95 ℃/5 min, 70 ℃/2 min x 1 cycle, 97 ℃/1 min, 54 ℃/2 min, 72 ℃/1 min, x 5 cycles; 95 ℃/0.5 min, 52 ℃/2 min, 72 ℃/1 min x 25 cycles; 72 ℃/3 min x 1 cycle. The first PCR products (2 μl) were used to perform the second PCR (PCR nested or semi-nested) under the same PCR conditions. PCR products were cloned into pGEM-T Easy Vector (Promega), and at least 20 independent clones for each fragment were sequenced with the T7 primer.

2.3 Results

To examine the relationship between DNA damage and gene silencing, we introduced a double strand break (DSB) in the genome and evaluated recombination and expression of the recombinant products. We also examined the structure at the DSB locus after repair. Finally, we asked how the inhibition of DNA methylation affected recombination and/or expression of the recombinant product during homologous recombination.

2.3.1 I-SceI Induces a Homologous Recombination in HeLa-DRGFP Cells.

Our recombination assay uses the DRGFP plasmid, which contains two mutated GFP genes separated by a drug selection marker (puromycin N-acetyltransferase gene) (Fig. 17). The 5' GFP gene (cassette I) has a unique recognition site for I-SceI, a rare-cutting homing endonuclease that does not cut human genomes (100). The I-SceI site was introduced at the BcgI site by substituting 11 bp using site-directed mutagenesis. This substitution also includes two in-frame stop codons thereby inactivating the GFP gene in cassette I. The downstream (3') GFP gene contains truncation at its 5' and 3' positions having only about 800 bp of GFP gene. This part of GFP is available as a template for HR. HeLa cells containing DRGFP integrated into the genome were generated and selected by puromycin resistance. Puromycin resistant pools of HeLa cells were then transiently transfected with a plasmid expressing I-SceI. The expression of I-SceI induced a single double strand break in the genome of the HeLa-DRGFP cells. The resultant DSBs trigger homologous recombination and recombinants products were analyzed. FACS analysis was used to detect cells expressing GFP. Wild type GFP formation is a product of gene conversion in this system. The percentage of GFP positive cells was counted (Fig. 18A). As shown in Fig. 18A, 5.5% of cells expressed GFP after transfection with I-SceI

plasmid. Control cells, which were not transfected, showed background level fluorescence showing that homologous recombination was induced by DSB. In addition, the expression of GFP following recombination was dependent on expression levels of I-SceI in transfected cells (Fig. 19). Cells were transiently transfected with different amount of I-SceI plasmid (0.5, 1.0, or 2.0 μg DNA). After 3 days incubation, cells were harvested, lysed, and analyzed by western blotting. Fig. 19 clearly showed that GFP expression is proportional to the level of expressed I-SceI enzyme.

The structure of the GFP locus was determined by PCR analysis. We used two 5' primers, Unrec, which amplified unrecombined units and Rec, which amplified only recombined units (Fig. 17). The 3' primer sequence is found in cassette I but not in cassette II. After 48 h I-SceI transfection, the Rec primer amplified a 459 bp fragment (Fig. 18B). Since Unrec priming site is gone after HR, this PCR product indicates a wild-type GFP gene generated by gene conversion at the I-SceI site. The Unrec products were detected in both cells transfected with/without I-SceI. However, the Rec PCR products were only detected in cells exposed to I-SceI (Fig. 18B) showing again gene conversion is dependent on DSB generated by I-SceI.

2.3.2 Methylation Reduces GFP Expression.

Homologous recombination is triggered by DSBs efficiently; however, we often observed rather low yields of GFP positive (GFP+) cells after I-SceI. This raised the possibility that some wild-type GFP recombinants were not particularly well expressed. The recombinant GFP gene might be silenced, possibly by DNA methylation. Accordingly, we asked whether inhibition of methylation might increase the yield of cells expressing GFP. The HeLa-DRGFP cells were transfected with I-SceI and split one day after transfection. Cells were further incubated with

either 0, 0.5, or 1.0 μM of aza-dC for 3 days, 5 days, or 9 days to block or reverse DNA methylation (101). As shown in Fig. 20, FACS analysis revealed that aza-dC significantly increased the number of GFP+ cells. Compared to non-aza-dC treated cell, aza-dC treated cells showed the increase of GFP+ cells by 0.4% (1 μM, 3 days), or ~2% (1 μM, 9 days). The aza-dC effect was observed as early as 3 days with 0.5 μM concentration. Treatment of cells not exposed I-SceI with aza-dC did not increase the yield of GFP+ clones above a background value (data not shown). Since aza-dC induces genome-wide hypomethylation, the increase of GFP+ cells by aza-dC indicates that methylation following DSB repair inhibits the expression of recombinant wild-type GFP.

2.3.3 Methylation does not Reduce Recombination Frequency.

Aza-dC significantly increased the number of GFP+ cells (Fig. 20); however, it is possible that aza-dC may increase the GFP+ cells by increasing the frequency of homologous recombination. To clarify this issue, we performed PCR analysis to see the recombinant products upon aza-dC treatment. PCR was carried out using the Rec primers, which only amplify the recombinant products and was performed at different cycles (25 and 30). Cells were transfected with I-SceI plasmid and treated with 5 μM aza-dC for 48 h. As shown in Fig. 21, PCR analysis clearly showed that aza-dC treatment after I-SceI exposure did not increase the number of recombinant products (compare lane 1 and 2, or 3 and 4). FACS analysis showed that the number of GFP+ cells was increased (data not shown); however, the recombinant gene products were not. These data indicate that aza-dC increased GFP+ cells by preventing DNA methylation at repair sites, not by stimulating the recombination frequency.

2.3.4 Recombination Generates Two Population of GFP+ Cells.

Transgenes are often known to be silenced in cultured cells (102); thus, we considered the possibility that the methylation at repaired sites was not induced by homology-directed repair, but resulted from subsequent transgene silencing. To distinguish these two events, we compared expression patterns of the wild type GFP gene driven by CMV promoter and of the recombinant GFP gene. HeLa cells carrying the DRGFP or wild type GFP plasmids were transfected with I-SceI or control plasmid and treated with aza-dC. In contrast to the expression of the recombinant GFP (which is of a bimodal), wild type GFP is unimodal (Fig 22A, compare upper and lower middle panel). Moreover, expression of wild type GFP gene was not enhanced by aza-dC, nor was it affected by I-SceI (Fig. 22A, lower middle and right panel). This bimodal distribution reflects the presence of two cell populations. One population expressing GFP with high fluorescence intensity (HR-H) and the other expressing GFP with low fluorescence intensity (HR-L) (Fig. 22A, upper middle panel). Interestingly, the expression of the recombinant GFP shifted to a unimodal distribution following aza-dC treatment (Fig. 22A, upper right panel). This suggests that the low GFP expression in HR-L population is a result of DNA methylation. To further study the nature of these two groups of cells, we sorted HR-H and HR-L cells. The separated cells were grown for a period time and parallel cultures were treated with aza-dC. GFP expression was monitored by FACS. As shown in Fig. 22B, only the HR-L cells were silenced over that period of time. The expression of GFP decreased quickly and the silencing reached a plateau about 14 days after I-SceI transfection. However, the GFP expression was maintained, even stimulated, in HR-L cells treated with aza-dC. This effect of aza-dC was not observed in aza-dC treated HR-H cells. These data confirm that the expression of GFP in HR-L cells was inhibited by DNA methylation.

2.3.5 DNA Methyltransferase 1 Suppresses Recombinant GFP Gene Expression.

The increase of GFP positive cells following aza-dC treatment suggested that a significant fraction of recombinant genes were silenced by methylation. To confirm the role of methylation in silencing GFP, we examined HCT116 human colorectal cells lacking DNMT1. In one specific cell line, exons 3-5 of DNMT1 are deleted (103). This deletion includes the PCNA binding domain, leaving the next exon out of frame and thus making cells *dnmt1*$^{-/-}$. Stable cell lines carrying DRGFP were generated with wild type HCT116 and HCT116 *dnmt1*$^{-/-}$ cells. Among the individual clones, colonies having similar level of Unrec genes were chosen from both DRGFP cell lines and analyzed (Fig. 23B compare Unrec products between wt and *dnmt1*$^{-/-}$ cells). Clones were then transfected with I-SceI and analyzed as described above for HeLa cells. As shown by FACS analysis (Fig. 23A), the number of *dnmt1*$^{-/-}$ cells that expressed GFP was more than 2-fold higher than wild-type cells. We conclude that DNMT1–dependent methylation silences GFP expression in HR repaired cells.

2.3.6 Repaired Molecules are heavily Methylated in HR-L cells.

Sodium bisulfite analysis of genomic DNA is a direct way of addressing the methylation status of cytosine residues (99). Bisulfite converts cytosine but not 5-methylcytosine to thymine. Bisulfite treated genomic DNA is amplified by PCR, cloned, and then sequenced. Cytosine residues detected by direct sequence analysis, therefore, represent methylated residues.

To analyze the methylation status of an individual DNA molecule before and after repair, we carried out bisulfite analysis and determined the methylation profile at the I-SceI site. DNA from HeLa DRGFP cells before and after I-SceI transfection was analyzed. The methylation profiles from various classes of recombinant DNAs are shown in Fig. 24: (1) uncut molecules; (2)

recombinant molecules from sorted HR-H (high expressor) or sorted HR-L (low expressor); and (3) molecules generated by non-homologous end joining (NHEJ). Compared to uncut molecules, molecules from HR-L cells were heavily methylated. The region approximately 300 bp downstream of the SceI site was mainly methylated. CpGs in this region were not methylated in the uncut molecules indicating that de novo methylation events occured. In contrast, molecules from HR-H were significantly hypomethylated both up- and downstream of the breakage site. The ratio of HR-H and HR-L was approximately 1:1.

2.3.7 DNMT1 is Associated with HR Chromatin.

The data shown above indicate that double strand break repair by homologous recombination leading to gene conversion is associated with methylation pattern changes in the region of the DSB and that DNMT1 is required for methylation induced by DSB repair. To find the relationship between recombination and DNA methylation, we investigated whether DNMT 1 was bound to GFP chromatin after I-SceI exposure. HeLa-DRGFP cells were transfected with I-SceI plasmid and further treated with 1 μM aza-dC. Fragmented chromatin was prepared (see material and methods) and was precipitated with mono specific anti-DNMT1 antibody. Under these conditions, incorporated aza-dC traps DNMT1 on the DNA and enriches the DNMT1 bound DNA during immunoprecipitation (101,104) without using formaldehyde to cross link the DNA and protein (11). The data shown in Fig. 25A indicate that DNMT1 is specifically localized to the recombined GFP DNA region. Although non-recombinant sequences are present in large excess relative to recombined GFP DNA in input chromatin DNA, the Unrec region was not enriched during immunoprecipitation suggesting that DNMT1 is primarily associated with GFP chromatin after DSB repair. The specificity of the assay was confirmed in positive controls

experiments (Fig. 25B). The promoter regions of MGMT and p16 are known to be methylated in HeLa cells.

2.4 Discussion

In this work we demonstrate the first evidence that DNA damage repair by homologous recombination (HR) is accompanied by DNA methylation resulting in gene silencing of repaired DNA. PCR and GFP expression assays were used to examine HR triggered by DSBs with I-SceI at a selected genomic site. We performed the analysis with pools of HeLa cells or in single HCT116 or HCT116 *dnmt1*$^{-/-}$ clones. In all cases, I-SceI induced HR resulted in the appearance of GFP+ cells and recombination based on PCR analyses. Also, we found that the DNA hypomethylating agent, aza-dC, significantly increased the % of GFP+ cells. Moreover, DNMT1 was associated with recombinant, but not non-recombinant chromatin.

Based on our collaborator's data, a significant fraction of recombinants expressed little or no GFP (105). Silencing of these genes was due to DNA methylation, since demethylation induced by aza-dC following DSB induction significantly increased the number of HeLa cells that expressed GFP at high levels. Demethylation prior to DSB generation was ineffective. Similarly, HCT116 *dnmt1*$^{-/-}$ cells lacking DNA methyltransferase 1 yielded more clones expressing GFP than wild-type controls. In addition, mouse ES cells lacking Dnmt1 was also showed the increase in GFP expression (105).

The DNA around the DSB in cassette I is retrieved by template in cassette II, with gene conversion at the I-SceI site, or by a sister chromatid, without gene conversion. We propose that DNMT1 methylates only one of the newly generated strands after DNA repair based on following pieces of evidence. First, an equivalent ratio (1:1) of hypo and hypermethylated molecules were observed in recombinants derived from single clones; therefore these two phenotypes did not segregate as individual clones. Thus, the two expression phenotypes, high

(HR-H) and low (HR-L) were generated in mass cultures or in clones containing a single integration site. Second, the expression pattern of wild type GFP (transfected GFP reporter plasmids) was unimodal, which is very different than the bimodal distribution of recombinant GFP. From these observations, we conclude that HR DNA repair results in one hypermethylated strand and one hypomethylated strand. Subsequent DNA replication yields daughter molecules that retain the methylation pattern of each parental template strand (Fig. 26). In the case of gene conversion, the length of the hyper- or hypomethylated track did not exceed the length of the cassette II template. We found that DNMT1 can act as a de novo methylase, that it can recognize unmethylated DNA as a substrate. Although it is commonly thought that DNMT1 cannot promote de novo methylation, in fact, the preference of DNMT1 for hemimethylated versus unmethylated DNA is not absolute but favored by 7-20 fold (106). The known de novo methylases, DNMT3a and DNMT3b, are not likely to be involved in HR repair for several reasons. First, we found that HCT116 *dnmt1*$^{-/-}$ cells show a greater frequency of GFP^{+} recombinants than wild-type cells. Second, these methylases are not recruited to the sites of DNA damage (95). Third, our colleagues showed that all GFP recombinants were unmethylated in *dnmt1*$^{-/-}$ mouse ES cells (105). The methylation profile of DNA molecules in untreated *dnmt1*$^{-/-}$ cells was similar to wild-type cells. This indicates that although DNMT3a and DNMT3b may partially substitute for DNMT1 during normal replication, neither cannot replace DNMT1 during HR repair (105).

In our collaborator lab, we showed that alteration of the methylation pattern following DNA repair by HR was restricted to 200-300 bp flanking the DSB. Changes in methylation patterns did not extend 5' to the CMV promoter that is ~1.7 kb upstream region from I-SceI site, or to cassette II (about 3.5 kb downstream) (105). This raises the question how restricted

methylation induced silencing of the recombinant GFP gene. We propose that local methylation initiates chromatin condensation, which is propagated near DSB regions, thereby silencing nearby genes (107). Presumably, propagation of the silencing signal involves histone modification, although this remains to be explored.

The protein tyrosine phosphatase, receptor type, J (PTPRJ) gene is located in an area of frequent loss of heterozygosity (LOH), and is often silenced in thyroid tumors (108). LOH at this locus was not caused by chromosome loss or cross translocation, as indicated by determination of PTPRJ copy number. LOH results from gene conversion associated with a DSB repaired by HR. Repair leaves behind an "epigenetic footprint" – a cluster of methyl CpGs that is remarkably similar in 3 independent thyroid tumors showing LOH. As was the case with the GFP model, about half the repaired DNA molecules were hypomethylated (105).

In conclusion, these results argue for a cause-effect relation between HR repair and de novo DNA methylation. Approximately one half of repaired molecules are marked by methylation. As a direct consequence, the gene in these repaired molecules is silenced. In the remaining molecules, the recombinant DNA is hypomethylated and highly expressed. We believe that this epigenetic modification of repaired DNA represents a powerful evolutionary force. If the expression of the repaired gene affects cell growth negatively, then only cells containing the hypermethylated copy will survive. In contrast, if the expression of the repaired gene is beneficial to cell growth, then cells inheriting hypomethylated copy will have a selective advantage (Fig. 27). Also, our model illustrates how HR repair and methylation could result in selecting an outgrowth of malignant cells. If a tumor suppressor gene is repaired by HR, the cells inheriting the silenced copy of the tumor suppressor gene will have a selective advantage. The frequent hypermethylation of DNA tracts in tumors or in aging may be induced by repair of

DSBs. We note that silencing of tumor suppressor genes by methylation is characteristic of tumor cells, as is frequent DNA breakage (13,109). Indeed, evidence of enhanced DSB formation in hyperplastic, precancerous cells, precedes the genomic instability and loss of p53 characteristic of more advanced tumors (110). Our data also imply that imprinting of genes may be linked to homologous recombination events. In this perspective, it is noteworthy that a systematic genome-wide analysis has revealed that human imprinted chromosomal regions are historical hot-spots of recombination (27).

Figure 17 Formation of a functional GFP gene by recombination initiated at a specific DSB.

The reporter plasmid, DRGFP, contains two mutated GFP genes oriented as direct repeats and separated by a puromycin selectable marker. The 5' GFP cassette (cassette I) carries an I-SceI recognition site. The I-SceI site was incorporated into a BcgI restriction site by substituting 11 bp of the wild-type GFP. The substituted base pairs also supply two in-frame stop codons that terminate translation, thereby inactivating cassette I. The 3' GFP cassette (cassette II) is inactivated by 5' and 3' truncations (triangles). The gene conversion of the I-SceI site to BcgI, initiated by a DBS, generates a functional GFP gene.

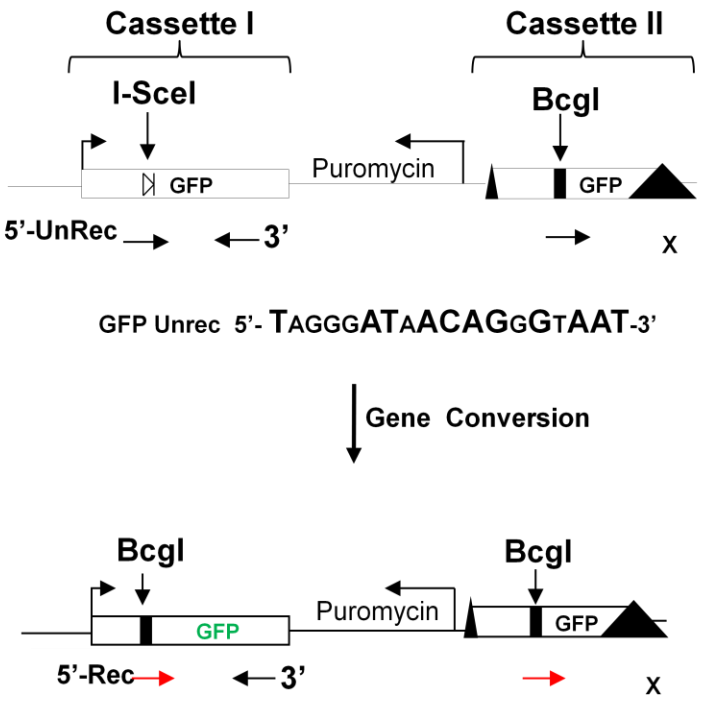

Figure 17 Formation of a functional GFP gene by recombination.

Figure 18 Recombination assay.

(A) Stable HeLa cells containing DRGFP plasmid were transiently transfected with I-SceI, and 3 days later, GFP+ cells were scored by FACS. The graph shows data from 3 experiments. (B) The recombined DNA products were analyzed using PCR. PCR was performed as described in Material and Methods.

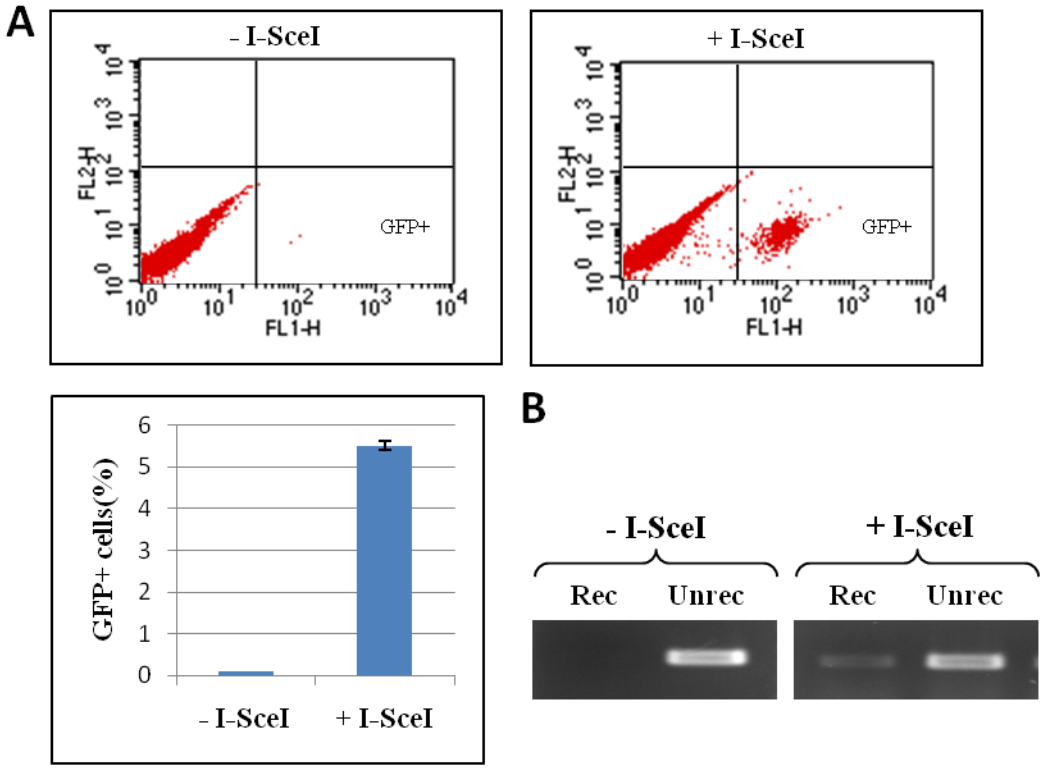

Figure 18 Recombination assay.

Figure 19 GFP expression is dependent on the level of I-SceI.

Stable HeLa cells containing DRGFP plasmid were transiently transfected with different amounts of I-SceI plasmids. After 3 days, cells were lysed and whole cell extracts were resolved on a SDS-PAGE gel, then subjected to western blot analysis with an anti-HA11 antibody to detect HA-epitope tagged I-SceI protein or with an anti-GFP antibody to detect GFP protein. Arrow indicates GFP protein expressed from recombined gene product. Arrow head indicates the HA epitope tagged I-SceI.

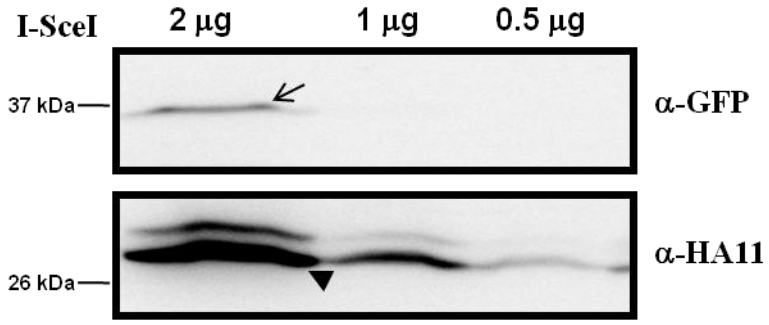

Figure 19 GFP expression is dependent on the level of I-SceI.

Figure 20 Aza-dC increases the level of GFP expression.

HeLa cells stably selected for the presence of DRGFP plasmid were transfected with 2 μg of I-SceI DNA and 1 day later, were trypsinized, pooled, and re-plated. Different amount of aza-dC were added and cells were further incubated for 3, 5, and 9 days. GFP+ cells were scored by FACS. The graph shows data from 3 experiments.

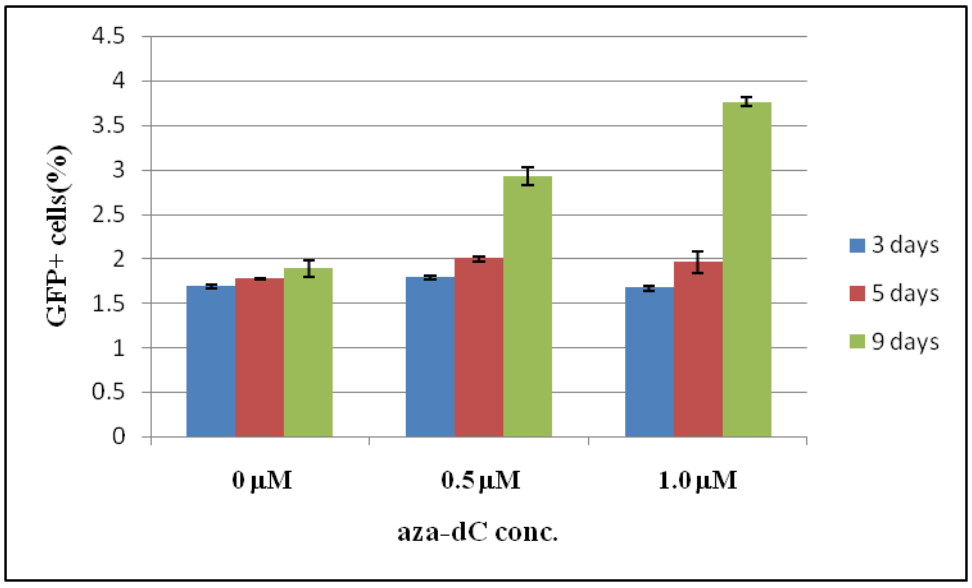

Figure 20 Aza-dC increases the level of GFP expression.

Figure 21 Aza-dC does not increase the recombination frequency.

HeLa DRGFP cells were transfected with I-SceI plasmid and treated with 5 μM aza-dC for 48 h. The HR DNA in individual clones was analyzed by PCR. PCR was performed at different cycles (25 and 30) as indicated, and GFP clones were analyzed by PCR with the Rec and 3' common primers indicated in Fig. 17. These primers amplify only recombinant products. (This figure was cited from Cuozzo et al. (105).)

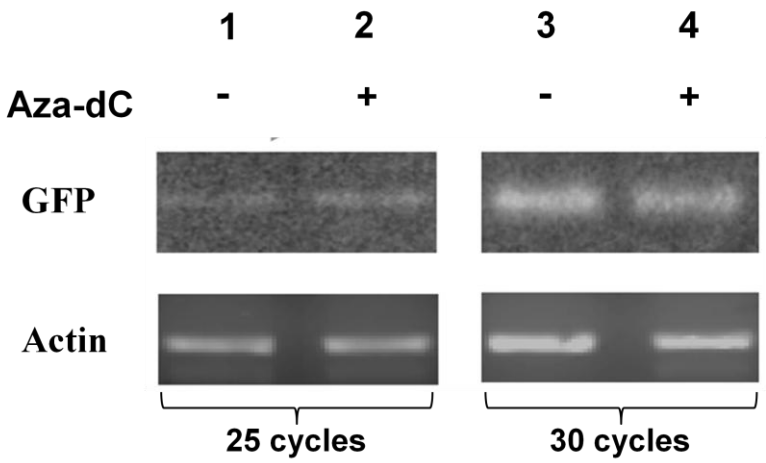

Figure 21 Aza-dC does not increase the recombination frequency.

Figure 22 Bimodal distribution of recombinant GFP expression.

(A) HeLa cells carrying either DRGFP or wild type GFP plasmid were transfected with I-SceI and treated with 5 μM aza-dC. GFP expression was analyzed by FACS. The mean fluorescence (arrow) and the % of GFP+ cells were: (1) DRGFP (no I-SceI) 7.4 and 0.4%; (I-SceI) 203.56 and 4.7%; and (I-SceI + aza-dC) 335.31 and 7.6%, respectively and (2) wild type GFP (no I-SceI) 357.51 and 95.4%; (I-SceI) 361.12 and 96.2%; and (I-SceI + aza-dC) 389.68 and 89.6%, respectively.

(B) Cells sorted by FACS and divided into two pools, HR-H and HR-L, 4 days after transfection. The sorted cells were monitored at 4, 6, 8, 14, and 21 days after transfection. Parallel cultures at 6, 12, and 19 days after transfection were treated with aza-dC (arrow heads) for 24 h; the drug was washed away and GFP fluorescence was determined 24 h later. This figure was cited from Cuozzo et al. (105).

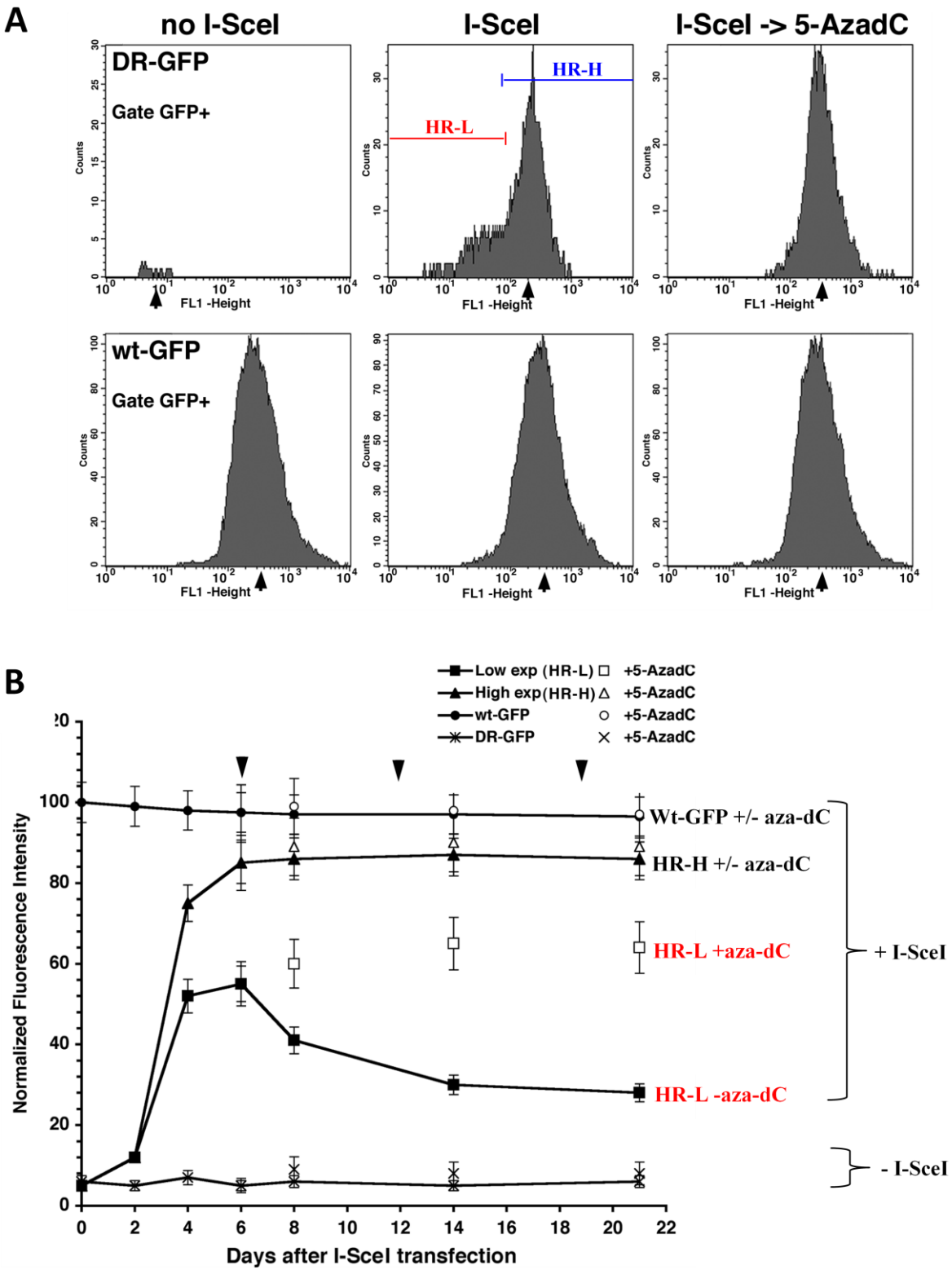

Figure 22 Bimodal distribution of recombinant GFP expression.

Figure 23 DNMT1 inhibits the expression of GFP.

HCT116-DRGFP or HCT116 *dnmt1*$^{-/-}$-DRGFP cells were transfected with I-SceI plasmid and grown 5 days, and analyzed for GFP recombination and expression. (A) FACS analysis of GFP+ cells from two cell lines. The histogram was obtained from three experiments. (B) Genomic DNA from two cell lines was PCR amplified with Unrec and Rec primers.

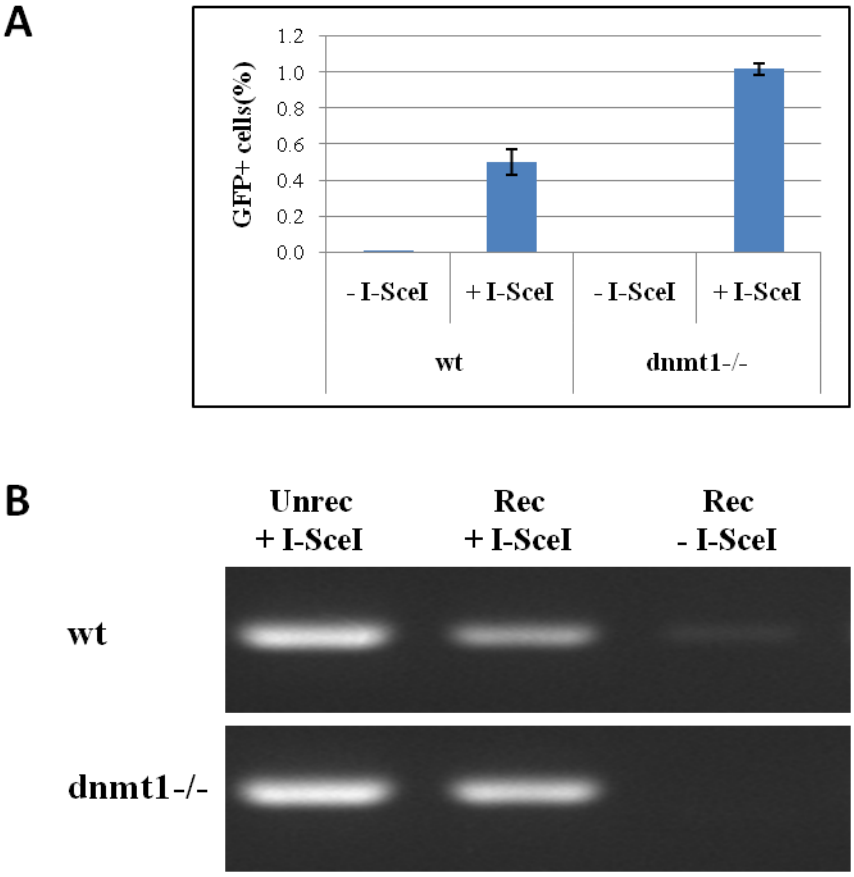

Figure 23 DNMT1 inhibits the expression of GFP.

Figure 24 CpG methylation status in repaired molecules.

DNAs from HeLa DRGFP cells transfected with I-SceI were subjected to bisulfite analysis. The number of molecules sequenced in each class was: 1. Uncut, 25 molecules; 2. HR-H, 15 molecules; 3. HR-L, 20 molecules; 4. NHEJ, 6 molecules. All CpGs (white circles) flanking the I-SceI site are shown. Gray circles, molecules methylated in ≥ 20% of molecules; black circles, molecules methylated in ≥ 40% of molecules. This figure was cited from Cuozzo et al. (105).

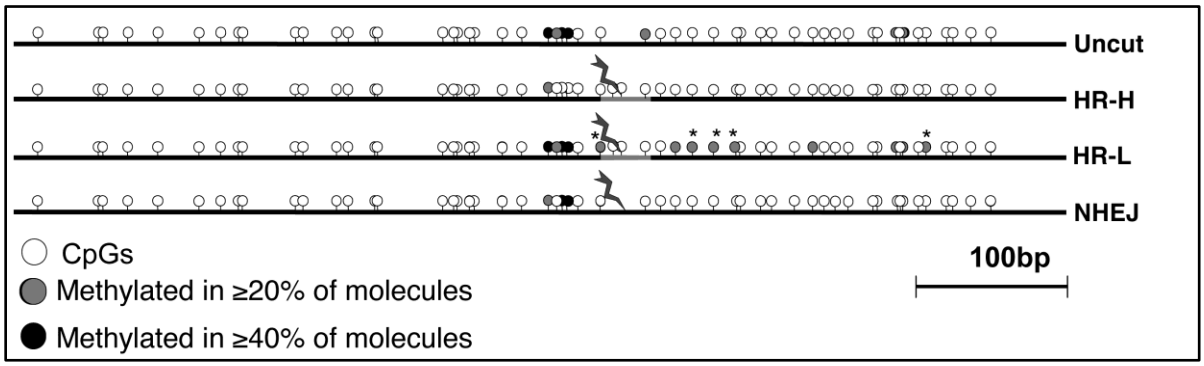

Figure 24 CpG methylation status in repaired molecules

Figure 25 DNMT1 selectively binds recombinant GFP chromatin.

HeLa-DRGFP cells were transfected with I-SceI and treated 24 h later with 1 μM aza-dC for 1, 2, and 4 days. Chromatin immunoprecipitation (Chip) was carried out as described in Material and Methods. (A) PCR of DNA immunoprecipitated with anti-DNMT1 antibody. "None" indicates chromatin derived from cells transfected with control plasmid, (-) or (+) indicates the treatment with aza-dC. Rec, and Unrec indicate the primers used for amplification (see Fig. 17). (B) PCR amplification of immunoprecipitated DNA with MGMT or p16 primers.

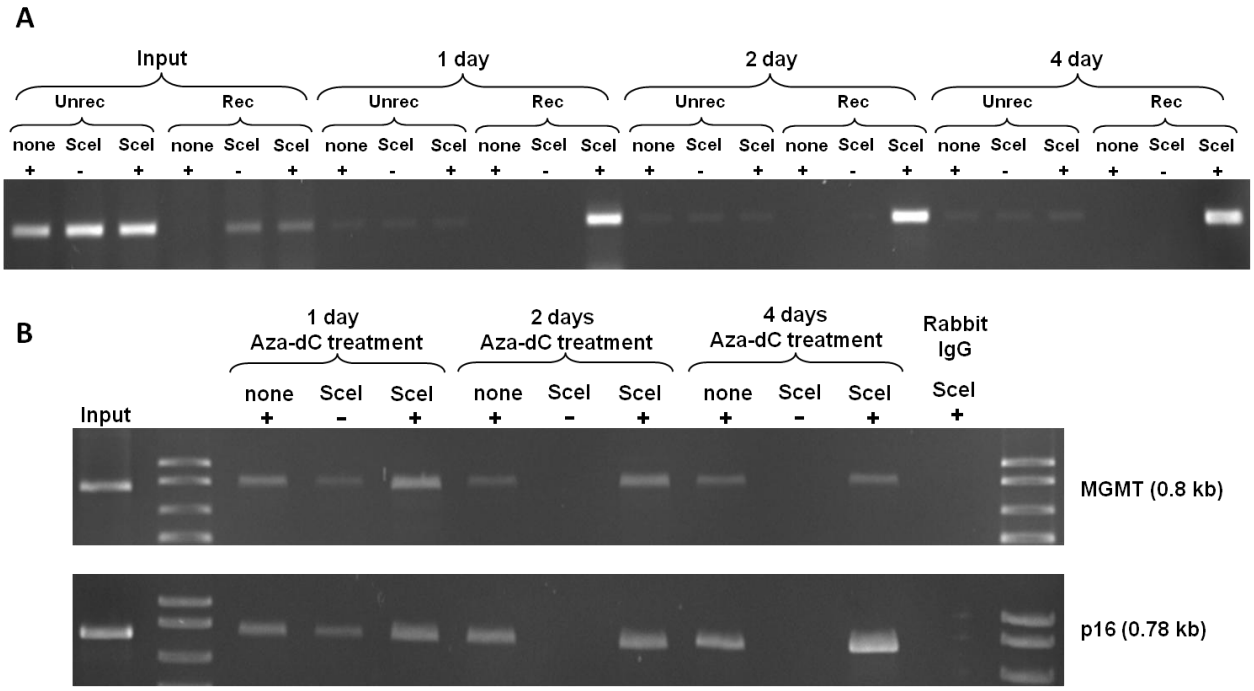

Figure 25 DNMT1 selectively binds recombinant GFP chromatin.

Figure 26 A model linking methylation and HR repair.

The model illustrates how HR repair affects DNA methylation. The primary product of repair is a hemimethylated DNA molecule. Replication of this molecule yields fully methylated and hypomethylated DNA molecules in a 1:1 ratio. The black and red lines correspond to parental DNA strands damaged by I-SceI. The green inset line represents the new DNA recovered by templating of cassette II (see Fig. 17). The faint gray line corresponds to new daughter DNA strands in cells that grow out from the original HR events.

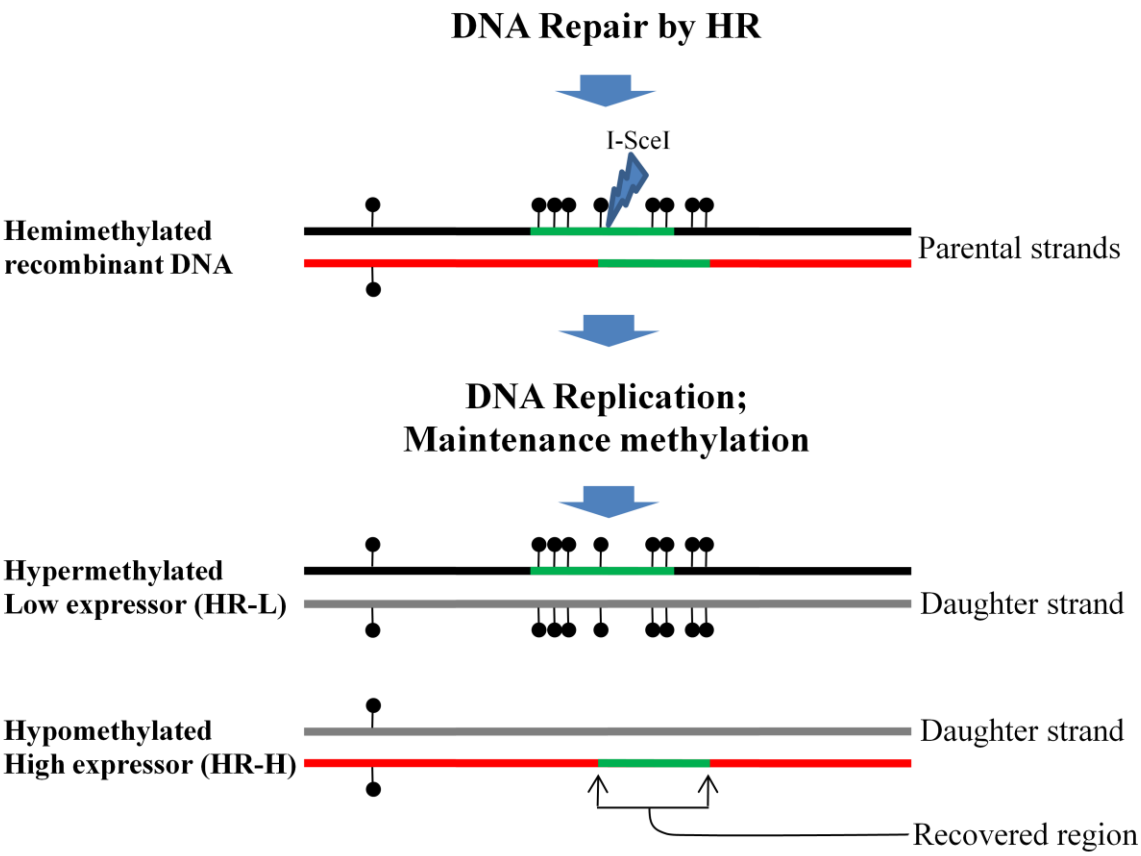

Figure 26 A model linking methylation and HR repair.

Figure 27 Biological consequences of repair-induced methylation.

This model illustrates how DNA damage, HR repair, and methylation could lead the selective outgrowth of cells. Red circles represent methylated CpGs induced by HR. Black circles represent methylated CpGs before HR. Silencing depends on the location of de novo methylated CpGs and sites of DNA damage, both of which are stochastic processes. Thus, HR-induced methylation is also random. If the expression of the repaired gene is harmful, only cells containing the silenced copy will survive. Conversely, if the expression of the repaired gene is beneficial, cells inheriting the hypomethylated copy will have a selective advantage.

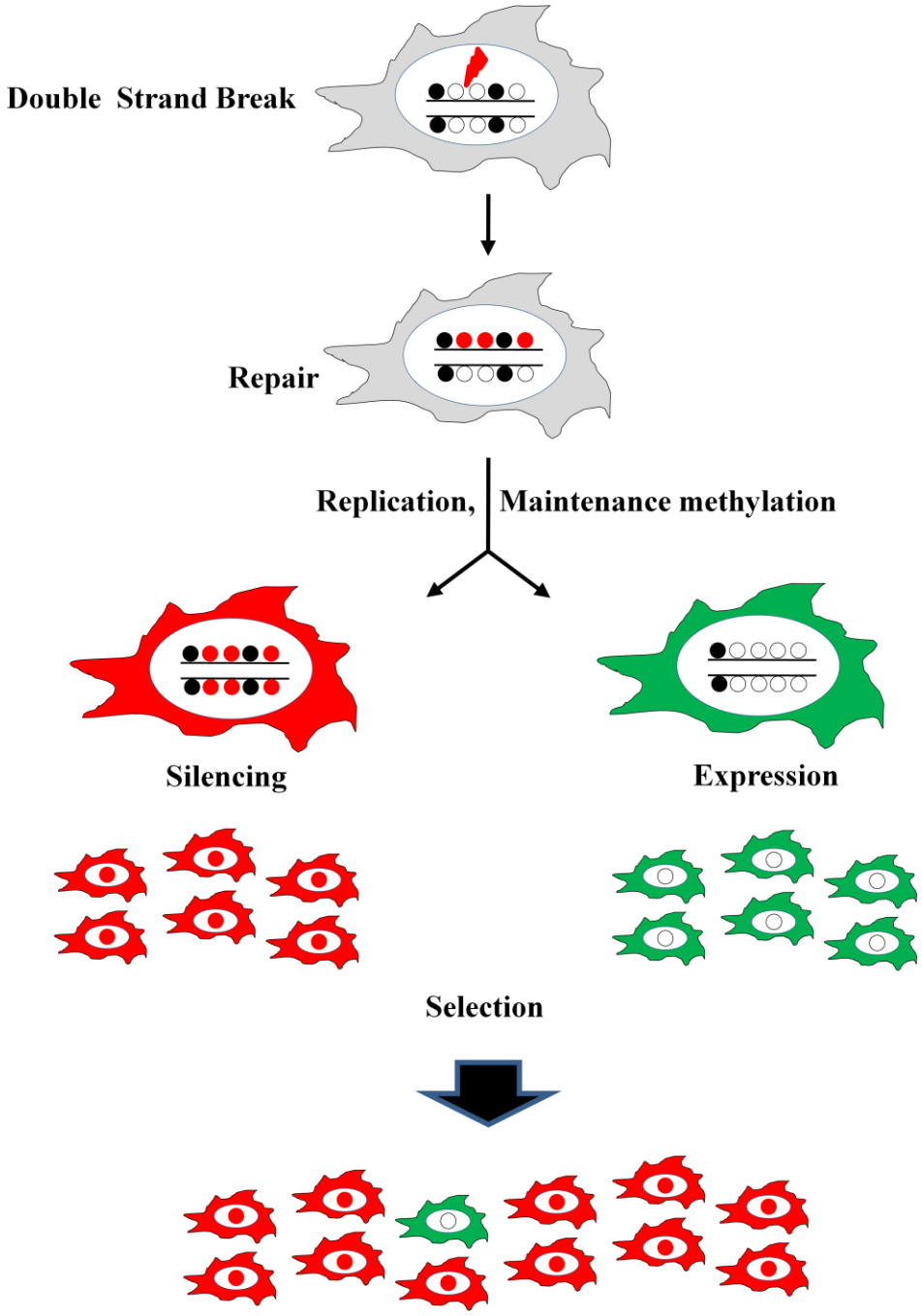

Figure 27 Biological consequences of repair-induced methylation.

CHAPTER 3: THE ROLE OF GADD45α IN MEDIATING STRAND SPECIFIC DNA METHYLATION INDUCED BY HOMOLOGY DIRECTED DNA REPAIR

3.1 Introduction

The growth arrest and DNA damage-inducible 45 alpha (GADD45α) is a small, 18.4 kDa, acidic protein and originally isolated from Chinese hamster ovarian (CHO) cells treated with UV irradiation (111). Subsequently, it was found to be induced by a variety of DNA-damage agents, including ionizing radiation (IR), methyl methansulfonate (MMS) and medium depletion (112,113). Three GADD45-like proteins, GADD45α (GADD45), GADD45β (MyD118), and GADD45γ (CR6), have been identified, and these GADD45 proteins share 55 to 60% sequence identity (114). All three genes are inducible by cellular stress, but their expression profile is distinct in various tissues (115). Among three GADD45 proteins, only GADD45α is up-regulated by p53 with a strong p53-binding site in the third intron (116). Its induction by IR is dependent on p53, but the induction by UV, MMS, and medium starvation is not dependent on p53 (116,117). GADD45α is also regulated by a BRCA1, in a p53 dependent manner (118,119).

The GADD45 proteins interact with multiple intracellular proteins such as, proliferating cell nuclear antigen (PCNA), p21 protein, Cdc2-cyclinB1 complex, core histones, and MTK1/MEKK4 in a JNK pathway (115,120-123). These various interactions suggest that the GADD45 pathway may have important roles in growth control, DNA repair, and the regulation of signaling. Some of these roles are common to all three isoforms and some roles are isoform specific. A known role for GADD45α is in growth arrest following genotoxic stress. GADD45 proteins bind to Cdc2 and displace cyclinB1 from Cdc2 inducing cell cycle G2/M arrest (124,125). In addition, the suppression of GADD45α or GADD45γ by siRNA abrogates growth arrest supporting the importance of their up-regulation after cellular stress (126). A role for

GADD45α in apoptosis is suggested by the fact that many apoptosis inducing agents up-regulate GADD45α expression (115). Moreover, GADD45α also interacts with MTK1/MEKK1 and activates the JNK/p38 pathway that induces apoptosis (115). However, the exact role of GADD45α in apoptosis is controversial because the activation of JNK pathway is not significantly changed in GADD45α-deficient mouse embryonic fibroblasts (MEFs). Also, both JNK and p38 MAPK were activated before the induction of GADD45α (127,128). Thus, it remains unclear whether GADD45α is induced as a consequence of apoptotic response or whether GADD45α activates apoptosis. Another potentially interesting biological role of GADD45α is in DNA repair. Early studies showed that GADD45α interacts with PCNA and have some role in nucleotide excision repair (NER) (120). Antisense RNA experiments revealed that reduced GADD45α levels affected DNA repair and sensitized cells to UV and cisplatin (129). GADD45α null mice exhibit increased genomic instabilities and are mainly susceptible to carcinogenesis induced by IR or UV (130,131). In addition, it has been reported that GADD45α interacts directly with core histones to destabilize histone-DNA complexes following UV irradiation (122). These findings imply that GADD45α may recognize an altered chromatin state and bind to damaged DNA in a chromatin setting. Finally, Carrier et al. (122) suggested that GADD45α may be involved in the coupling chromatin assembly with DNA repair.

Another relevant and interesting role of GADD45α is its involvement in DNA demethylation. Recently, Barreto et al. (132) reported that GADD45α promotes DNA demethylation and erases epigenetic marks. They showed that GADD45α over-expression activated a methylation silenced reporter plasmid and that it interacts with repair endonuclease XPG to direct DNA demethylation; however, this finding has been challenged. Jin et al. (133)

could not confirm the role of GADD45α in the demethylation of mammalian DNA using similar approaches; thus, the mechanism of active demethylation remains in question. In plants, genomic methylation patterns can be changed in part by active demethylation. The demethylation in plants is mediated by a family of methyl-cytosine glycosylases (134-136). The active demethylation in mammals is controversial due to the lack of a confirmed enzymatic mechanism and defined pathways. The existence of mammalian demethylases has been a recurrent subject that has remained obscure.

Here, we investigate the role of GADD45α in DNA demethylation. We have found that the region repaired by homologous recombination is marked by DNA methylation and, interestingly, only one of strand in repaired region was methylated suggesting the possible involvement of demethylation machinery. We have found that GADD45α interacts with the catalytic domains of DNMT1, 3a, and 3b and inhibits their enzyme activity. Since GADD45α is induced by genotoxic stress, we hypothesized that GADD45α may inhibit DNA methylation of one strand of recombinant DNAs during DNA repair in passive manner. Using a homologous recombination system as a reporter, we found that GADD45α increases the expression of GFP. This indicates that GADD45α may provide the choreography associated with strand specific methylation. GADD45α prevents complete silencing of repaired region by interaction with DNMT1 suggesting its role in passive DNA demethylation during homology-directed repair.

3.2 Material and Methods

3.2.1 Plasmids

The construction of DNMT1-V5, DNMT3a-V5, and deletion mutants of DNMT1 is described in material and methods of Chapter 1. All Glutathione-S-transferase (GST) fused DNMT1 deletion mutants were constructed by inserting PCR products into pGEX-5X-1 (GE Healthcare Life Sciences) using EcoRI and NotI. Flag-DNMT3b was constructed by inserting DNMT3b PCR products into pCMV-Tag2 (Stratagene) vector using EcoRI and XhoI sites. To clone the Myc-GADD45α, first, a pCMV-Myc1 plasmid was constructed by inserting a Myc linker containing one copy of the epitope into pcDNA3.1(+) (Invitrogen) using the HindIII and BamHI sites (HindIII site was mutated by inserting the Myc linker). GADD45α PCR products were digested with EcoRV and XbaI and cloned into pCMV-Myc1 plasmid. Each point mutant of Myc-GADD45α was generated by replacing one or two consecutive amino acids residues with alanine residues using site-directed mutagenesis kit (Stratagene). To make an intein fused GADD45α, GADD45α PCR products was cut with NdeI and SapI and cloned into pTXB1 vector (NEB) using these same sites.

3.2.2 Co-immunoprecipitation and Western Blotting

Whole cell extracts were prepared by lysing cells in RIPA buffer (1X PBS pH 7.5, 1% NP-40, 0.5% deoxycholate, 0.1% SDS, 10% glycerol) containing 1X protease inhibitor cocktail (Roche), 1 mM DTT, 1 mM $MgCl_2$, and 2 mM PMSF. For immunoprecipitation, whole cell extracts were diluted 5 times with 0.5X PBS containing 1X protease inhibitor cocktail, 1 mM DTT, 1 mM EDTA, and 2 mM PMSF. Antibody (1 μg) was added to samples for 3 h, followed by 30 μl of protein A Sepharose 4B beads (Zymed) overnight. Beads were washed three times

with 1X RIPA and once with 1X PBS. Bound proteins were eluted with sample buffer and analyzed by western blotting. Antibodies used are as follows: anti-V5 (Invitrogen), anti-DNMT1 (NEB), anti-Topoisomerase IIα (TopoGEN), anti-GADD45α (Santa Cruz), anti-lamin A/C (Santa Cruz), anti-Flag (Sigma) and anti-Myc (Upstate).

3.2.3 In Vivo Complex of Methylase Assay

In vivo complex of methylase (ICM) assays were performed as described in Liu et al. (11). A detailed procedure is also described in material and methods of Chapter 1. For the double CsCl gradient experiment, the first gradient DNA fractions were pooled, ethanol precipitated and resuspended in TE buffer (20 mM Tris/HCl, pH 8.0, 1 mM EDTA). RNaseA (100 U, Roche) was added and incubated for 1 h at 37 ^{o}C. RNase A treated or not treated samples were loaded onto a second CsCl gradient. To see the effect of GADD45α on DNMT1-DNA complex formation, cells were transfected with Myc-GADDD45α for 4 h and fresh medium was added (or medium containing 1 μM aza-dC). After 1 or 2 days, cells were treated with 1 μM aza-dC for 1 day or 10 μM for 1 h. DNMT1-DNA complexes were resolved by CsCl gradient and analyzed by slot blot assay. The immune complex was detected with Amersham's enhanced chemiluminescence kit. Signals were quantified using the GeneTools program (SynGene, Cambridge, UK).

3.2.4 Recovery of GADD45α from ICM DNA Pools

DNA was purified by CsCl centrifugation as described in the ICM protocol. The DNA fractions were pooled, ethanol precipitated and resuspended in digestion buffer (20 mM Tris/HCl, pH 8.0, 5 mM NaCl, 2.5 mM $MgCl_2$, 2.5 mM $CaCl_2$, 5% glycerol). S7 nuclease (200 units, Roche) and 100 U of DNase I (Roche) were added and incubated for 1 h at 37 ^{o}C. The whole

mixture was then analyzed on a 15% SDS-PAGE gel and by western blotting using anti-Myc-antibody.

3.2.5 Cellular Fractionation and Nuclear Matrix Isolation

HEK293 cells were transfected with Myc-GADD45α. For endogenous GADD45α, 10^7 HCT116 cells were irradiated by UV (10 mJ/cm^2). For the nuclear matrix preparation, cells were extracted sequentially as described in Grondin et al. (137). In brief, cells were washed in phosphate-buffered saline and subjected to hypotonic lysis in RSB buffer (10 mM Tris/HCl, pH 7.4, 10 mM NaCl, 3 mM $MgCl_2$, 0.5 mM PMSF). Cells were incubated on ice for 10 min, homogenized with a Dounce homogenizer, and centrifuged at 750g for 10 min. The supernatant was designated fraction number 1 and corresponds to the cytoplasm-containing fraction. The nuclei recovered in the pellet were subjected to subsequent subnuclear fractionation and nuclear matrix isolation. The washed nuclei were freed of the chromatin by digestion with 400 units of RNase-free DNase I (Roche) at 30 ℃ for 50 min in digestion buffer (10 mM HEPES, pH 8.0, 50 mM NaCl, 300 mM sucrose, 3 mM $MgCl_2$, 1 mM EGTA, 0.5% (v/v) Triton X-100, 1.2 mM PMSF, and 1X protease inhibitor cocktail (Roche)). The digested nuclei were then extracted by the addition of ammonium sulfate to a final concentration of 0.25 M. The 750g supernatant containing the digested chromatin was designated fraction number 2. The pellet was further fractionated after resuspension of the pellet in digestion buffer containing 2 M NaCl. The supernatant obtained after a 750g centrifugation was designated fraction number 3. The pellet was resuspended in digestion buffer and incubated for 1 h at room temperature with RNase A (Roche) at 2000 μg/ml. The fractions were then centrifuged at 750g. The supernatant and pellet treated with RNase A were designated fraction numbers 4 and 5, respectively. The fractions were subjected to western blot analysis with either anti-Myc antibody, anti-GADD45α antibody,

anti-topoisomerase IIα antibody, or anti-lamin A/C antibody. All steps used for cell fractionation and nuclear matrix isolation were performed at 4 ℃ unless otherwise specified.

3.2.6 Surface Plasmon Resonance

DNA-protein interaction analysis was performed by Surface Plasmon Resonance (SPR) experiments using a Reichert SR7000 SPR refractometer (Reichert Inc., Depew, NY, USA). Biotinylated hemi- or unmethylated DNA oligomers (50 μl) were immobilized to neutravidin-coated sensor slide (Reichert Inc., Depew, NY, USA) at a flow rate 6.67 μl/min. Unbound oligomers were washed off with PBS containing 0.2% Tween 20. HBS buffer (10 mM HEPES, pH 7.4, 150 mM NaCl, 3 mM EDTA) was used as running buffer. To determine equilibrium dissociation constants (K_D) for DNA-protein interactions, various concentrations of each protein were applied to the immobilized DNA oligomers at a flow rate of 13.3 μl/min at 37 ℃ in HBS buffer. Reichert Labview software was used for data collection. Biologic Scrubber 2 software (Campbell, Australia) was used for curve fitting and data analysis.

3.2.7 DNA Oligomers

The following DNA oligomers were used in this study. For SPR experiments, biotinylated hemi- or unmethylated DNA oligomers were prepared by annealing complimentary single strand DNAs. D1subHMF: 5'-GAA GCT GGG ACT TCM GGC AGG AGA GTG CAA-3' or D1subUMF: 5'-GAA GCT GGG ACT TCC GGC AGG AGA GTG CAA-3' single strand DNA was annealed to Bt-D1subUMR: 5'-Bt-TTG CAC TCT CCT GCC GGA AGT CCC AGC TTC-3' generating hemi- or unmethylated DNA oligomers (where M and Bt denote 5-methylcytosine and biotin, respectively). Oligonucleotides were purchased from Integrated DNA Technologies. Double-stranded oligonucleotides were annealed by mixing equal amounts

of complimentary oligonucleotides, heating to 95 ℃ for 5 min, 65 ℃ for 10 min, and slowly cooling to 20 ℃. For in vitro DNA methyltransferase assays, the same single strand DNAs were used without biotinylation, to make hemi- or unmethylated DNA oligomer substrates.

3.2.8 Flow Cytometry Analysis

Cells were transfected with I-SceI and wild type or mutant Myc-GADD45α and after 3 or 7 days, were treated with trypsin and collected. After two washes with PBS, cells were resuspended in 500 µl of PBS 1X and 6 X 10^4 cells were analyzed using FACSCalibur (BD Biosciences).

3.2.9 In Vitro Methyltransferase Assays

DNA methylation activity of purified DNMT1 was measured by the incorporation of tritiated methyl group from labeled S-adenosyl-L-[methyl-^{3}H] methionine (PerkinElmer) into an oligonucleotide substrate containing a single CpG site in hemimethylated form. Methylation reactions were carried out at concentration with 0.5 µM DNA oligomers, 0.5 µCi SAM, and 100 ng of DNMT1 in assay buffer (20 mM Tris/HCl, pH7.5, 5 mM EDTA, 5 mM DTT, 1 mM PMSF, and 10% glycerol) at 37 ℃. Reactions were stopped by adding phenol/chloroform and DNA was precipitated by adding same volume of isopropyl alcohol. DNA pellets were dissolved in TE buffer and transferred to Whatman filter paper, and radioactivity was determined using LS6500 scintillation counter (Beckman Coulter).

3.2.10 Intein Mediated Purification of GADD45α

pTXB1-GADD45α was transformed into *E.coli* BL21(DE3). The cells were grown in LB broth with 100 µg/ml ampicillin at 37 ℃ and induced with 0.5 mM IPTG at an OD_{600} of 0.4

for 4 h. The cells were collected by centrifugation and the pellet resuspended and sonicated in pH 8.5 chitin column buffer (20 mM Tris/HCl, 0.5 M NaCl, 1 mM DTT, 0.1 mM EDTA and 0.1% Triton X-100) supplemented with 1X protease inhibitor cocktail (Roche). The clarified cell lysate was loaded onto a chitin column equilibrated with pH 8.5 column buffer and the column was washed with 20 bed volumes of Wash buffer (20 mM Tris/HCl, pH 8.5, 1 M NaCl, 1 mM EDTA, and 0.3% Triton X-100). The column was then flushed with cleavage buffer (30 mM Tris/HCl, pH 8.5, 0.5 M NaCl, and 40 mM DTT) to trigger splicing. After 18 h, the splicing and cleavage products were eluted. The eluted fractions were pooled and dialyzed against dialysis buffer (25 mM MOPS/KOH pH 7.0, 1 mM EDTA, 1 mM DTT, 0.2 mM KCl, and 10% glycerol). The entire purification process was conducted at 4 ℃.

3.3 Results

3.3.1 GADD45α Strongly Binds to DNA.

To gain insight into the function of GADD45α in DNA demethylation, we first sought to address whether GADD45α interacts or associates with DNA under physiological conditions. Although it has been reported that it lacks discernable demethylase activity (132), we want to confirm it using ICM assay. If GADD45α has a similar activity to that of glycosylase (removes methyl group from methyl-cytosine), it might form a stable or covalent intermediate with cytosine (138,139). Since the ICM assay involves the separation of DNA bound protein from free protein by CsCl density buoyant gradient (11), we tested whether over-expressed GADD45α could be detected in the DNA fraction from CsCl density gradient. HCT116 cells were transfected with Myc epitope tagged GADD45α (Myc-GADD45α), incubated for 20 h or 40 h, and harvested. Cells were lysed and loaded onto CsCl gradient separating DNA and free protein. The gradient fractions were analyzed by slot blot assay. We found that Myc-GADD45α was readily detected in the DNA peak fraction (Fig. 28) in proportion to the duration of GADD45α expression (compare row 1 and 2) and was not seen in negative controls that did not contain Myc-GADD45α (row 3). The positive signal in DNA fraction with anti-GADD45α was confirmed by probing a twin membrane with anti-Myc antibody (Fig. 28 right panel).

Although we have shown that the DNA fraction reacts with anti-GADD45α or anti-Myc antibody, additional data confirm that the positive signal was indeed due to GADD45α protein. To rigorously address this question, we recovered Myc-GADD45α protein from DNA fractions (DNA fractions were pooled and precipitated using isopropyl alcohol). The DNA was digested fully with S7 nuclease and analyzed by SDS-PAGE followed by western blot analysis. As

shown in Fig. 29, a polypeptide of the predicted size of Myc-GADD45α (~20 kDa) was recovered from DNA fractions indicating that the signal in DNA fractions was indeed GADD45α and not simple "carry over" in the gradient. Note also that S7 digestion was essential for GADD45α release from the DNA. Taken together, these data suggest that GADD45α forms a highly stable, possibly covalent intermediate with DNA.

3.3.2 DNA Binding of GADD45α is not Dependent on DNMTs.

Since Barreto et al. (132) has reported that GADD45α is not a demethylase, our ICM data raised a question of how GADD45α could bind DNA under conditions of high salt (> 5 M CsCl). One possible mechanism is that GADD45α interacts strongly with a DNA bound protein, which itself is connected to DNA covalently. Thus, we tested whether the localization of GADD45α to DNA is dependent on endogenous DNA methyltransferase activity. Cells transfected with Myc-GADD45α were treated with aza-dC to trap endogenous DNM/DNA adducts. If GADD45α depends on a methylase "tether", its DNA binding should also be dependent on aza-dC; however, this was not a case, as shown in Fig. 30. The GADD45α signal in DNA fraction did not depend on aza-dC (right panel). In contrast, the DNMT1 signal was strongly dependent on aza-dC (left panel). GADD45α was detected in both samples regardless of aza-dC. The data show that DNA binding by GADD45α is independent of DNMT1.

GADD45α is a small protein with an amino acids sequence homology to ribosomal proteins (140). Since many ribosomal proteins are known to interact with multiple RNA elements (141), we were concerned about RNA contamination in the DNA region of the CsCl density gradient; thus, we tested whether the signal in ICM assay was possibly due to RNA

bound GADD45α. To clarify this issue, we performed two successive CsCl density gradients pooling the first DNA peak and rerunning on a second gradient. Briefly, DNA fractions were pooled from the first gradient and digested with RNase A extensively. The RNase A treated DNA was then loaded onto a second CsCl gradient. This double CsCl gradient procedure allows us to obtain high purity RNA-free genomic DNA. Fig. 31 shows that the GADD45α signal in DNA fraction is not dependent on the presence of RNA. The signal was detected in both RNase A treated and non-treated samples (compare row 3 and 4). In addition, the double CsCl gradient also eliminates a potential false positive signals caused by the contamination of free protein in the DNA pool. Although the signal strength in the 2nd DNA pools is reduced due to poor recovery, the GADD45α signal was readily detected in DNA fraction (compare row 1 and 2).

Taken together, the GADD45α signal in DNA fractions suggests that GADD45α strongly binds to or associates stably with DNA, in living cells.

3.3.3 GADD45α is a Nuclear Matrix Protein.

In the ICM assay, cells are lysed with the ionic detergent, sarkosyl. Sarkosyl, at 1%, effectively disrupts electrostatic protein-protein, and protein-DNA complexes. In addition, the very high concentration of CsCl (> 5 M ionic strength) further disrupts ionic interactions. In other words, the GADD45α signal in the DNA fraction must be exceptionally robust. Often nuclear matrix associated proteins show strong stable DNA binding, especially in matrix regions (142). This prompted us to examine whether GADD45α localizes to the nuclear matrix.

HEK293 cells were transfected with Myc-GADD45α plasmid and 24 h later nuclear matrix preparations were performed according to the protocol of Grondin et al. (137) with some slight modification (see material and methods and Fig. 32). Nuclei were prepared from

transfected cells and proteins were sequentially removed by treating nuclei with DNase I, 2 M NaCl, and RNase A (Fig. 32). An equal portion of each extract was then analyzed by western blotting. Human topoisomerase IIα (topo IIα, a known nuclear matrix control protein (143)) served as an internal marker for the nuclear matrix fractionation protocol (Fig. 33 upper panel). Most of topo IIα was released in the DNase I chromatin fraction, however, a small, but reproducible amount was recovered from nuclear matrix fractions. Most of Myc-GADD45α was also associated with nuclear matrix (Fig. 33 bottom panel, lane 5). Significant amounts of Myc-GADD45α were also localized to cytosol and chromatin fractions (Fig. 33 lane 1 and 2). The localization of Myc-GADD45α in chromatin fraction agrees with other reports since GADD45α is known to interact with core histones (122). However, the localization to cytosol fraction is not clear, and may be an overexpression artifact.

To confirm the localization of GADD45α to nuclear matrix region, we determined the localization of endogenous GADD45α using the same fractionation method. Since GADD45α is UV inducible (111), we UV irradiated HCT116 cells. Cells were then incubated for 6 h, harvested, and subjected to fractionation. Much of the endogenous GADD45α was found in the cytosol fraction with very little in matrix fraction (Fig. 34 middle panel, lane 1); however, endogenous GADD45α was observed in matrix region when we loaded five fold more of the matrix fraction (Fig. 34 middle panel, lane 6). The GADD45α bands shown in middle panel are specific, because there were no bands observed in fractions from non-UV treated cells (Fig. 34 upper panel). To further demonstrate that the cytosol localization of GADD45α is not caused by contamination of nuclear fraction, we probed membrane with anti lamin A/C antibody. This antibody allows us to confirm clear separation between cytosol and nuclear fractions, and lamin

A/C serves as a nuclear matrix marker. As expected, lamin A (74 kDa) and C (65 kDa) were predominantly found in nuclear matrix region (Fig. 34 bottom panel, lane 5 and 6). Also these data show that the cytosol fraction was not contaminated by nuclear fractions (compare lane 1 and 2 at bottom panel). Thus, endogenous UV induced GADD45α is found in both the cytosol and the nuclear matrix.

3.3.4 GADD45α Binds to DNA and Prefers Hemimethylated DNA.

The results of the ICM assay and the localization to nuclear matrix suggest that GADD45α binds strongly to DNA. However, it is still unclear whether GADD45α binds to DNA directly or through other proteins (we know it does not bind through DNMT, see Fig. 30). We therefore employed the surface plasmon resonance (SPR) technique to quantify the physical interaction of GADD45α with DNA. SPR assay is a real-time analysis that was developed as a methodology for determining molecular binding constants (144). With this method, a protein of interest is injected over a sensor slide containing DNA. An interaction between DNA and protein increases the mass on the sensor slide changing the resonance angle of reflected light. Two sensor slides containing hemimethylated or unmethylated DNA were prepared as described in Material and Methods. Our detection system was validated by the robust signal produced with purified DNMT1 and hemimethylated DNA oligomers (Fig. 35C). We analyzed the interaction between GADD45α and DNA at various concentrations (100, 200, 400, and 1600 nM) of GADD45α (Fig. 35). Fig. 35 shows the association, represented by an increase in Micro Refractive Index Unit (Micro RIU). Hemimethylated DNA oligomers immediately associated with GADD45α and slowly dissociated from it (Fig. 35B), while unmethylated DNA oligomers slowly associated with GADD45α (Fig. 35A). Micro RIU values of GADD45α to both hemi-

and unmethylated DNA increased in a dose dependent manner. The equilibrium dissociation constant (K_D) values were determined to be 0.28 μM and 44.9 μM for hemimethylated DNA and unmethylated DNA, respectively; thus, the K_D for hemimethylated DNA is 160 times lower than for unmethylated DNA, indicating that GADD45α has much higher binding affinity for hemimethylated DNA. Even the K_D value of GADD45α for hemimethylated DNA is much lower than that of DNMT1 (3.8 times lower, compare Fig. 35 B and C). This is the first demonstration that GADD45α directly binds to DNA and has a substantial preference for hemimethylated DNA.

3.3.5 GADD45α Interacts with DNMT1.

DNMT1 methylates repaired region during HR (105). Interestingly, the initial DNA methylation seems to be directed to only one strand and subsequent cell division generates two populations of GFP positive cells (high and low expressor clones). In high expressor cells, the recombined region was hypomethylated and in low expressors, the region was hypermethylated. This raised an obvious mechanistic question regarding how one strand is methylated during homologous recombination (HR). One intriguing idea is that DNMT1 might methylate one or both strands; however, one strand could be demethylated or, alternatively, one strand protected from methylation. Since active demethylation has not been reported in mammals, we hypothesized that some factor might inhibit or redirect DNMT1 resulting in single strand specific methylation yielding a hemimethylated template. As a putative factor we examined GADD45α, which as noted above, is induced by DNA damage and implicated in active demethylation (112,132). In addition, GADD45α has an acute preference for hemimethylated DNA. We first, investigated whether GADD45α interacts with DNMT1. HEK293FT cells were co-transfected

with DNMT1-V5, Myc tagged GADD45α, and 24h later, cells harvested and lysed. Whole cells extracts were subjected to immunoprecipitation using anti-V5 antibody to bring down DNMT1. The immune complexes were eluted, separated on SDS-PAGE followed by western blot analysis, and probed with anti-Myc antibody to test for co-immunoprecipitated Myc-GADD45α. As shown in Fig. 36, DNMT1-V5 and Myc-GADD45α are binding partners. In figure 36A, Myc-GADD45α was co-immunoprecipitated with DNMT1-V5 (lane 1). Although some amount of Myc-GADD45α was precipitated by itself (lane 3), more Myc-GADD45α was co-immunoprecipitated with DNMT1-V5 (compare lanes 1 and 3). To confirm this interaction, we performed immunoprecipitation using anti-Myc antibody to bring down Myc-GADD45α first, and checked co-immunoprecipitated DNMT1-V5 using anti-DNMT1 antibody. Figure 36B shows that DNMT1 was co-immunoprecipitated with Myc-GADD45α (lane 1) and was dependent on Myc-GADD45α (lane 2).

3.3.6 Catalytic Domain of DNMT1 is Required for the Interaction with GADD45α.

To map the interaction domain of DNMT1, we generated a series of DNMT1 deletion mutants. All three deletion mutants were V5 tagged (Fig. 37A). HEK293FT cells were transfected with each DNMT1 deletion mutant plus Myc tagged GADD45α, and 24h later, cells were harvested and lysed. Whole cell extracts were subjected to immunoprecipitation using anti-V5 antibody to recover DNMT1. The immune complexes were analyzed by western blotting using anti-Myc antibod. As shown in Fig. 37B, Myc-GADD45α was co-immunoprecipitated with a DNMT1 deletion mutant containing residues 1114 to 1616, which contains only the catalytic domain of DNMT1.

To determine whether the interaction between GADD45α and the catalytic domain of DNMT1 is direct or not, we applied a GST pull-down assay with recombinant human GADD45α and GST fused DNMT1 deletion mutants (Fig. 38A) purified from *E.coli*. As shown in Fig. 38B, GADD45α was co-purified with GST fused DNMT1 catalytic domain (GST-D1-1100-1616), but not with GST alone or other DNMT1 deletion mutants. This confirms the interaction of GADD45α with the catalytic domain of DNMT1 and indicates that the two proteins bind directly without the need for an intermediate factor, at least in vitro.

3.3.7 GADD45α Interacts with DNMT3a and DNMT3b.

The catalytic domains of all major mammalian DNMTs are quite conserved. Since GADD45α interacts with the catalytic domain of DNMT1, we tested whether GADD45α also interacts with de novo methylase enzymes, DNMT3a and DNMT3b. We performed a co-immunoprecipitation experiment with V5 epitope tagged DNMT3a, Flag epitope tagged DNMT3b and Myc-GADD45α. HEK293FT cells were co-transfected with Myc-GADD45α and DNMT3a-V5 or Flag-DNMT3b. We immunoprecipitated each DNMT using anti-V5 antibody for DNMT3a or anti-Flag antibody for Flag-DNMT3b. Immune complexes were separated on SDS-PAGE and subjected to western blot using anti-Myc antibody to check co-immunoprecipitated Myc-GADD45α. Myc-GADD45α co-immunoprecipitated with full length DNMT3a and DNMT3b (Fig. 39 lane 1, 2, and 4). Without co-expressed DNMTs, no Myc-GADD45α was recovered (lane 3 and 5).

Taken together, GADD45α interacts with all major mammalian DNMTs and the catalytic domain of each DNMT might be required for the interaction with GADD45α.

3.3.8 Analysis of GADD45α Point Mutations that Reduces DNMT1 Interaction.

GADD45α is a small, acidic protein of 165 residues. It does not have any obvious or distinctive DNA binding motif or domain. To determine the region of GADD45α involved in interaction with DNMT1, we systematically changed two consecutive amino acids, which reside in clustered charged, polar, or hydrophobic regions. Four point mutants were generated, RT34AD (R34A, T35D), LC56AA (L56A, C57A), ED63AA (E63A, D64A), and CE83AA (C83A, E83A) (Fig. 40). These four mutants were tested for interaction with DNMT1 by co-immunoprecipitation analyses. HEK293FT cells were co-transfected with Myc epitope tagged point mutants and DNMT1-V5. DNMT1-V5 was immunoprecipitated using an anti-V5 antibody and co-immunoprecipitation with each GADD45α mutant was evaluated by western blotting. As shown in Fig. 41, all four mutants showed less interaction than that of wild type GADD45α (Fig. 41A). Note that the yield of immunoprecipitated DNMT1-V5 in each sample is different; therefore, the amount of co-immunoprecipitated GADD45α mutant was adjusted with the amount of precipitated DNMT1-V5 after bands were quantified. Each immunoprecipitated mutant signal was normalized with regard to immunoprecipitated DNMT1 levels and expressed as a percent of wild type control (Fig. 41B). The RT34AA mutant showed the lowest binding with DNMT1 (its interaction was reduced by 76%). The interaction of CE83AA mutant with DNMT1 was also reduced to 32%, compared to that of wild type (Fig. 41B); thus, this mutant is interesting since the L80E in GADD45γ has a defect in dimerization and the position of C83 and E84 residues are very close to L77 residue, which corresponds to L80 of GADD45γ (see below and Fig. 42). Thus, we made two additional single point mutants, L77E and C83E. As expected, both mutants showed reduced interaction with DNMT1.

3.3.9 The Di- or Oligomerization of GADD45α is Required for DNMT1 Interaction.

GADD45α is known to oligomerize with self or with other GADD monomers (145). In addition, a recent report showed that the L80E mutation of GADD45γ abolishes its dimerization (146) Leu80 of GADD45γ resides in a α-helix 3 (α3) domain, which is highly conserved among all GADD proteins (Fig. 42B). Interestingly, CE83AA mutation is also part of the α3 region. This raised a question whether oligo- or dimerization of GADD45α might be important in DNMT1 interaction. Thus, we tested whether the CE83AA mutant of GADD45α could self-associate in the cell using Myc tagged GADD45α CE83AA and V5 epitope tagged GADD45α CE83AA. In addition, other point mutants, RT34AA, LC56AA, ED63AA, L77E, and C83E, were similarly tested using Myc or V5 tagged versions of each point mutant. HEK293FT cells were transfected with both constructs (Myc- and V5 tagged). From whole cell extracts, Myc tagged GADD45α mutants were immunoprecipitated to check for the corresponding V5 tagged partner. As a control, cells were transfected with the Myc tagged point mutant. These controls demonstrate the specificity of the analysis. As shown in Fig. 43A, the mutants co-immunoprecipitated less than the wild type. That is, the point mutations impaired self-association of GADD45α suggesting that those residues are important for di- or oligomerization of GADD45α. Since the yield of immunoprecipitated mutants is variable (Fig. 43A, bottom panel), we adjusted the band intensity of co-immunoprecipitated proteins relative to the amount of immunoprecipitated signal for each GADD45α point mutant (Fig. 43B). The data show that the CE83AA mutant displayed the lowest self-association (reduced to 30%). However, the self-association was recovered in C83E mutant to 62% suggesting that both Cys 83 and Glu

84 play an important role in di- or oligomerization of GADD45α. Other mutants showing less interaction with DNMT1 also showed the defects in self-association (Fig. 43B).

These collective data support the notion that the oligo- or dimerization of GADD45α is important for interacting with DNMT1.

3.3.10 GADD45α Reduces DNMT1-DNA Complex Formation.

To investigate the physiological role for GADD45α in its interaction with DNMT1, we examined the effect of GADD45α overexpression on endogenous DNA methylation using the ICM assay. As described above, DNMT1 forms a covalent intermediate with its target cytosine residue during catalysis (104); however, when aza-dC is present, DNMT1 is not released from DNA resulting in irreversibly bound DNMT1 to DNA. This DNMT1-DNA complex is then measured using the in vivo complex of methylase (ICM) assay (11). Myc-GADD45α was transiently expressed in HCT116 cell lines and the transfected cells were treated with 1 μM aza-dC for 24 h or 10 μM aza-dC for 1 h. The amount of DNMT1-DNA complex was compared in the presence or absence of Myc-GADD45α. DNMT1 in the slot blot was dependent on aza-dC, as expected. As shown in Fig. 44, DNMT1-DNA complex formation is significantly reduced in the presence of overexpressed Myc-GADD45α. As noted, the DNMT1-DNA complex formation is dependent on aza-dC (compare row 1 and 2). However, DNMT1/DNA complex formation is severely reduced when GADD45α is overexpressed (row 5 and 6). In this experiment (row 5 and 6), cells were treated with aza-dC after 24 h or 48 h post-transfection. Since GADD45α may suppress cell growth and arrest cells at G2/M phase (147), it is possible that aza-dC might not be incorporated into genome during S phase resulting in less trapped DNMT1. To rule out this possibility, we transfected cells without serum for 4 h, then added

fresh media containing serum and aza-dC. In this way, cells were allowed an additional window for incorporating aza-dC into genome, while GADD45α was being expressed. Fig. 44 row 4 clearly showed that DNMT1-DNA complex formation is still inhibited by the presence of GADD45α (compare row 2 and 4). Since we have evidence that GADD45α interacts with the catalytic domain of DNMT1 (Fig. 37 and 38), it is reasonable to suggest that GADD45α decreases the DNMT1-DNA complex formation in the cell, probably by binding to the catalytic domain of DNMT1.

3.3.11 GADD45α Stimulates the Expression of HR Repaired GFP.

We have shown that ~50% of the cells expressing a functional GFP by gene conversion expressed GFP poorly and that silencing was associated with DNA methylation of the HR gene (Fig. 20 , 23, and ref (105)). Half of the recombinant DNA molecules were de novo methylated and half were essentially hypomethylated. DNMT1 appears to have a primary role in this process. However, the mechanism of hypomethylation of the same DNA template is mechanistically unclear. Since GADD45α is induced post-DNA damage, binds to the catalytic domain of DNMT1 and inhibits the formation of DNMT1-DNA complex (Fig. 37 and 44), we hypothesized that GADD45α might be recruited to the recombination region during HR and block the DNA methylation on one strand only. To address this, we analyzed the GFP expression following HR in HeLa-DRGFP cells in the presence or absence of transfected GADD45α. HeLa-DRGFP cells were transfected with I-SceI plasmid along with Myc-GADD45α or Myc-GADD45α CE83AA. Cells were further incubated for 7 days and GFP+ cells were analyzed by FACS. Co-expression of Myc-GADD45α significantly increased the number of GFP+ cells (Fig. 45). The increase of GFP+ cells was proportional to the amount of

Myc-GADD45α plasmid up to 0.5 μg. Above 0.5 μg, the rate of increase was not proportional (see Fig. 45 for SceI + Myc-GADD45α 1 μg sample). We note that Myc-GADD45α CE83AA mutant did not increase GFP expression. Interestingly, CE83AA mutant decreased the GFP+ cells at high dosage. That is, the cells transfected with 0.25 μg DNA showed an increase in GFP+ cells (comparable to that of wild type). However, cells transfected with more than 0.5 μg DNA showed the decrease in GFP+ cells. To determine whether other point mutants could repress the GFP+ cells, we performed the same basic experiment with the other point mutants. Since the expression levels of each point mutants varied, the level of expression was adjusted by transfecting cells with different amounts of plasmid DNA (checked by western blot, data not shown). Figure 46 clearly shows that all of other GADD45α point mutants repressed the GFP+ cells during HR. Currently, it is not clear how CE83AA and other point mutants decrease the GFP+ cells although a dominant negative mechanism seems most likely. In support of this model, we observed that each point mutant still self-associates and forms di- or oligomer, although such self-interactions are weak (Fig. 43).

We conclude that stimulation of recombinant GFP gene expression by GADD45α is caused by direct or indirect inhibition of DNMT1. These data suggest a model, where GADD45α might be involved in coordinating on regulating strand specific methylation.

3.3.12 GADD45α Inhibits the Methyltransferase Activity of DNMT1 In Vitro.

We have shown that DNA methylation decreases the expression of HR repaired DNA and that GFP expression is recovered when we inhibit DNMT1. As noted above, this increase in GFP+ cells by GADD45α overexpression strongly suggests that GADD45α inhibits DNA methylation during HR. The interaction with the catalytic domain of DNMT1 and the binding

ability to DNA also support the idea that DNA methylation was inhibited by GADD45α. However, the exact mechanism for inhibiting DNA methylation is still unclear. To directly examine a role of GADD45α in catalytic action of DNA methylase, we performed in vitro methyltransferase assays in the presence or absence of purified GADD45α. The catalytic activity of purified DNMT1 was measured using S-[methyl-^{3}H] adenosyl methionine as a methyl donor with hemimethylated or unmethylated oligonucleotide substrates. First, to determine the proper concentrations of GADD45α for the inhibition of DNMT1 activity, we performed activity assays with various concentration of GADD45α. The catalytic activity of DNMT1 was inhibited by GADD45α in dose dependent manner (Fig. 47A). The activity of DNMT1 on hemimethylated DNA substrate was reduced to 56% in the presence of 100 ng GADD45α (Fig 47B). Further reduction was not observed, even after increasing GADD45α more than 100 ng (compare 100 ng and 200 ng samples in Fig. 47A). The DNMT1 activity on unmethylated DNA substrate was also reduced to 42% with incubation of 200 ng GADD45α. Next, we determined how GADD45α might affect DNMT1 catalytic activity. To address this question, we performed a time course enzyme assay with fixed levels of GADD45α (100 ng) and DNMT1 (100 ng). At specific times, reactions were terminated and the amount of methylated DNA was determined. Without GADD45α, the reaction reached to plateau in 40 min, however, the reaction rate was reduced by 2.8 fold in the presence of GADD45α (Fig. 47C).

In summary, GADD45α inhibits the catalytic activity of DNMT1 and the degree of inhibition was dependent on the concentration of GADD45α. Also, addition of GADD45α caused a 2.8-fold reduction in reaction rate.

3.4 Discussion

We provide evidence for a plausible link between DNA repair and DNA methylation (Chapter 2). In mouse and human cells, half of the DNA molecules repaired by homology-directed repair (HR) are marked by de novo DNA methylation. As a result, linked gene expression in these repaired molecules was silenced. In the remaining molecules, the repaired molecules are hypomethylated and robustly expressed. During this study, we noticed both hypermethylated and hypomethylated products segregate in roughly 1:1 ratio. This suggests a model where DNA repair erases, then resets methylation patterns generating one hypermethylated and one hypomethylated strand. Subsequent replication of this molecule yields fully methylated and nonmethylated double-stranded daughter molecules. In other words, the methylation induced by HR is strand-selective. The mechanism of strand-selective methylation is currently unknown. However, we propose that GADD45α might be involved in the coordinating methylation events such that only one strand is methylated post HR.

Our previous data suggested that DNMT1 mediates the methylation of one strand close to the HR site, leaving the opposing strand unmethylated. How might this strand specific methylation be achieved? As a putative regulator of this process, we tested GADD45α. GADD45α is a small acidic protein that is well known as a growth suppressor following genotoxic stress. Interestingly, it has been implicated in methylation/demethylation events (132,133). A role for GADD45α in the strand specific methylation during HR can be summarized as follows. First, GADD45α physically interacts with the catalytic domain of DNMT1 (Fig. 36, 37, and 38). Coimmunoprecipitation data showed that DNMT1 deletion mutant lacking the catalytic domain did not bind GADD45α. In addition, GADD45α interacts

with other DNA methyltransferases, like DNMT3a and 3b (Fig. 39). Second, GADD45α binding to DNMT1 inhibits the methylation activity of DNMT1 in vitro and in vivo. For the in vivo experiments, we used the methylase inhibitory drug, aza-dC. The amount of endogenous DNMT1 in covalent protein/DNA complexes reflects the global methylation state in the cell. Overexpressed GADD45α strongly reduced the DNMT1/DNA complexes and thus affected global methylation (Fig. 44). The in vivo inhibition data were corroborated by in vitro methyltransferase activity assays in the presence of GADD45α (Fig. 47) using purified DNMT1. Third, the silencing of recombinant DNA following HR was partially reversed by high level expression of GADD45α. GFP expression following HR repair was reproducibly increased when GADD45α was overexpressed (Fig. 45 and 46). Fourth, DNMT1/GADD45α interaction was reduced by altering the di- or oligomerization interface of GADD45α. GADD45α CE83AA (and other point mutants) displayed reduced self-association and interacted poorly with DNMT1, relative to wild type GADD45α (Fig. 41 and 43). Fifth, GADD45α appears to inhibit DNMT1 activity at recombination sites. GADD45α or its CE83AA mutant were overexpressed in the HR repair system. When GFP expression, as a readout for methylation status, was compared, wild type GADD45α increased GFP expression, whereas CE83AA mutant did not. (Fig. 45 and 46). In summary, we provide new data suggesting that GADD45α might regulate the epigenetic silencing following homologous recombination. Based on these, a model is presented depicting DNMT1/GADD45α interplay during HR (Fig. 48). The HR repair involves strand assimilation, excision of ½ of I-SceI site and recruitment of DNMT1 to upper strand as a complex with GADD45α (dimer or oligomer). At HR sites, GADD45α might modulate DNMT1 activity by inhibiting its enzymatic activity or preventing the access of DNMT1 to the bottom strand. As a result, the methylation will be introduced on only upper strand leading two populations of GFP

expression cells. Hypermethylation will silence the HR site and hypomethylation will produce high GFP expression. We note that the dimerization (or oligomerization) of GADD45α and the stoichiometric ratio between GADD45α di- or oligomer and DNMT1 may also be important. CE83AA mutant showed weak self-association and interacted weakly with DNMT1. When this mutant was expressed at low gene dosage, it behaved like wild type GADD45α and increased GFP expression (see Fig. 45). However, at higher gene dosage, CE83AA mutant decreased GFP expression. This suggests that C83AA might bind to endogenous GADD45α and inhibit its binding to DNMT1; yet when expressed above a certain level, it resulted in a decrease of GFP expression. This model is based on an assumption that GADD45α interacts with DNMT1 and inhibits its catalytic activity. However, the detailed mechanism of inhibition is far from clear. Although we assume that the interaction between two proteins is a key mechanism for the inhibition of DNMT1 activity, we cannot rule out other direct or indirect mechanisms. For example, GADD45α binds naked DNA with a strong preference for hemimethylated over unmethylated DNA. This finding suggests another way that GADD45α might link up with hemimethylated DNA and hinder radial access of DNMT1 to its substrate DNA. Indeed, the equilibrium dissociation constant (K_D) value of GADD45α for hemimethylated DNA is 3.8 times lower than that of DNMT1 suggesting that GADD45α could compete for DNA substrate with DNMT1. Thus, GADD45α could inhibit the activity of DNMT1 by occupying its substrate DNA site. With current recombination assay system, we could not determine whether GADD45α inhibits DNMT1 activity by masking the catalytic domain of DNMT1 or the substrate of DNMT1, hemimethylated DNA.

Although detailed mechanisms of DNMT1/GADD45α interplay are not clear, our data suggest that GADD45α plays a pivotal role in modulating epigenetic silencing at HR sites. Future studies will be focused on testing following roles: 1) GADD45α might recruit DNMT1 to site of HR or vise versa. 2) GADD45α aids in chromatin remodeling at HR sites. 3) GADD45α modulates DNMT1 activity by interacting with its catalytic domain or occupying its substrate DNA. 4) GADD45α protects the cells from inappropriate gene silencing following HR repair.

Figure 28 ICM assay of Myc-GADD45α in HCT116 cells.

HCT116 cells were transiently transfected with Myc tagged GADD45α. After 20 h and 40 h post-transfection, cells were harvested and lysed. The lysates were loaded CsCl gradient. The DNA fractions of CsCl gradient were pooled, slot blotted onto membranes, and probed with anti-Myc antibody.

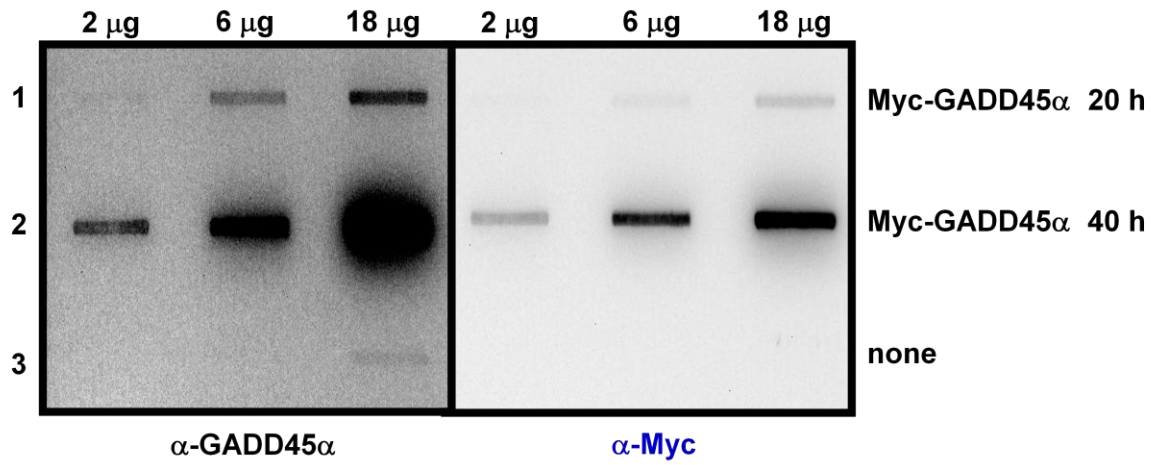

Figure 28 ICM assay of Myc-GADD45α in HCT116 cells.

Figure 29 Recovery of GADD45α from ICM DNA fractions.

HEK293FT cells were transiently transfected with Myc tagged GADD45α or empty vector, and 24 h later, cells harvested. The cellular lysates were loaded onto CsCl gradients. The DNA containing fractions were pooled and ethanol precipitated. DNA pellets were dissolved in buffer containing S7 nuclease and incubated for 1 h at 37 ℃. The whole mixture was subjected onto SDS-PAGE followed by western blot analysis, probing with anti-Myc antibody to detect the recovered Myc-GADD45α.

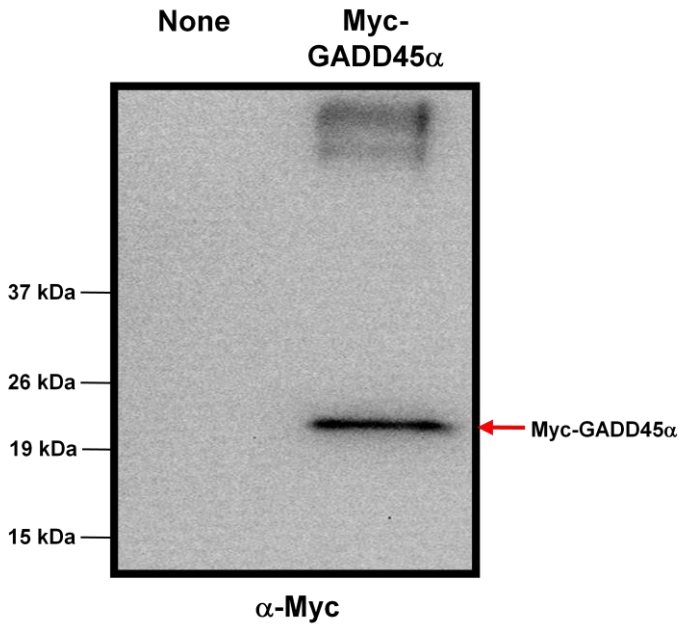

Figure 29 Recovery of GADD45α from ICM DNA fractions.

Figure 30 DNA binding of GADD45α is not dependent on DNMTs.

HeLa cells were transiently transfected with Myc tagged GADD45α,. and 24 h later, treated with 10 μM aza-dC for 1 h. The DNA fractions of CsCl gradient were pooled and probed with anti-DNMT1 antibody or anti-Myc antibody.

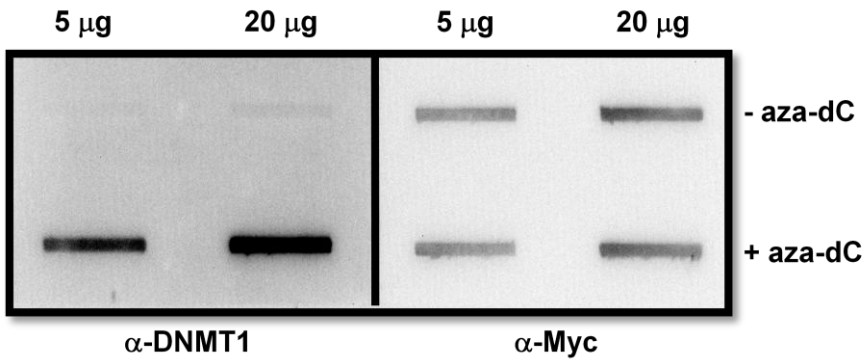

Figure 30 DNA binding of GADD45α is not dependent on DNMTs.

Figure 31 DNA binding of GADD45α is not dependent on RNA.

HEK293FT cells were transiently transfected with Myc tagged GADD45α. And analyzed 24 h later by sarkosyl lysis (see Material and Methods). The lysates were loaded onto a CsCl gradient. The DNA fractions of CsCl gradient were pooled, ethanol precipitated, and treated with RNase A extensively. The RNase A treated DNA fractions were loaded onto the 2nd CsCl density gradient. The DNA fractions from the 2nd CsCl gradient were analyzed by immunoblotting with anti-Myc antibody.

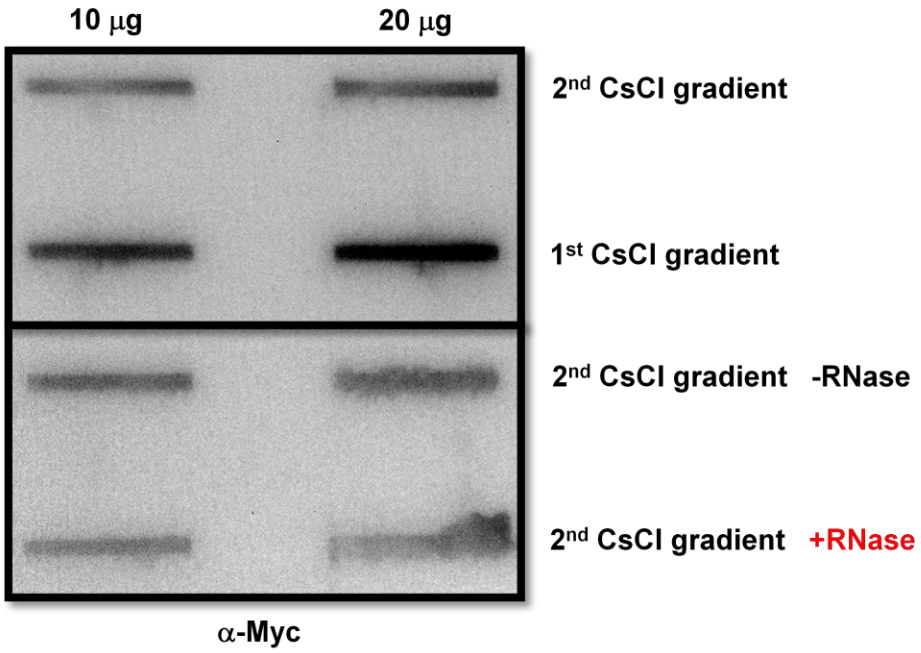

Figure 31 DNA binding of GADD45α is not dependent on RNA.

Figure 32 Schematic diagram of nuclear matrix preparation.

Nuclei were prepared as described in material and methods. The subsequent steps allowing subnuclear fractionation and nuclear matrix isolation were performed essentially as described by Grondin et al. (137).

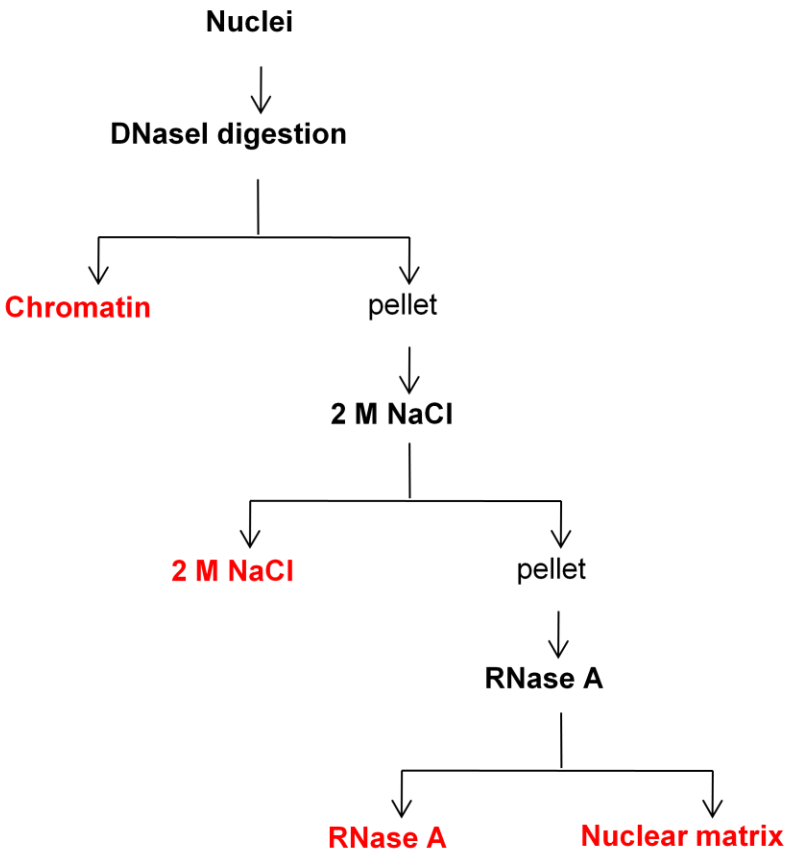

Figure 32 Schematic diagram of nuclear matrix preparation.

Figure 33 Myc-GADD45α localizes to nuclear matrix in HEK293 cells.

HEK293 cells were transfected with Myc-GADD45α and nuclei were prepared as described in material and methods. Subnuclear fractionation and nuclear matrix isolation were performed and an equal portion of each fraction was analyzed by western blot with anti-Myc antibody or anti-Topo IIα antibody. Note that part of membrane for Topo IIα western blot was replaced with high exposed image (in lane 5).

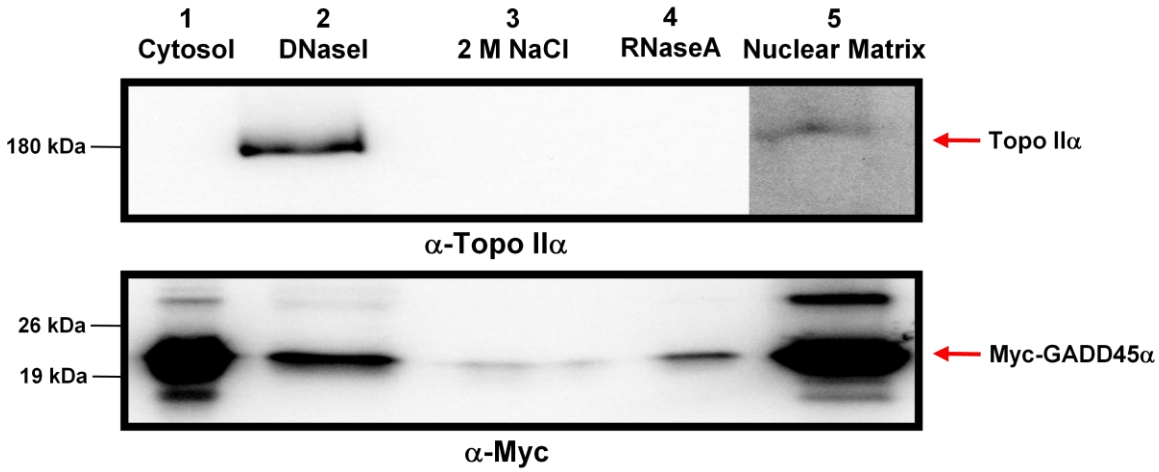

Figure 33 Myc-GADD45α localizes to nuclear matrix in HEK293 cells.

Figure 34 Endogenous GADD45α localizes to nuclear matrix in HCT116 cells.

HCT116 cells were irradiated with UV (10 mJ/cm^2) and further incubated for 6h. Nuclei were prepared and subnuclear fractionation was performed (Fig. 32). Subnuclear fractionation from control cells (non UV irradiated) is shown in upper panel. Middle and lower panels show the subnuclear fractionation from UV irradiated cells. An equal portion of each fraction was analyzed by western blot with anti-GADD45α antibody or anti-lamin A/C antibody. In lane 6, five fold more protein was loaded to detect low levels of GADD45α protein. Note that anti-lamin A/C antibody detects both lamin A (74 kDa) and lamin C (65 kDa).

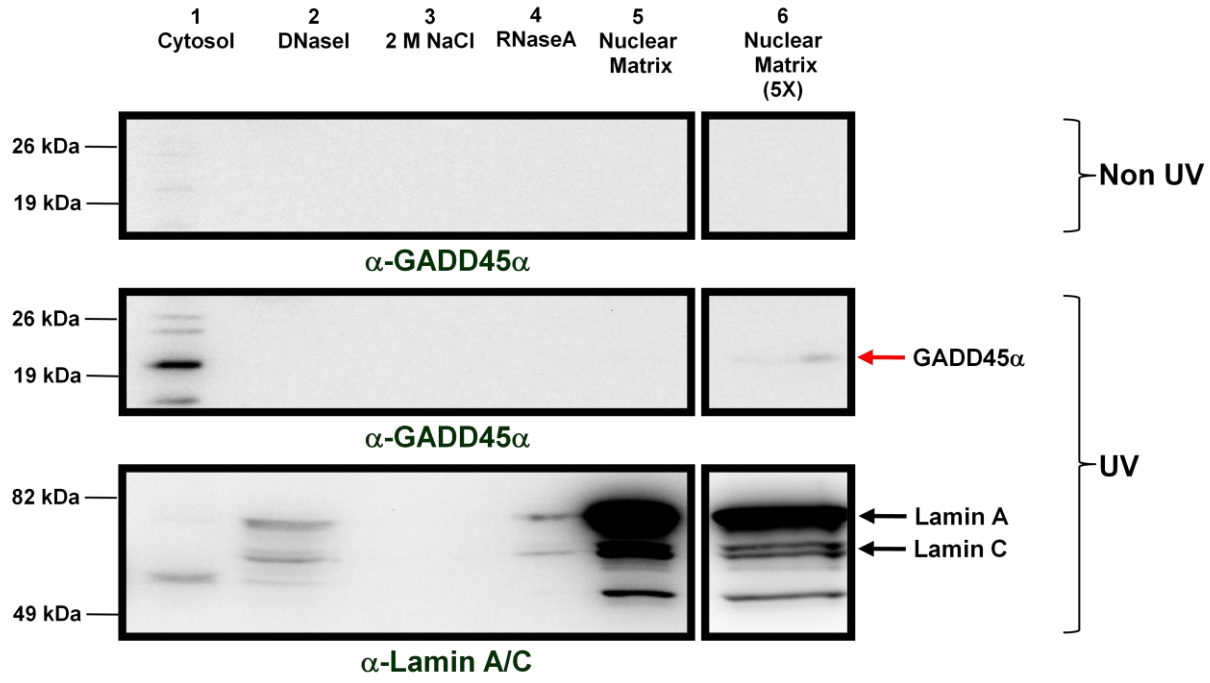

Figure 34 Endogenous GADD45α localizes to nuclear matrix in HCT116 cells.

Figure 35 GADD45α binds to DNA and prefers hemimethylated DNA.

Biotinylated hemi- or unmethylated oligomer DNA was immobilized on the neutravidin surface of a gold sensor slide. Various concentrations of GADD45α or DNMT1 were applied to each DNA-immobilized sensor slide. Exactly 25 μl of each concentration was injected at a flow rate of 13.3 μl/min. The Micro Refractive Index Unit (Micro RIU) reflects DNA-protein interactions. The micro RIU of GADD45α or DNMT1 binding to DNA increased in proportion to concentration. (A) GADD45α binding to unmethylated oligomers. (B) GADD45α binding to hemimethylated oligomers. (C) DNMT1 binding to hemimethylated oligomers. The sensorgrams have been corrected by subtraction of a reference cell and zeroed on the y and x-axes, where y gives the increase in Micro RIU, and x is time in seconds.

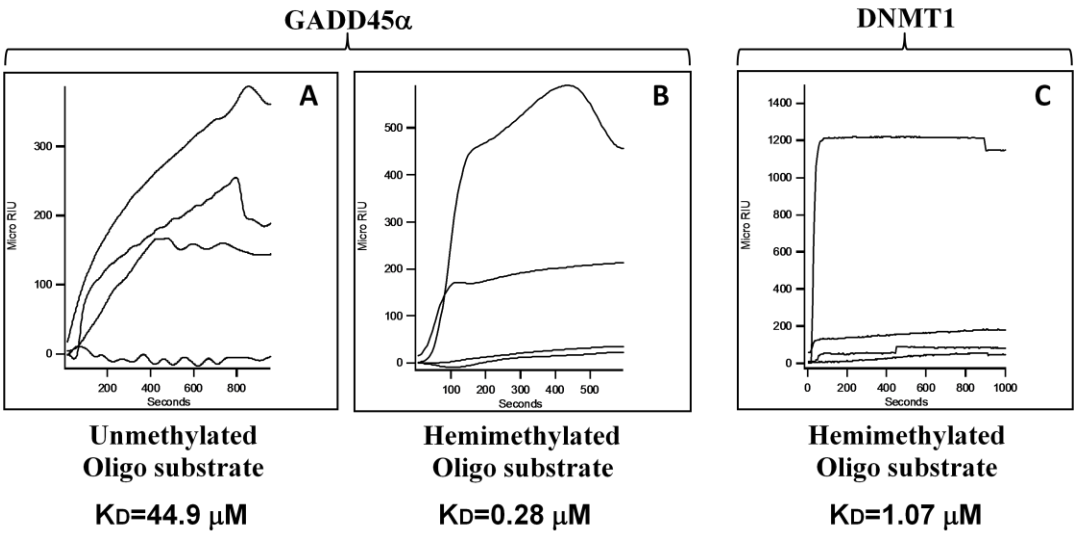

Figure 35 GADD45α binds to DNA and prefers hemimethylated DNA.

Figure 36 DNMT1 interacts with GADD45α.

DNMT1-V5 was co-transfected with Myc-GADD45α into HEK293FT cells. (A) DNMT1-V5 was immunoprecipitated from the transfected whole cell extracts with anti-V5 antibody. Immunoprecipitates were analyzed by western blotting using anti-Myc antibody. The yield of immunoprecipitated DNMT1-V5 was monitored using anti-DNMT1 antibody (lower panel). (B) Whole cell extracts were immunoprecipitated with anti-Myc antibody and precipitated proteins analyzed by western blotting with an anti-DNMT1 antibody to probe co-immunoprecipitated DNMT1-V5 or with anti-Myc to measure the total recovery of Myc-GADD45α (lower panel).

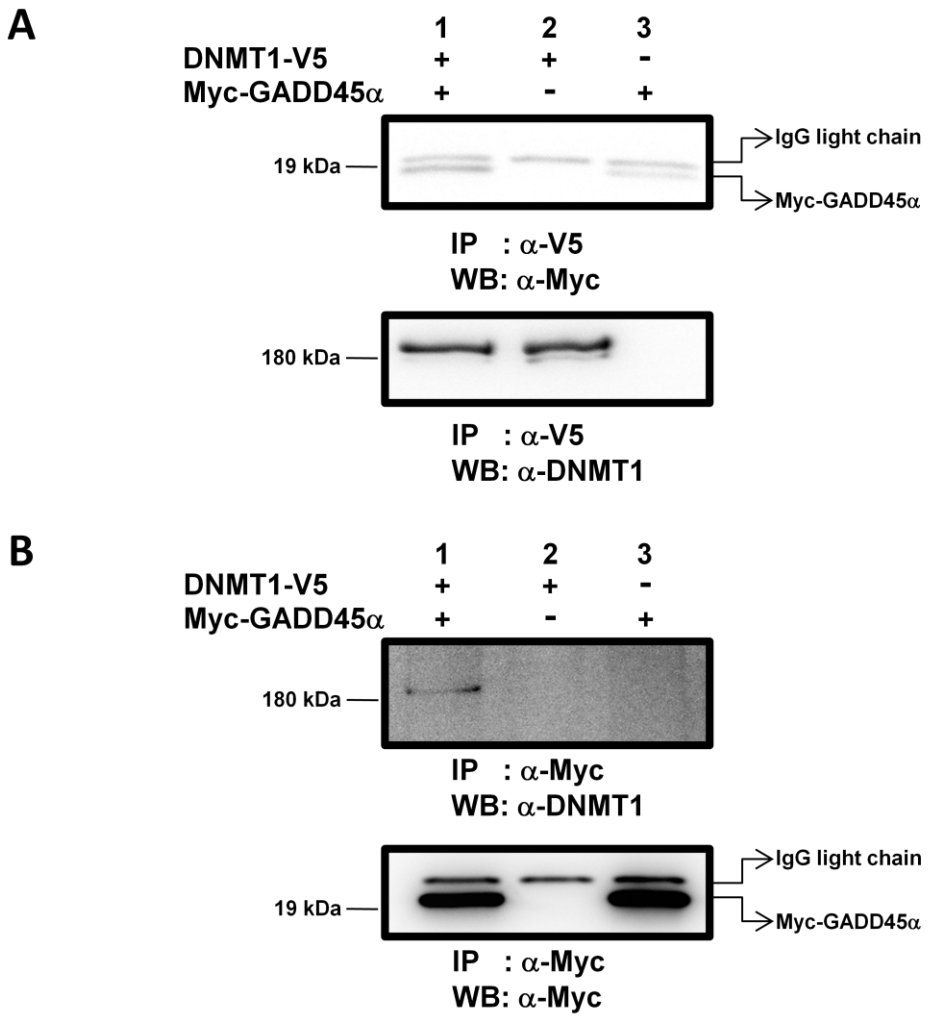

Figure 36 DNMT1 interacts with GADD45α.

Figure 37 GADD45α interacts with the catalytic domain of DNMT1.

Panel A depicts a schematic representation of V5 epitope tagged DNMT1 deletion mutants. Panel B tests for interactions of each DNMT1 deletion mutant with GADD45α. Each of the DNMT1 deletion mutants was co-transfected with Myc-GADD45α into HEK293FT cells. Whole cell extracts were immunoprecipitated with anti-V5 antibody and precipitated proteins analyzed by western blotting with an anti-Myc antibody to probe co-immunoprecipitated GADD45α or with anti-V5 to measure the total recovery of each deletion mutant (lower panel).

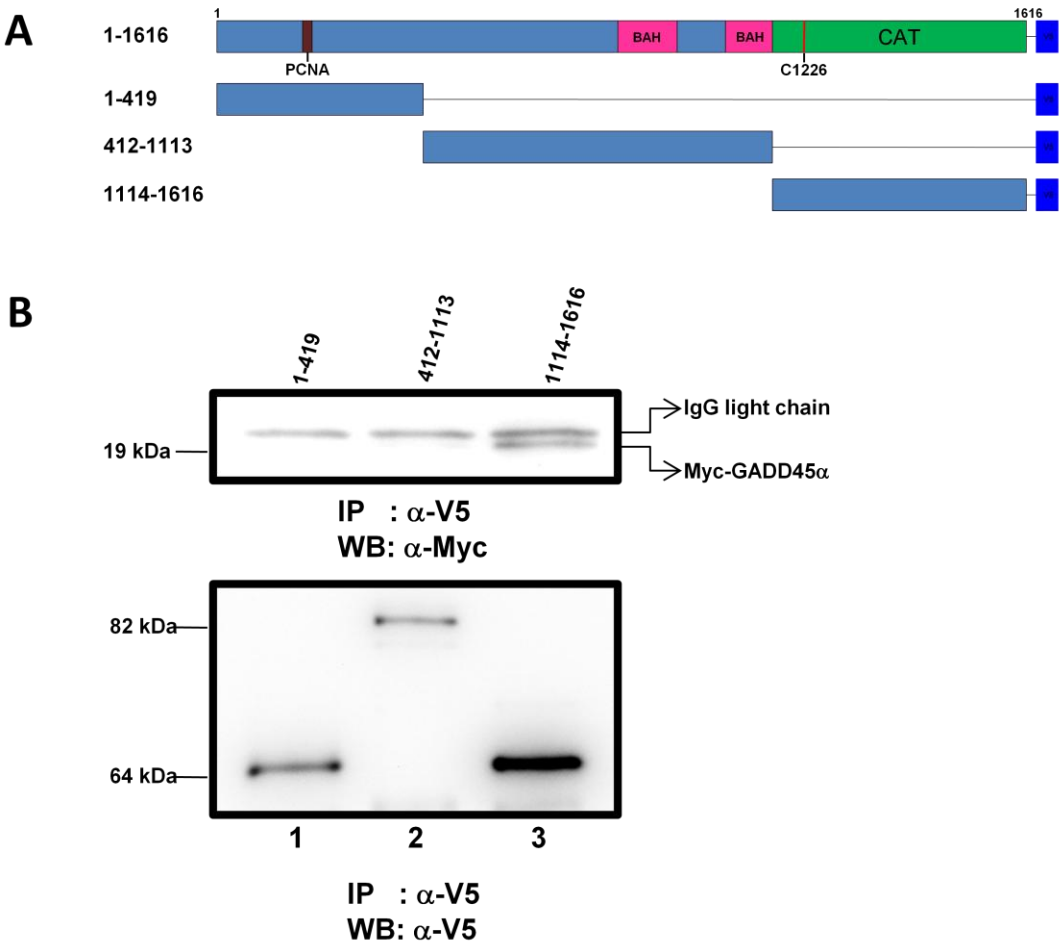

Figure 37 GADD45α interacts with the catalytic domain of DNMT1.

Figure 38 GADD45α interacts directly with the catalytic domain of DNMT1 in vitro.

(A) A schematic representation of GST fused DNMT1 deletion mutants. (B) Panel B tests for direct interaction of each DNMT1 deletion mutant with GADD45α. Each deletion mutant was purified from *E.coli* and mixed with purified GADD45α. The GST deletion mutants were purified using Glutathione-Sepharose 4B and determined whether GADD45α co-purified with DNMT1 deletion mutant. Upper panel shows coommassie blue staining of each protein and lower panel shows western blotting with anti-GADD45α antibody.

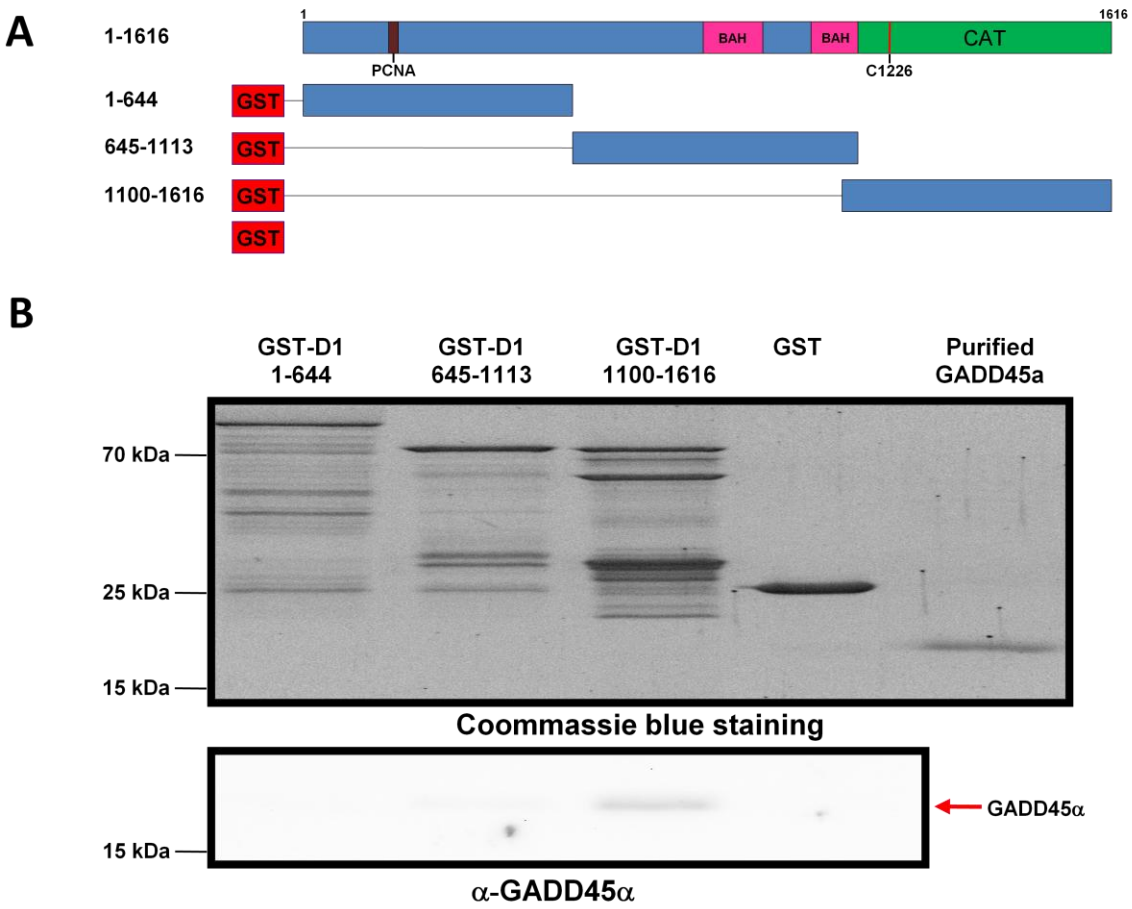

Figure 38 GADD45α interacts directly with the catalytic domain of DNMT1 in vitro.

Figure 39 GADD45α interacts with DNMT3a and DNMT3b.

Myc-GADD45α was co-transfected with DNMT1-V5, DNMT3a-V5, or Flag-DNMT3b into HEK293FT cells. DNMT1-V5 and DNMT3a-V5 were immunoprecipitated from the transfected whole cell extracts with anti-V5 antibody. Flag-DNMT3b was immunoprecipitated with anti-Flag antibody. The immunoprecipitates were analyzed by western blotting using anti-Myc antibody. The yield of immunoprecipitated DNMT1-V5 was checked using anti-V5 antibody for DNMT1-V5 and DNMT3a-V5 (lower left panel) or anti-Flag antibody for Flag-DNMT3b (lower right panel).

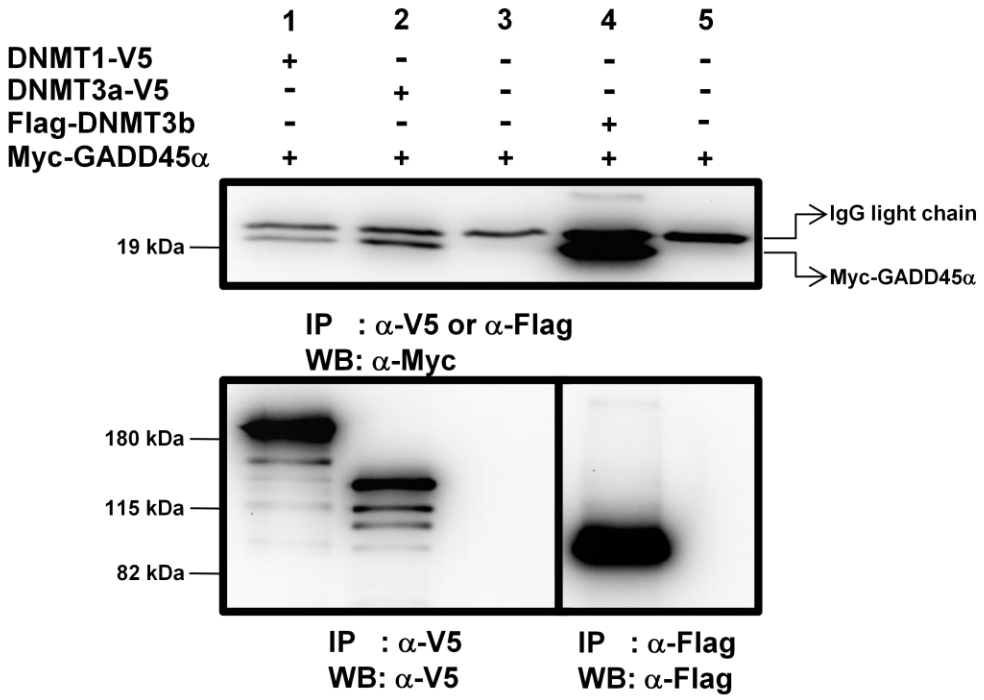

Figure 39 GADD45α interacts with DNMT3a and DNMT3b.

Figure 40 Alanine scanning mutagenesis of GADD45α.

The locations of al point mutations are indicated. The regions having four to six consecutive polar, hydrophobic, or charged amino acids were selected as primary targets for mutagenesis. Two consecutive amino acid residues in those regions were replaced with two alanine residues.

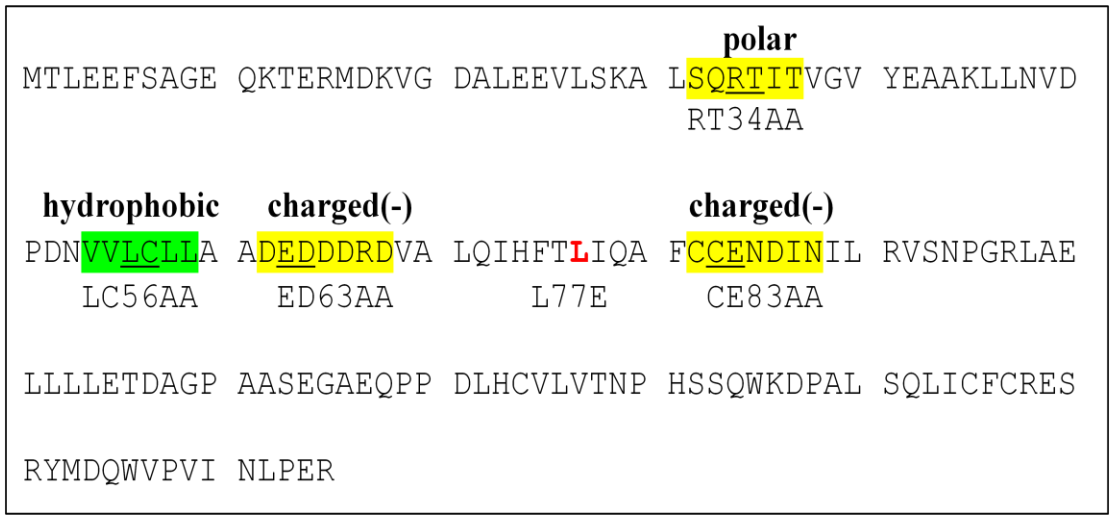

Figure 40 Alanine scanning mutagenesis of GADD45α.

Figure 41 Interaction of each GADD45α point mutant with DNMT1.

(A) Interactions of GADD45α mutants with DNMT1 was evaluated. Each GADD45α point mutant was co-transfected with DNMT1-V5 into HEK293FT cells. Whole cell extracts were immunoprecipitated with an anti-V5 antibody and precipitated proteins analyzed by western blotting with an anti-Myc antibody to probe co-immunoprecipitated GADD45α or with anti-V5 to measure the recovery of DNMT1-V5 (lower panel). An asterisk indicates IgG light chain and an arrow indicates the co-immunoprecipitated each GADD45α point mutant.

(B) Band intensities of co-immunoprecipitated GADD45α point mutants (A) were quantified using the GeneTools program (SynGene, Cambridge, UK). The amount of co-immunoprecipitated GADD45α was normalized by the amount of immunoprecipitated DNMT1 and plotted as a relative amount against wild type band intensity. The statistical data are based on three independent experiments.

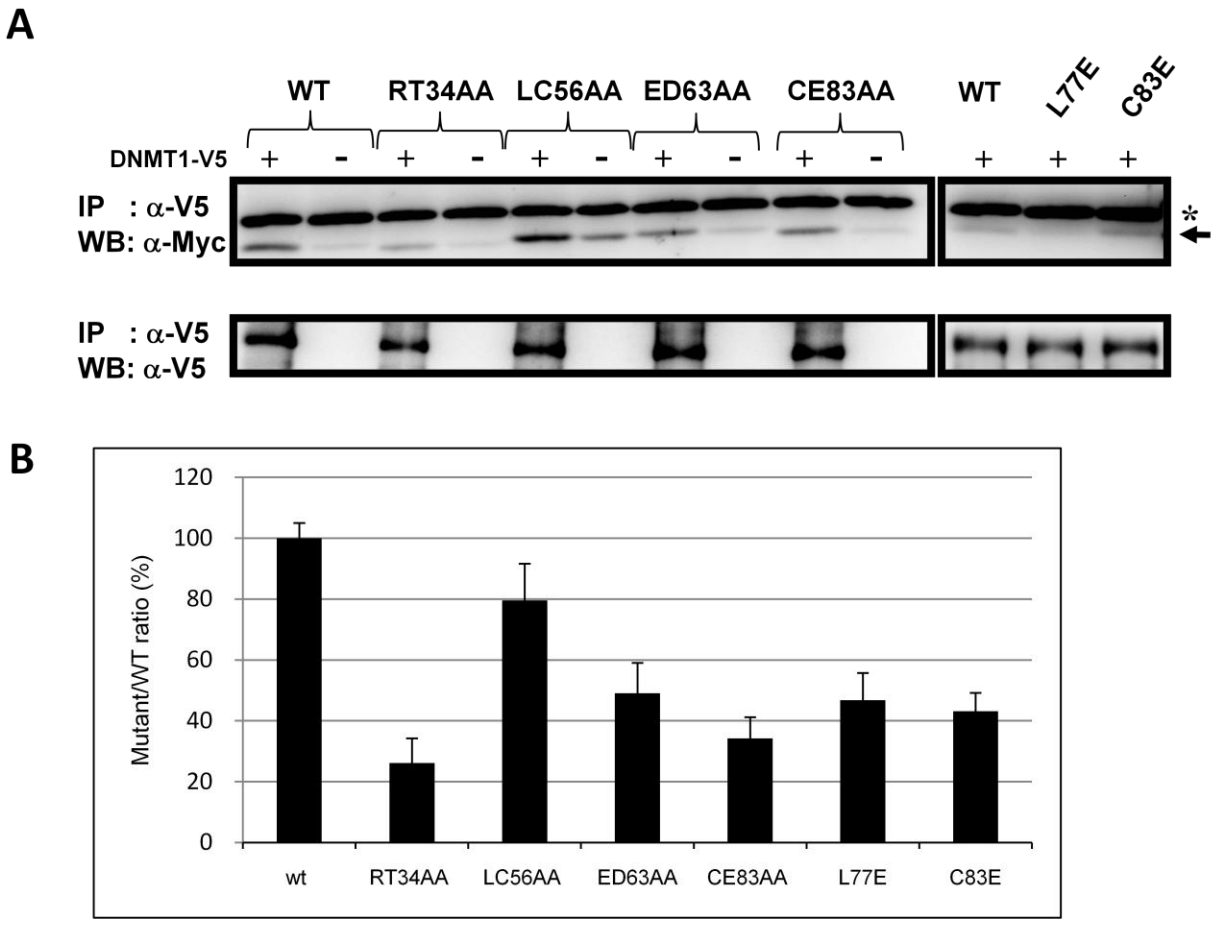

Figure 41 Interaction of each GADD45α point mutant with DNMT1.

Figure 42 Structure of GADD45γ and sequence alignment of GADD45 isoforms.

(A) The structure of GADD45γ. Corresponding position of CE83AA mutation of GADD45α in the structure of GADD45γ.

(B) Amino acid sequence alignment of GADD45 isoforms. Identical residues are boxed in gray. Secondary structure of GADD45γ is marked above the sequences. Leu80 residue in helix 3 (α3) is involved in the dimerization of GADD45γ and the corresponding residue in GADD45α is Leu77. According to this alignment, CE83AA is in helix 3, which is consisting dimerization surface with helix 2. These figures are from Schrag et al. (146).

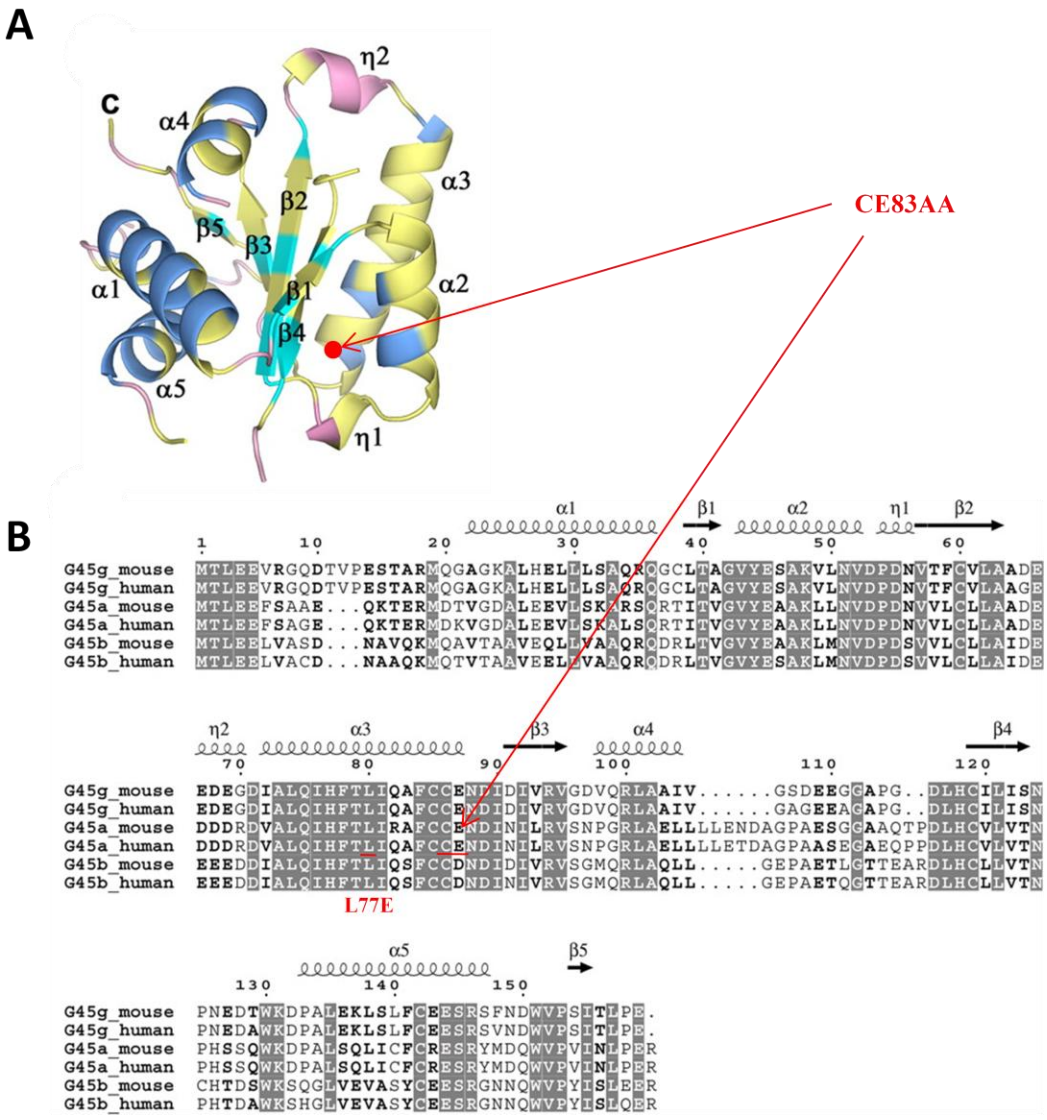

Figure 42 Structure of GADD45γ and sequence alignment of GADD45 isoforms.

Figure 43 Oligo- or dimerization of GADD45α.

(A) Self-association of GADD45α. V5 tagged GADD45α point mutant was co-transfected with Myc-tagged corresponding point mutant or alone into HEK293FT cells. Whole cell extracts were immunoprecipitated with an anti-Myc antibody and precipitated proteins analyzed by western blotting with an anti-V5 antibody. Note that some of point mutants self-precipitated.

(B) Band intensities of co-immunoprecipitated V5 tagged GADD45α point mutants (A) were quantified using the GeneTools program (SynGene, Cambridge, UK). First, the band intensity of co-immunoprecipitated V5 tagged point mutant was subtracted with the band intensity of self-precipitation. The amount of co-immunoprecipitated V5 tagged point mutant was normalized by the amount of immunoprecipitated Myc tagged point mutants and plotted as a relative amount against wild type band intensity. Note that the self-association of L77E mutant was not determined because V5 tagged L77E was not expressed.

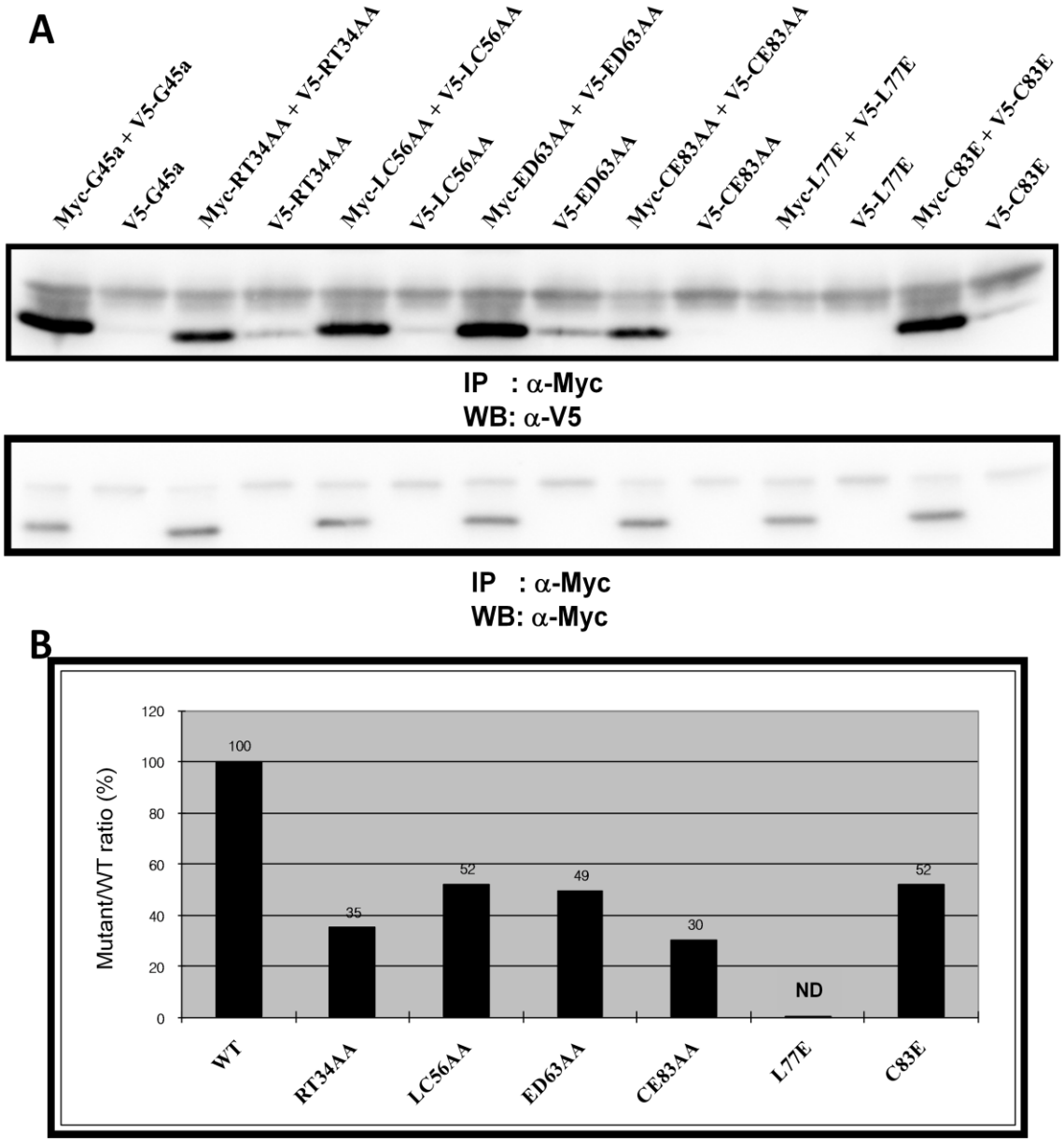

Figure 43 Oligo- or dimerization of GADD45α.

Figure 44 Effect of GADD45α on DNMT1-DNA complex formation.

HCT116 cells were treated with 1 μM aza-dC for 24 h or 10 μM for 1 h. DNMT1-DNA complexes were resolved on CsCl gradients and DNA fractions were pooled. Either 5 or 10 μg of DNA was loaded onto the membrane which was then probed with anti-DNMT1 antibody. HCT116 cells were transfected with 1 μg of Myc-GADD45α plasmid and incubated for 4 h, 24 h, or 48 h before aza-dC was added (rows 4 - 6).

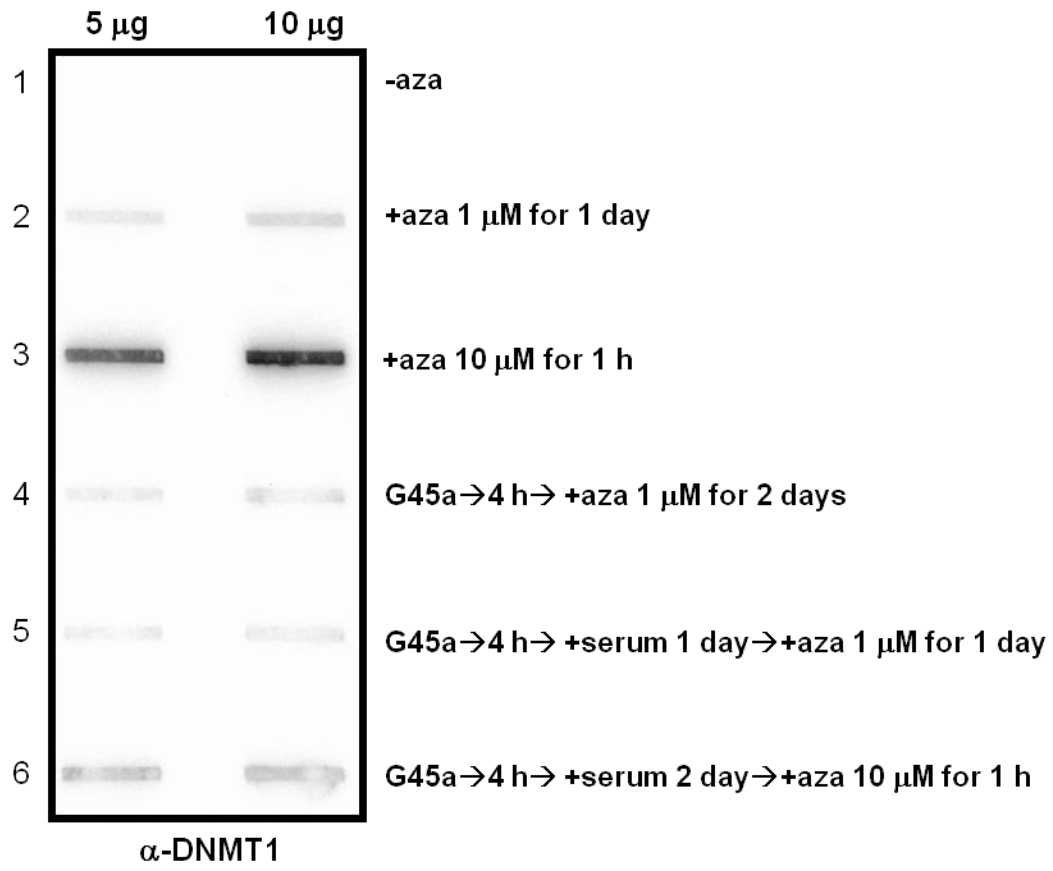

Figure 44 Effect of GADD45α on DNMT1-DNA complex formation.

Figure 45 Stimulation of recombinant GFP gene expression by GADD45α.

HeLa-DRGFP cells were transfected with 2 μg of I-SceI plasmid and different amount of Myc-GADD45α or Myc-GADD45α CE83AA. After 7 days, GFP+ cells were analyzed by FACS. Co-expression of Myc-GADD45α significantly increased the number of GFP+ cells, while CE83AA repressed.

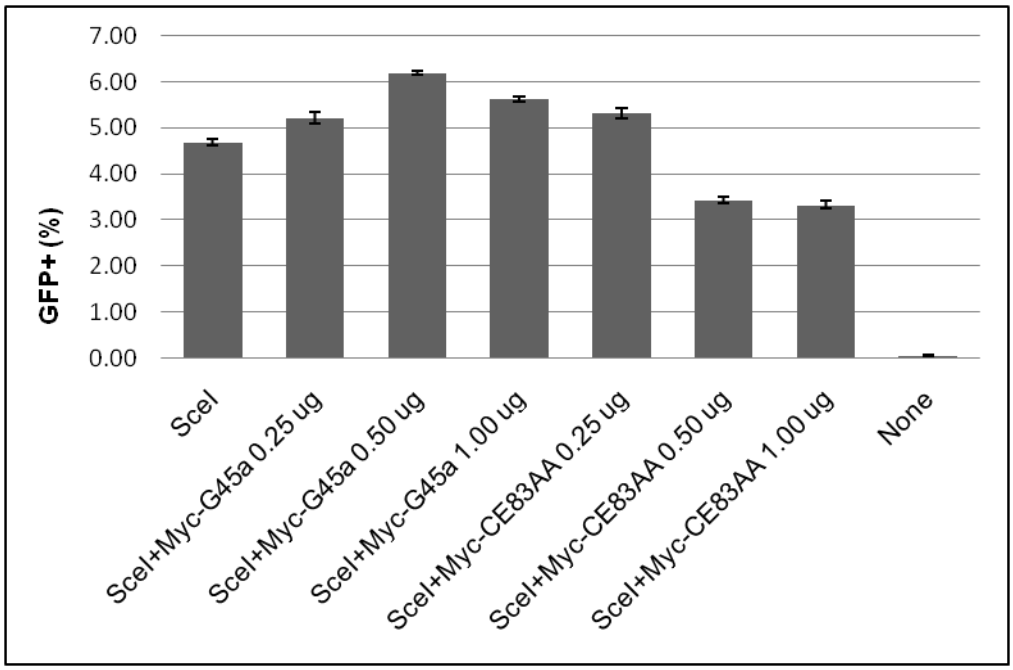

Figure 45 Stimulation of recombinant GFP gene expression by GADD45α.

Figure 46 Repression of recombinant GFP gene expression by GADD45α point mutation.

HeLa-DRGFP cells were transfected with 2 μg of I-SceI plasmid and different amount of Myc-GADD45α or Myc-GADD45α point mutants. The amount of each plasmid DNA used for transfection was adjusted to get similar levels of expression (expression levels were checked, data not shown). After 3 days, GFP+ cells were analyzed by FACS. Co-expression of wild type Myc-GADD45α significantly increased the number of GFP+ cells, while the point mutants repressed the expression of GFP.

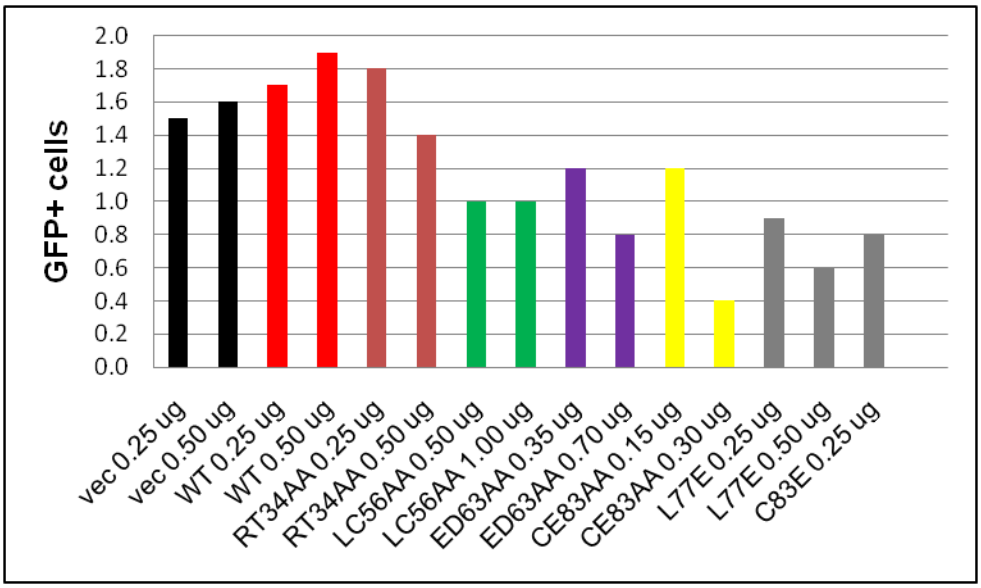

Figure 46 Repression of recombinant GFP gene expression by GADD45α point mutation.

Figure 47 GADD45α inhibits the catalytic activity of DNMT1 in vitro.

(A) DNA methyltransferase activity of DNMT1 on hemi- (blue bars) or un- (red bars) methylated DNA substrate in the presence of GADD45α. DNA methyltransferase activity was measured as described in "Material and Method" in the presence of various amounts of purified GADD45α (0, 50, 100, and 200 ng). (B) The relative % of DNA methyltransferase activity shown in panel A. (C) Time course measurement of DNMT1 activity on hemimethylated DNA substrate in the presence (-◆-) or absence (-■-) of GADD45α. The reaction mixtures contained 100 ng of purified GADD45α. At the indicated time points, reactions were stopped and the incorporation of methyl group on the hemimethylated DNA substrate was determined. Values are average ± SD of three independent experiments. Methyl group (CH_3) incorporation was corrected for background (in reactions lacking DNMT1).

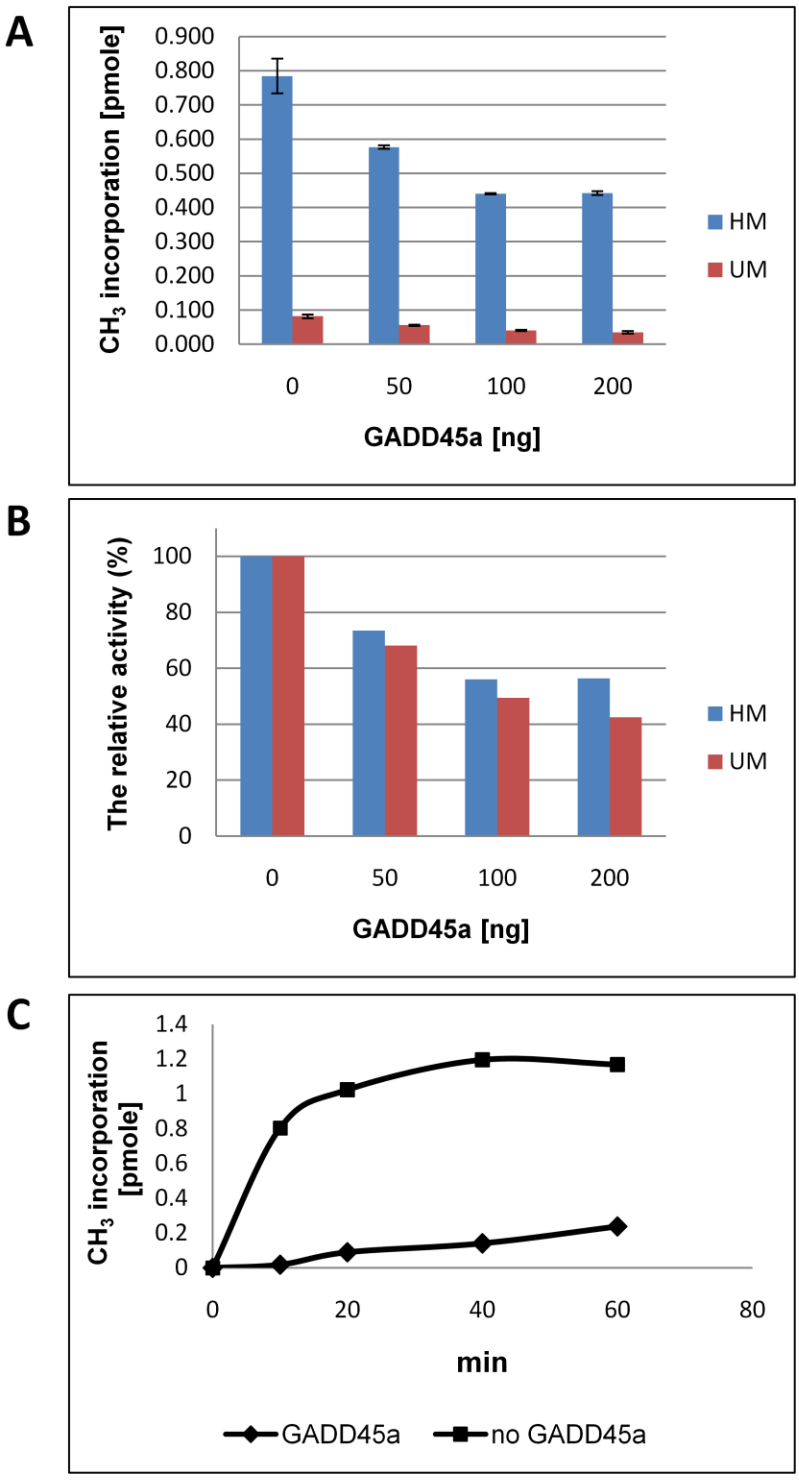

Figure 47 GADD45α inhibits the catalytic activity of DNMT1 in vitro.

Figure 48 Model for DNMT1/GADD45α interplay during HR repair.

A drawing illustrates the possible interplay between DNMT1 and GADD45α during HR leading to silencing, low expression, or high expression of HR DNA segments. Filled rollipops represent methylated CpGs induced by HR. In this model, GADD45α modulates DNMT1 activity at HR site. Depending on the availability of GADD45α, HR DNA segments could be hyper- or hypomethylated.

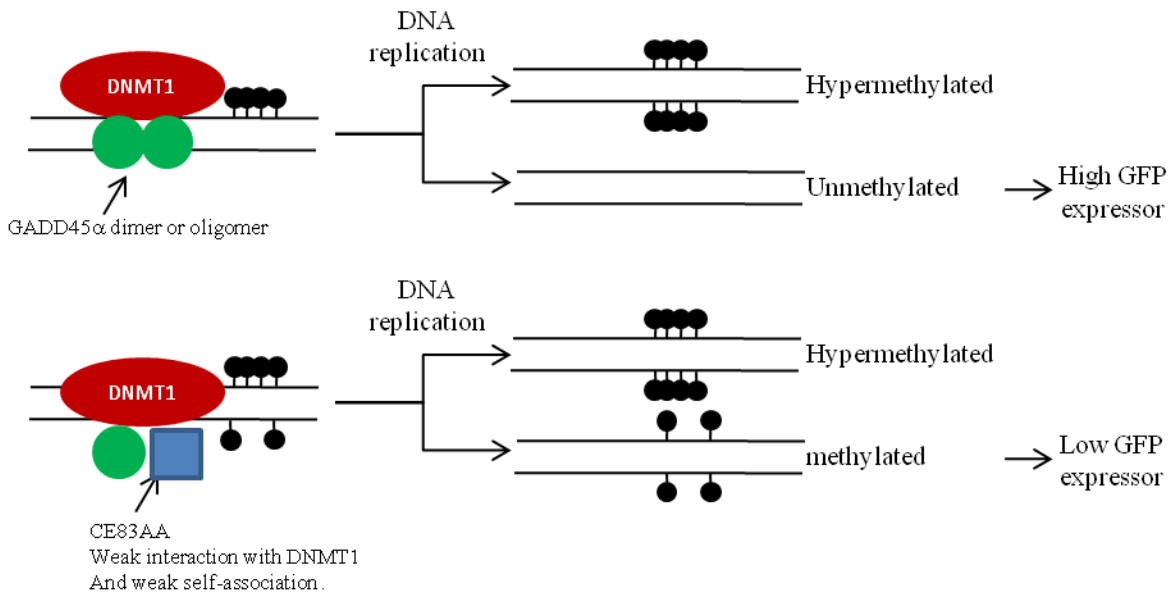

Figure 48 Model for DNMT1/GADD45α interplay during HR repair.

GENERAL DISCUSSION

This dissertation focuses on the regulation of a prominent methylation pathway in somatic cells. We hypothesized that post-translational modifications and a variety of protein-protein interactions processes are key regulatory elements that set global and local methylation patterns of CpG elements essential for normal growth behavior in somatic cells. These fundamental processes can be disrupted by DNA damage leading to inappropriate gene silencing and loss of growth control in somatic cells. We studied the regulatory features of human DNA methyltransferase 1 (DNMT1) at the post-translational level and examined novel functions of DNMT1 in DNA damage repair.

DNMT1 enzyme activity is enhanced by SUMO1 modification.

To explore physiological roles of post-translational modifications of DNMT1, we examined how sumoylation influences methylation in vivo using ICM analysis. This in vivo assay takes advantage of the transient covalent complex formation of the methyltransferase with cytosine base ring (148,149) which is trapped when aza-dC is added. The DNA methyltransferase inhibitor aza-dC is widely used in research as a hypomethylating drug that is incorporated into DNA in living cells. The incorporated aza-dC prevents release of the methyltransferase from DNA resulting in permanently bound DNMTs at the position of their genomic active site. These trapped DNMTs are then quantified with mono specific antibodies to specific DNMT isoforms. Because aza-dC is a mechanism-based inhibitor, immobilization of the DNMT1 is a direct measure of endogenous global methyltransferase activity on genomic DNA. As shown in Fig. 9, mutating a conserved Pro-Cys motif, (which is involved in the covalent complex formation), destroyed the activity and C1226A mutant failed to form a

covalent complex. Using this ICM analysis, we also could determine the post-translational modification status of DNA bound DNMT1, which by definition is catalytically active in a chromatin (in vivo) setting. The data shown in Fig. 8 indicate that the DNMT1 trapped on DNA was modified by SUMO1. This SUMO1 modification of DNMT1 could affect the function of DNMT1 in various ways; thus, one important objective of this work was to determine the physiological consequences of sumoylation of DNMT1. To investigate this, we used pathway relevant genes (SUMO E3 ligase, PIASy, and a SUMO de-conjugating enzyme, SENP1), and the ICM analysis to correlate changes in sumoylation status with DNA binding and catalytic efficiency of DNMT1. We found, for example, that PIASy increased both the sumoylation of DNMT1 and DNA binding efficiency. SENP1, in contrast, did just the opposite. These data indicate that DNMT1 is most likely sumoylated before engaging DNA and that sumoylation of DNMT1 may facilitate the access of DNMT1 to the genomic substrate. The mechanism how SUMO1 modification modulates the activity of protein is not entirely clear. It has been proposed that sumoylation may alter the three-dimensional structure of the modified protein resulting in disruption or creation of new protein-protein interaction surfaces (150,151). Considering that DNMT1 interacts with many different proteins, it is possible that the sumoylation of DNMT1 could alter its interaction with other binding partners, thereby, affecting its activity on DNA or its access to sites in chromatin.

DNMT1 marks HR DNA molecule by methylation.

A DNA double strand break (DSB) is a critical lesion that can promote genomic instability. Cells have evolved complex signal-transduction, cell-cycle checkpoint and repair pathways to deal with such DNA damage. Studies using a range of approaches have advanced our knowledge of the mechanism of the DNA damage response pathways. A major DNA

damage response pathway is linked with HR (homologous recombination). One principle aim of this study is to understand the role of this pathway in cancer. Here, we and our colleagues defined a new relationship between DNA methylation and homologous recombination (105). Using a system developed by Jasin (92), we examined the structure and methylation status at DSB loci following repair and asked how inhibition of DNA methylation may influence expression of recombinant products. In this system, a reporter plasmid containing two mutated GFP cassettes (DRGFP) with a single unique I-SceI cleavage site is engineered in HeLa cells. I-SceI is a homing endonuclease that is then transfected into the indicator cells, resulting in a gene conversion or HR repair event leading to the appearance of GFP+ cells. The methylation and expression status of the repaired indicator DNA molecules was rigorously evaluated. We induced double strand breaks in HeLa or HCT116 cells carrying DRGFP using I-SceI. The unique double strand break triggers a homology-directed repair (HR) and gene conversion generating functional GFP; however, ~50% of recombinants expressed poorly. The silencing of these recombinants was due to DNA methylation. Moreover, we found that DNMT1 is responsible for silencing. We propose that only one of the newly repaired strands is methylated by DNMT1, which is recruited to the DSB locus by proliferating cell nuclear antigen (PCNA) (6). That is, the DNA methylation induced by homology-directed repair is strand-selective and generates a hemimethylated intermediate DNA molecule. Replication of this hemimethylated strand during S phase generates hypermethylated and hypomethylated DNA products in a 1:1 ratio. Based on this observation, we propose a model illustrating how HR repair and DNA methylation could lead to inappropriate gene silencing and possibly selective growth advantage of affected cells (Fig. 27). This hypothetical model also suggests how HR repair could result in selecting an outgrowth of malignant cells. Silencing of tumor suppressor genes or over

expression of oncogenes can cause tumor development. Since the location of methylated CpGs and DNA damage is random, HR-induced methylation is also random. If the DNA damage and HR repair locus occurs either in the gene body or in the promoter region of a tumor suppressor gene, the cells inheriting the silenced copy of the tumor suppressor gene will have a growth advantage and may expand. Also, if an oncogene is affected by HR DNA repair, the cells inheriting the hypomethylated copy will have a selective advantage. Both cases result in an unbalanced outgrowth of immortalized cells. In conclusion, we propose that a cause-effect relationship exists between HR repair and de novo DNA methylation. Discontinuous LOH is a signature associated with oxidative DNA damage and mutations resembling discontinuous LOH are commonly observed in a wide variety of human cancers (152). In addition, the tumor suppressor gene silencing by methylation is prevalent in human tumors (13). Indeed, at a very early stage, cancer development is associated with DNA double strand breaks preceding the genomic instability and loss of p53 (110).

Due to its strong preference for hemimethylated substrate DNA in vitro (153,154) and its accumulation at replication sites during S-phase (155), DNMT1 is thought to act as a maintenance methylase acting on replicating DNA during cell division. In contrast, DNMT3a and -3b have no preference for hemi- versus non-methylated DNA (7) and are not guided by the methylation of the parental strand. They have been termed the “de novo” methylases. Although it is believed that DNMT1 cannot promote de novo methylation, in vitro data showed that it also has de novo methyltransferase activity (106). Our observation of methylation following HR is the first evidence for de novo methylation activity by DNMT1 in vivo. In agreement with our results, DNMT1 is also associated with methylation activity following recombination mediated by Cre-LoxP interaction in meiotic cells (156).

Many proteins involved in DNA repair pathways are sumoylated. For example, Rad52 (RADiation sensitive), a protein that mediates the exchange of the early recombination factor RPA (Replication Protein A) by Rad51 and promotes strand annealing, is sumoylated. Its sumoylation is sustained by the Rad52 activity and concomitantly protects the protein from proteasomal degradation (157). So far, sumoylation of DNA methyltransferases has been limited to the de novo methyltransferases, (DNMT3a and DNMT3b) (58,59,68). It was thought that sumoylation might distinguish the de novo from the maintenance DNA methyltransferases. Thus, it would be of interest to examine the role of DNMT1 sumoylation in DNA damage repair. It is possible that de novo methyltransferase activity of DNMT1 is regulated by sumoylation. Future studies will be aimed at testing this idea.

DNMT1 activity is regulated by GADD45α during HR.

GADD45α is induced by various cellular stresses including DNA damage. It is a regulatory protein functioning primarily to protect cells by inducing cell cycle arrest and DNA repair (112,158). In addition, there is evidence that it may be involved in DNA demethylation (132,159,160). Previously, we found that DNA methylation by DNMT1 was induced by homology-directed repair followed by DNA damage. Interestingly, the methylation is strand specific, in other words, one strand close to the repair site is hypermethylated leaving other strand hypomethylated. As a putative mechanism of this strand specific methylation, we propose that GADD45α is a regulator of DNMT1 activity during HR. GADD45α appears to inhibit DNMT1 activity at the site of HR. It might protect one strand from methylation by DNMT1 or inhibit the extended methylation to that strand by binding to the catalytic domain of DNMT1. Previously, GADD45α was implicated in the active demethylation events and was reported to

recruit the repair endonuclease XPG (132). Although this result was questioned by others (133), our findings suggest that GADD45α may be involved in DNA demethylation in passive manner, as opposed to an active methyl reversal. We have shown that it plays a role in coordinating strand specific methylation during HR.

GADD45α is known to be specifically involved in nucleotide excision repair (NER) (161) by delaying cell cycle progression. In addition to cell cycle arrest, its involvement in NER pathway seems to be more active, judged by its interaction with XPG, an NER pathway component (132). Our findings also expand its function in another type of DNA repair pathway, HR, where it modulates DNA methylation. Taken together, these findings suggest that GADD45α plays an important role in maintaining genomic stability. It is known that genomic instability, such as incorrect centromere amplification, may contribute prominently to tumor development and progression. Indeed, GADD45α deletion has been found to lead to significant genomic instability (161). Many cancer cells have reduced GADD45α expression levels (126) and low levels of GADD45α might contribute more frequent gene silencing after damage repair. Further studies are necessary to understand the detailed mechanism of regulating DNA methylation during HR by GADD45α and DNMT1 interplay.

In summary, in order to examine the regulatory features of DNMT1, three hypotheses are examined; 1. The epigenetic state of somatic cell methylation is mediated by sumoylation of a key methylase activity. 2. Alterations in DNA methylation of growth regulatory genes following double strand DNA damage are mediated by DNMT1 leading to inappropriate gene silencing antecedent to malignant transformation. 3. DNA repair related methylation is mediated by protein-protein interactions through a class of DNA damage responsive factors that directing

bind DNMT1. We show here that DNMT1 is modified by a small ubiquitin like modifier, SUMO1, and the modification of DNMT1 by SUMO1 strongly enhances its ability to methylate DNA in vitro and in vivo. With respect to DNA damage repair, we found that the methylation status at HR repair sites are erased and reset by DNMT1 acting as a de novo methylase. These data support a role that DNA methylation marks HR repaired genomic regions to at least partially prevent unregulated gene expression following DNA damage. The DNA methylation during HR is, we believe, further regulated by the interplay between GADD45α and DNMT1.

REFERENCES

1. Herman, J.G. and Baylin, S.B. (2003) Gene silencing in cancer in association with promoter hypermethylation. *N Engl J Med*, **349**, 2042-2054.

2. Jones, P.A. and Laird, P.W. (1999) Cancer epigenetics comes of age. *Nat Genet*, **21**, 163-167.

3. Robertson, K.D. and Wolffe, A.P. (2000) DNA methylation in health and disease. *Nat Rev Genet*, **1**, 11-19.

4. Robertson, K.D., Uzvolgyi, E., Liang, G., Talmadge, C., Sumegi, J., Gonzales, F.A. and Jones, P.A. (1999) The human DNA methyltransferases (DNMTs) 1, 3a and 3b: coordinate mRNA expression in normal tissues and overexpression in tumors. *Nucleic Acids Res*, **27**, 2291-2298.

5. Liu, Y., Oakeley, E.J., Sun, L. and Jost, J.P. (1998) Multiple domains are involved in the targeting of the mouse DNA methyltransferase to the DNA replication foci. *Nucleic Acids Res*, **26**, 1038-1045.

6. Chuang, L.S., Ian, H.I., Koh, T.W., Ng, H.H., Xu, G. and Li, B.F. (1997) Human DNA-(cytosine-5) methyltransferase-PCNA complex as a target for p21WAF1. *Science*, **277**, 1996-2000.

7. Okano, M., Xie, S. and Li, E. (1998) Cloning and characterization of a family of novel mammalian DNA (cytosine-5) methyltransferases. *Nat Genet*, **19**, 219-220.

8. Okano, M., Bell, D.W., Haber, D.A. and Li, E. (1999) DNA methyltransferases Dnmt3a and Dnmt3b are essential for de novo methylation and mammalian development. *Cell*, **99**, 247-257.

9. Yoder, J.A. and Bestor, T.H. (1998) A candidate mammalian DNA methyltransferase related to pmt1p of fission yeast. *Hum Mol Genet*, **7**, 279-284.

10. Hermann, A., Schmitt, S. and Jeltsch, A. (2003) The human Dnmt2 has residual DNA-(cytosine-C5) methyltransferase activity. *J Biol Chem*, **278**, 31717-31721.

11. Liu, K., Wang, Y.F., Cantemir, C. and Muller, M.T. (2003) Endogenous assays of DNA methyltransferases: Evidence for differential activities of DNMT1, DNMT2, and DNMT3 in mammalian cells in vivo. *Mol Cell Biol*, **23**, 2709-2719.

12. Robertson, K.D. (2002) DNA methylation and chromatin - unraveling the tangled web. *Oncogene*, **21**, 5361-5379.

13. Jones, P.A. and Baylin, S.B. (2002) The fundamental role of epigenetic events in cancer. *Nat Rev Genet*, **3**, 415-428.

14. Bird, A. (2002) DNA methylation patterns and epigenetic memory. *Genes Dev*, **16**, 6-21.

15. Stirzaker, C., Millar, D.S., Paul, C.L., Warnecke, P.M., Harrison, J., Vincent, P.C., Frommer, M. and Clark, S.J. (1997) Extensive DNA methylation spanning the Rb promoter in retinoblastoma tumors. *Cancer Res*, **57**, 2229-2237.

16. Herman, J.G., Latif, F., Weng, Y., Lerman, M.I., Zbar, B., Liu, S., Samid, D., Duan, D.S., Gnarra, J.R., Linehan, W.M. *et al.* (1994) Silencing of the VHL tumor-suppressor gene by DNA methylation in renal carcinoma. *Proc Natl Acad Sci U S A*, **91**, 9700-9704.

17. Costello, J.F., Fruhwald, M.C., Smiraglia, D.J., Rush, L.J., Robertson, G.P., Gao, X., Wright, F.A., Feramisco, J.D., Peltomaki, P., Lang, J.C. *et al.* (2000) Aberrant CpG-island methylation has non-random and tumour-type-specific patterns. *Nat Genet*, **24**, 132-138.

18. Rauch, T.A., Zhong, X., Wu, X., Wang, M., Kernstine, K.H., Wang, Z., Riggs, A.D. and Pfeifer, G.P. (2008) High-resolution mapping of DNA hypermethylation and hypomethylation in lung cancer. *Proc Natl Acad Sci U S A*, **105**, 252-257.

19. Shen, L., Kondo, Y., Guo, Y., Zhang, J., Zhang, L., Ahmed, S., Shu, J., Chen, X., Waterland, R.A. and Issa, J.P. (2007) Genome-wide profiling of DNA methylation reveals a class of normally methylated CpG island promoters. *PLoS Genet*, **3**, 2023-2036.

20. Smith, J.F., Mahmood, S., Song, F., Morrow, A., Smiraglia, D., Zhang, X., Rajput, A., Higgins, M.J., Krumm, A., Petrelli, N.J. *et al.* (2007) Identification of DNA methylation in 3' genomic regions that are associated with upregulation of gene expression in colorectal cancer. *Epigenetics*, **2**, 161-172.

21. Weber, M., Davies, J.J., Wittig, D., Oakeley, E.J., Haase, M., Lam, W.L. and Schubeler, D. (2005) Chromosome-wide and promoter-specific analyses identify sites of differential DNA methylation in normal and transformed human cells. *Nat Genet*, **37**, 853-862.

22. Opavsky, R., Wang, S.H., Trikha, P., Raval, A., Huang, Y., Wu, Y.Z., Rodriguez, B., Keller, B., Liyanarachchi, S., Wei, G. *et al.* (2007) CpG island methylation in a mouse model of lymphoma is driven by the genetic configuration of tumor cells. *PLoS Genet*, **3**, 1757-1769.

23. Frigola, J., Song, J., Stirzaker, C., Hinshelwood, R.A., Peinado, M.A. and Clark, S.J. (2006) Epigenetic remodeling in colorectal cancer results in coordinate gene suppression across an entire chromosome band. *Nat Genet*, **38**, 540-549.

24. Keshet, I., Schlesinger, Y., Farkash, S., Rand, E., Hecht, M., Segal, E., Pikarski, E., Young, R.A., Niveleau, A., Cedar, H. *et al.* (2006) Evidence for an instructive mechanism of de novo methylation in cancer cells. *Nat Genet*, **38**, 149-153.

25. Fang, F., Fan, S., Zhang, X. and Zhang, M.Q. (2006) Predicting methylation status of CpG islands in the human brain. *Bioinformatics*, **22**, 2204-2209.

26. Feltus, F.A., Lee, E.K., Costello, J.F., Plass, C. and Vertino, P.M. (2006) DNA motifs associated with aberrant CpG island methylation. *Genomics*, **87**, 572-579.

27. Di Croce, L., Raker, V.A., Corsaro, M., Fazi, F., Fanelli, M., Faretta, M., Fuks, F., Lo Coco, F., Kouzarides, T., Nervi, C. *et al.* (2002) Methyltransferase recruitment and DNA hypermethylation of target promoters by an oncogenic transcription factor. *Science*, **295**, 1079-1082.

28. Lei, H., Oh, S.P., Okano, M., Juttermann, R., Goss, K.A., Jaenisch, R. and Li, E. (1996) De novo DNA cytosine methyltransferase activities in mouse embryonic stem cells. *Development*, **122**, 3195-3205.

29. Jackson-Grusby, L., Beard, C., Possemato, R., Tudor, M., Fambrough, D., Csankovszki, G., Dausman, J., Lee, P., Wilson, C., Lander, E. *et al.* (2001) Loss of genomic methylation causes p53-dependent apoptosis and epigenetic deregulation. *Nat Genet*, **27**, 31-39.

30. Vertino, P.M., Yen, R.W., Gao, J. and Baylin, S.B. (1996) De novo methylation of CpG island sequences in human fibroblasts overexpressing DNA (cytosine-5-)-methyltransferase. *Mol Cell Biol*, **16**, 4555-4565.

31. Wu, J., Issa, J.P., Herman, J., Bassett, D.E., Jr., Nelkin, B.D. and Baylin, S.B. (1993) Expression of an exogenous eukaryotic DNA methyltransferase gene induces transformation of NIH 3T3 cells. *Proc Natl Acad Sci U S A*, **90**, 8891-8895.

32. Kanai, Y., Ushijima, S., Kondo, Y., Nakanishi, Y. and Hirohashi, S. (2001) DNA methyltransferase expression and DNA methylation of CPG islands and peri-centromeric satellite regions in human colorectal and stomach cancers. *Int J Cancer*, **91**, 205-212.

33. Saito, Y., Kanai, Y., Sakamoto, M., Saito, H., Ishii, H. and Hirohashi, S. (2001) Expression of mRNA for DNA methyltransferases and methyl-CpG-binding proteins and DNA methylation status on CpG islands and pericentromeric satellite regions during human hepatocarcinogenesis. *Hepatology*, **33**, 561-568.

34. Mizuno, S., Chijiwa, T., Okamura, T., Akashi, K., Fukumaki, Y., Niho, Y. and Sasaki, H. (2001) Expression of DNA methyltransferases DNMT1, 3A, and 3B in normal hematopoiesis and in acute and chronic myelogenous leukemia. *Blood*, **97**, 1172-1179.

35. Peng, D.F., Kanai, Y., Sawada, M., Ushijima, S., Hiraoka, N., Kosuge, T. and Hirohashi, S. (2005) Increased DNA methyltransferase 1 (DNMT1) protein expression in precancerous conditions and ductal carcinomas of the pancreas. *Cancer Sci*, **96**, 403-408.

36. Eden, A., Gaudet, F., Waghmare, A. and Jaenisch, R. (2003) Chromosomal instability and tumors promoted by DNA hypomethylation. *Science*, **300**, 455.

37. Gaudet, F., Hodgson, J.G., Eden, A., Jackson-Grusby, L., Dausman, J., Gray, J.W., Leonhardt, H. and Jaenisch, R. (2003) Induction of tumors in mice by genomic hypomethylation. *Science*, **300**, 489-492.

38. Kimura, F., Seifert, H.H., Florl, A.R., Santourlidis, S., Steinhoff, C., Swiatkowski, S., Mahotka, C., Gerharz, C.D. and Schulz, W.A. (2003) Decrease of DNA methyltransferase 1 expression relative to cell proliferation in transitional cell carcinoma. *Int J Cancer*, **104**, 568-578.

39. Bestor, T., Laudano, A., Mattaliano, R. and Ingram, V. (1988) Cloning and sequencing of a cDNA encoding DNA methyltransferase of mouse cells. The carboxyl-terminal domain of the mammalian enzymes is related to bacterial restriction methyltransferases. *J Mol Biol*, **203**, 971-983.

40. Rountree, M.R., Bachman, K.E. and Baylin, S.B. (2000) DNMT1 binds HDAC2 and a new co-repressor, DMAP1, to form a complex at replication foci. *Nat Genet*, **25**, 269-277.

41. Bestor, T.H. and Verdine, G.L. (1994) DNA methyltransferases. *Curr Opin Cell Biol*, **6**, 380-389.

42. Robertson, K.D., Ait-Si-Ali, S., Yokochi, T., Wade, P.A., Jones, P.L. and Wolffe, A.P. (2000) DNMT1 forms a complex with Rb, E2F1 and HDAC1 and represses transcription from E2F-responsive promoters. *Nat Genet*, **25**, 338-342.

43. Fuks, F., Hurd, P.J., Deplus, R. and Kouzarides, T. (2003) The DNA methyltransferases associate with HP1 and the SUV39H1 histone methyltransferase. *Nucleic Acids Res*, **31**, 2305-2312.

44. Tatematsu, K.I., Yamazaki, T. and Ishikawa, F. (2000) MBD2-MBD3 complex binds to hemi-methylated DNA and forms a complex containing DNMT1 at the replication foci in late S phase. *Genes Cells*, **5**, 677-688.

45. Kimura, H. and Shiota, K. (2003) Methyl-CpG-binding protein, MeCP2, is a target molecule for maintenance DNA methyltransferase, Dnmt1. *J Biol Chem*, **278**, 4806-4812.

46. Kim, G.D., Ni, J., Kelesoglu, N., Roberts, R.J. and Pradhan, S. (2002) Co-operation and communication between the human maintenance and de novo DNA (cytosine-5) methyltransferases. *Embo J*, **21**, 4183-4195.

47. Glickman, J.F., Pavlovich, J.G. and Reich, N.O. (1997) Peptide mapping of the murine DNA methyltransferase reveals a major phosphorylation site and the start of translation. *J Biol Chem*, **272**, 17851-17857.

48. Hershko, A. and Ciechanover, A. (1998) The ubiquitin system. *Annu Rev Biochem*, **67**, 425-479.

49. Ghoshal, K., Datta, J., Majumder, S., Bai, S., Kutay, H., Motiwala, T. and Jacob, S.T. (2005) 5-Aza-deoxycytidine induces selective degradation of DNA methyltransferase 1 by a proteasomal pathway that requires the KEN box, bromo-adjacent homology domain, and nuclear localization signal. *Mol Cell Biol*, **25**, 4727-4741.

50. Agoston, A.T., Argani, P., Yegnasubramanian, S., De Marzo, A.M., Ansari-Lari, M.A., Hicks, J.L., Davidson, N.E. and Nelson, W.G. (2005) Increased protein stability causes DNA methyltransferase 1 dysregulation in breast cancer. *J Biol Chem*, **280**, 18302-18310.

51. Deshaies, R.J. (1999) SCF and Cullin/Ring H2-based ubiquitin ligases. *Annu Rev Cell Dev Biol*, **15**, 435-467.

52. Naumann, M., Bech-Otschir, D., Huang, X., Ferrell, K. and Dubiel, W. (1999) COP9 signalosome-directed c-Jun activation/stabilization is independent of JNK. *J Biol Chem*, **274**, 35297-35300.

53. Matunis, M.J., Coutavas, E. and Blobel, G. (1996) A novel ubiquitin-like modification modulates the partitioning of the Ran-GTPase-activating protein RanGAP1 between the cytosol and the nuclear pore complex. *J Cell Biol*, **135**, 1457-1470.

54. Bayer, P., Arndt, A., Metzger, S., Mahajan, R., Melchior, F., Jaenicke, R. and Becker, J. (1998) Structure determination of the small ubiquitin-related modifier SUMO-1. *J Mol Biol*, **280**, 275-286.

55. Melchior, F. (2000) SUMO--nonclassical ubiquitin. *Annu Rev Cell Dev Biol*, **16**, 591-626.

56. Sampson, D.A., Wang, M. and Matunis, M.J. (2001) The small ubiquitin-like modifier-1 (SUMO-1) consensus sequence mediates Ubc9 binding and is essential for SUMO-1 modification. *J Biol Chem*, **276**, 21664-21669.

57. Desterro, J.M., Rodriguez, M.S. and Hay, R.T. (1998) SUMO-1 modification of IkappaBalpha inhibits NF-kappaB activation. *Mol Cell*, **2**, 233-239.

58. Kang, E.S., Park, C.W. and Chung, J.H. (2001) Dnmt3b, de novo DNA methyltransferase, interacts with SUMO-1 and Ubc9 through its N-terminal region and is subject to modification by SUMO-1. *Biochem Biophys Res Commun*, **289**, 862-868.

59. Ling, Y., Sankpal, U.T., Robertson, A.K., McNally, J.G., Karpova, T. and Robertson, K.D. (2004) Modification of de novo DNA methyltransferase 3a (Dnmt3a) by SUMO-1 modulates its interaction with histone deacetylases (HDACs) and its capacity to repress transcription. *Nucleic Acids Res*, **32**, 598-610.

60. Langereis, M.A., Rosas-Acosta, G., Mulder, K. and Wilson, V.G. (2007) Production of sumoylated proteins using a baculovirus expression system. *J Virol Methods*, **139**, 189-194.

61. Fey, E.G., Wan, K.M. and Penman, S. (1984) Epithelial cytoskeletal framework and nuclear matrix-intermediate filament scaffold: three-dimensional organization and protein composition. *J Cell Biol*, **98**, 1973-1984.

62. Kotaja, N., Karvonen, U., Janne, O.A. and Palvimo, J.J. (2002) PIAS proteins modulate transcription factors by functioning as SUMO-1 ligases. *Mol Cell Biol*, **22**, 5222-5234.

63. Horie, K., Tomida, A., Sugimoto, Y., Yasugi, T., Yoshikawa, H., Taketani, Y. and Tsuruo, T. (2002) SUMO-1 conjugation to intact DNA topoisomerase I amplifies cleavable complex formation induced by camptothecin. *Oncogene*, **21**, 7913-7922.

64. Callebaut, I., Courvalin, J.C. and Mornon, J.P. (1999) The BAH (bromo-adjacent homology) domain: a link between DNA methylation, replication and transcriptional regulation. *FEBS Lett*, **446**, 189-193.

65. Chou, C.C., Chang, C., Liu, J.H., Chen, L.F., Hsiao, C.D. and Chen, H. (2007) Small ubiquitin-like modifier modification regulates the DNA binding activity of glial cell missing Drosophila homolog a. *J Biol Chem*, **282**, 27239-27249.

66. Spada, F., Haemmer, A., Kuch, D., Rothbauer, U., Schermelleh, L., Kremmer, E., Carell, T., Langst, G. and Leonhardt, H. (2007) DNMT1 but not its interaction with the replication machinery is required for maintenance of DNA methylation in human cells. *J Cell Biol*, **176**, 565-571.

67. Denison, C., Rudner, A.D., Gerber, S.A., Bakalarski, C.E., Moazed, D. and Gygi, S.P. (2005) A proteomic strategy for gaining insights into protein sumoylation in yeast. *Mol Cell Proteomics*, **4**, 246-254.

68. Venturelli, S., Armeanu, S., Pathil, A., Hsieh, C.J., Weiss, T.S., Vonthein, R., Wehrmann, M., Gregor, M., Lauer, U.M. and Bitzer, M. (2007) Epigenetic combination therapy as a tumor-selective treatment approach for hepatocellular carcinoma. *Cancer*, **109**, 2132-2141.

69. Bell, S.P., Kobayashi, R. and Stillman, B. (1993) Yeast origin recognition complex functions in transcription silencing and DNA replication. *Science*, **262**, 1844-1849.

70. Connelly, J.J., Yuan, P., Hsu, H.C., Li, Z., Xu, R.M. and Sternglanz, R. (2006) Structure and function of the Saccharomyces cerevisiae Sir3 BAH domain. *Mol Cell Biol*, **26**, 3256-3265.

71. Pak, D.T., Pflumm, M., Chesnokov, I., Huang, D.W., Kellum, R., Marr, J., Romanowski, P. and Botchan, M.R. (1997) Association of the origin recognition complex with heterochromatin and HP1 in higher eukaryotes. *Cell*, **91**, 311-323.

72. Henikoff, S. and Comai, L. (1998) A DNA methyltransferase homolog with a chromodomain exists in multiple polymorphic forms in Arabidopsis. *Genetics*, **149**, 307-318.

73. Malagnac, F., Gregoire, A., Goyon, C., Rossignol, J.L. and Faugeron, G. (1999) Masc2, a gene from Ascobolus encoding a protein with a DNA-methyltransferase activity in vitro, is dispensable for in vivo methylation. *Mol Microbiol*, **31**, 331-338.

74. Schwaiger, M. and Schubeler, D. (2006) A question of timing: emerging links between transcription and replication. *Curr Opin Genet Dev*, **16**, 177-183.

75. Smallwood, A., Esteve, P.O., Pradhan, S. and Carey, M. (2007) Functional cooperation between HP1 and DNMT1 mediates gene silencing. *Genes Dev*, **21**, 1169-1178.

76. Uchimura, Y., Ichimura, T., Uwada, J., Tachibana, T., Sugahara, S., Nakao, M. and Saitoh, H. (2006) Involvement of SUMO modification in MBD1- and MCAF1-mediated heterochromatin formation. *J Biol Chem*, **281**, 23180-23190.

77. Johnson, E.S. (2004) Protein modification by SUMO. *Annu Rev Biochem*, **73**, 355-382.

78. Margot, J.B., Aguirre-Arteta, A.M., Di Giacco, B.V., Pradhan, S., Roberts, R.J., Cardoso, M.C. and Leonhardt, H. (2000) Structure and function of the mouse DNA methyltransferase gene: Dnmt1 shows a tripartite structure. *J Mol Biol*, **297**, 293-300.

79. Fuks, F., Burgers, W.A., Brehm, A., Hughes-Davies, L. and Kouzarides, T. (2000) DNA methyltransferase Dnmt1 associates with histone deacetylase activity. *Nat Genet*, **24**, 88-91.

80. Fatemi, M., Hermann, A., Pradhan, S. and Jeltsch, A. (2001) The activity of the murine DNA methyltransferase Dnmt1 is controlled by interaction of the catalytic domain with the N-terminal part of the enzyme leading to an allosteric activation of the enzyme after binding to methylated DNA. *J Mol Biol*, **309**, 1189-1199.

81. Zimmermann, C., Guhl, E. and Graessmann, A. (1997) Mouse DNA methyltransferase (MTase) deletion mutants that retain the catalytic domain display neither de novo nor maintenance methylation activity in vivo. *Biol Chem*, **378**, 393-405.

82. Schermelleh, L., Spada, F., Easwaran, H.P., Zolghadr, K., Margot, J.B., Cardoso, M.C. and Leonhardt, H. (2005) Trapped in action: direct visualization of DNA methyltransferase activity in living cells. *Nat Meth*, **2**, 751-756.

83. Cheng, J., Kang, X., Zhang, S. and Yeh, E.T. (2007) SUMO-specific protease 1 is essential for stabilization of HIF1alpha during hypoxia. *Cell*, **131**, 584-595.

84. Richardson, C. and Jasin, M. (2000) Frequent chromosomal translocations induced by DNA double-strand breaks. *Nature*, **405**, 697-700.

85. Lin, Y., Lukacsovich, T. and Waldman, A.S. (1999) Multiple pathways for repair of DNA double-strand breaks in mammalian chromosomes. *Mol Cell Biol*, **19**, 8353-8360.

86. Essers, J., van Steeg, H., de Wit, J., Swagemakers, S.M., Vermeij, M., Hoeijmakers, J.H. and Kanaar, R. (2000) Homologous and non-homologous recombination differentially affect DNA damage repair in mice. *Embo J*, **19**, 1703-1710.

87. Takata, M., Sasaki, M.S., Sonoda, E., Morrison, C., Hashimoto, M., Utsumi, H., Yamaguchi-Iwai, Y., Shinohara, A. and Takeda, S. (1998) Homologous recombination

and non-homologous end-joining pathways of DNA double-strand break repair have overlapping roles in the maintenance of chromosomal integrity in vertebrate cells. *Embo J*, **17**, 5497-5508.

88. Cromie, G.A., Connelly, J.C. and Leach, D.R. (2001) Recombination at double-strand breaks and DNA ends: conserved mechanisms from phage to humans. *Mol Cell*, **8**, 1163-1174.

89. Taghian, D.G. and Nickoloff, J.A. (1997) Chromosomal double-strand breaks induce gene conversion at high frequency in mammalian cells. *Mol Cell Biol*, **17**, 6386-6393.

90. Elliott, B., Richardson, C., Winderbaum, J., Nickoloff, J.A. and Jasin, M. (1998) Gene conversion tracts from double-strand break repair in mammalian cells. *Mol Cell Biol*, **18**, 93-101.

91. Johnson, R.D., Liu, N. and Jasin, M. (1999) Mammalian XRCC2 promotes the repair of DNA double-strand breaks by homologous recombination. *Nature*, **401**, 397-399.

92. Pierce, A.J., Johnson, R.D., Thompson, L.H. and Jasin, M. (1999) XRCC3 promotes homology-directed repair of DNA damage in mammalian cells. *Genes Dev*, **13**, 2633-2638.

93. Difilippantonio, M.J., Zhu, J., Chen, H.T., Meffre, E., Nussenzweig, M.C., Max, E.E., Ried, T. and Nussenzweig, A. (2000) DNA repair protein Ku80 suppresses chromosomal aberrations and malignant transformation. *Nature*, **404**, 510-514.

94. Gao, Y., Ferguson, D.O., Xie, W., Manis, J.P., Sekiguchi, J., Frank, K.M., Chaudhuri, J., Horner, J., DePinho, R.A. and Alt, F.W. (2000) Interplay of p53 and DNA-repair protein XRCC4 in tumorigenesis, genomic stability and development. *Nature*, **404**, 897-900.

95. Mortusewicz, O., Schermelleh, L., Walter, J., Cardoso, M.C. and Leonhardt, H. (2005) Recruitment of DNA methyltransferase I to DNA repair sites. *Proc Natl Acad Sci U S A*, **102**, 8905-8909.

96. Chen, R.Z., Pettersson, U., Beard, C., Jackson-Grusby, L. and Jaenisch, R. (1998) DNA hypomethylation leads to elevated mutation rates. *Nature*, **395**, 89-93.

97. Avvedimento, E.V., Obici, S., Sanchez, M., Gallo, A., Musti, A. and Gottesman, M.E. (1989) Reactivation of thyroglobulin gene expression in transformed thyroid cells by 5-azacytidine. *Cell*, **58**, 1135-1142.

98. Bird, A.P. and Wolffe, A.P. (1999) Methylation-induced repression--belts, braces, and chromatin. *Cell*, **99**, 451-454.

99. Frommer, M., McDonald, L.E., Millar, D.S., Collis, C.M., Watt, F., Grigg, G.W., Molloy, P.L. and Paul, C.L. (1992) A genomic sequencing protocol that yields a positive display of 5-methylcytosine residues in individual DNA strands. *Proc Natl Acad Sci U S A*, **89**, 1827-1831.

100. Jasin, M. (1996) Genetic manipulation of genomes with rare-cutting endonucleases. *Trends Genet*, **12**, 224-228.

101. Juttermann, R., Li, E. and Jaenisch, R. (1994) Toxicity of 5-aza-2'-deoxycytidine to mammalian cells is mediated primarily by covalent trapping of DNA methyltransferase rather than DNA demethylation. *Proc Natl Acad Sci U S A*, **91**, 11797-11801.

102. Pikaart, M.J., Recillas-Targa, F. and Felsenfeld, G. (1998) Loss of transcriptional activity of a transgene is accompanied by DNA methylation and histone deacetylation and is prevented by insulators. *Genes Dev*, **12**, 2852-2862.

103. Rhee, I., Jair, K.W., Yen, R.W., Lengauer, C., Herman, J.G., Kinzler, K.W., Vogelstein, B., Baylin, S.B. and Schuebel, K.E. (2000) CpG methylation is maintained in human cancer cells lacking DNMT1. *Nature*, **404**, 1003-1007.

104. Schermelleh, L., Spada, F., Easwaran, H.P., Zolghadr, K., Margot, J.B., Cardoso, M.C. and Leonhardt, H. (2005) Trapped in action: direct visualization of DNA methyltransferase activity in living cells. *Nat Methods*, **2**, 751-756.

105. Cuozzo, C., Porcellini, A., Angrisano, T., Morano, A., Lee, B., Di Pardo, A., Messina, S., Iuliano, R., Fusco, A., Santillo, M.R. *et al.* (2007) DNA damage, homology-directed repair, and DNA methylation. *PLoS Genet*, **3**, e110.

106. Pradhan, S., Bacolla, A., Wells, R.D. and Roberts, R.J. (1999) Recombinant human DNA (cytosine-5) methyltransferase. I. Expression, purification, and comparison of de novo and maintenance methylation. *J Biol Chem*, **274**, 33002-33010.

107. Padjen, K., Ratnam, S. and Storb, U. (2005) DNA methylation precedes chromatin modifications under the influence of the strain-specific modifier Ssm1. *Mol Cell Biol*, **25**, 4782-4791.

108. Iuliano, R., Le Pera, I., Cristofaro, C., Baudi, F., Arturi, F., Pallante, P., Martelli, M.L., Trapasso, F., Chiariotti, L. and Fusco, A. (2004) The tyrosine phosphatase PTPRJ/DEP-1 genotype affects thyroid carcinogenesis. *Oncogene*, **23**, 8432-8438.

109. Pierce, A.J., Stark, J.M., Araujo, F.D., Moynahan, M.E., Berwick, M. and Jasin, M. (2001) Double-strand breaks and tumorigenesis. *Trends Cell Biol*, **11**, S52-59.

110. Gorgoulis, V.G., Vassiliou, L.V., Karakaidos, P., Zacharatos, P., Kotsinas, A., Liloglou, T., Venere, M., Ditullio, R.A., Jr., Kastrinakis, N.G., Levy, B. *et al.* (2005) Activation of the DNA damage checkpoint and genomic instability in human precancerous lesions. *Nature*, **434**, 907-913.

111. Fornace, A.J., Jr., Alamo, I., Jr. and Hollander, M.C. (1988) DNA damage-inducible transcripts in mammalian cells. *Proc Natl Acad Sci U S A*, **85**, 8800-8804.

112. Fornace, A.J., Jr., Nebert, D.W., Hollander, M.C., Luethy, J.D., Papathanasiou, M., Fargnoli, J. and Holbrook, N.J. (1989) Mammalian genes coordinately regulated by growth arrest signals and DNA-damaging agents. *Mol Cell Biol*, **9**, 4196-4203.

113. Papathanasiou, M.A., Kerr, N.C., Robbins, J.H., McBride, O.W., Alamo, I., Jr., Barrett, S.F., Hickson, I.D. and Fornace, A.J., Jr. (1991) Induction by ionizing radiation of the gadd45 gene in cultured human cells: lack of mediation by protein kinase C. *Mol Cell Biol*, **11**, 1009-1016.

114. Zhang, W., Bae, I., Krishnaraju, K., Azam, N., Fan, W., Smith, K., Hoffman, B. and Liebermann, D.A. (1999) CR6: A third member in the MyD118 and Gadd45 gene family which functions in negative growth control. *Oncogene*, **18**, 4899-4907.

115. Takekawa, M. and Saito, H. (1998) A family of stress-inducible GADD45-like proteins mediate activation of the stress-responsive MTK1/MEKK4 MAPKKK. *Cell*, **95**, 521-530.

116. Kastan, M.B., Zhan, Q., el-Deiry, W.S., Carrier, F., Jacks, T., Walsh, W.V., Plunkett, B.S., Vogelstein, B. and Fornace, A.J., Jr. (1992) A mammalian cell cycle checkpoint pathway utilizing p53 and GADD45 is defective in ataxia-telangiectasia. *Cell*, **71**, 587-597.

117. Zhan, Q., Chen, I.T., Antinore, M.J. and Fornace, A.J., Jr. (1998) Tumor suppressor p53 can participate in transcriptional induction of the GADD45 promoter in the absence of direct DNA binding. *Mol Cell Biol*, **18**, 2768-2778.

118. Fan, W., Jin, S., Tong, T., Zhao, H., Fan, F., Antinore, M.J., Rajasekaran, B., Wu, M. and Zhan, Q. (2002) BRCA1 regulates GADD45 through its interactions with the OCT-1 and CAAT motifs. *J Biol Chem*, **277**, 8061-8067.

119. Harkin, D.P., Bean, J.M., Miklos, D., Song, Y.H., Truong, V.B., Englert, C., Christians, F.C., Ellisen, L.W., Maheswaran, S., Oliner, J.D. *et al.* (1999) Induction of GADD45 and JNK/SAPK-dependent apoptosis following inducible expression of BRCA1. *Cell*, **97**, 575-586.

120. Smith, M.L., Chen, I.T., Zhan, Q., Bae, I., Chen, C.Y., Gilmer, T.M., Kastan, M.B., O'Connor, P.M. and Fornace, A.J., Jr. (1994) Interaction of the p53-regulated protein Gadd45 with proliferating cell nuclear antigen. *Science*, **266**, 1376-1380.

121. Kearsey, J.M., Coates, P.J., Prescott, A.R., Warbrick, E. and Hall, P.A. (1995) Gadd45 is a nuclear cell cycle regulated protein which interacts with p21Cip1. *Oncogene*, **11**, 1675-1683.

122. Carrier, F., Georgel, P.T., Pourquier, P., Blake, M., Kontny, H.U., Antinore, M.J., Gariboldi, M., Myers, T.G., Weinstein, J.N., Pommier, Y. *et al.* (1999) Gadd45, a p53-responsive stress protein, modifies DNA accessibility on damaged chromatin. *Mol Cell Biol*, **19**, 1673-1685.

123. Zhan, Q., Antinore, M.J., Wang, X.W., Carrier, F., Smith, M.L., Harris, C.C. and Fornace, A.J., Jr. (1999) Association with Cdc2 and inhibition of Cdc2/Cyclin B1 kinase activity by the p53-regulated protein Gadd45. *Oncogene*, **18**, 2892-2900.

124. Jin, S., Tong, T., Fan, W., Fan, F., Antinore, M.J., Zhu, X., Mazzacurati, L., Li, X., Petrik, K.L., Rajasekaran, B. *et al.* (2002) GADD45-induced cell cycle G2-M arrest associates with altered subcellular distribution of cyclin B1 and is independent of p38 kinase activity. *Oncogene*, **21**, 8696-8704.

125. Vairapandi, M., Balliet, A.G., Hoffman, B. and Liebermann, D.A. (2002) GADD45b and GADD45g are cdc2/cyclinB1 kinase inhibitors with a role in S and G2/M cell cycle checkpoints induced by genotoxic stress. *J Cell Physiol*, **192**, 327-338.

126. Zerbini, L.F., Wang, Y., Czibere, A., Correa, R.G., Cho, J.Y., Ijiri, K., Wei, W., Joseph, M., Gu, X., Grall, F. *et al.* (2004) NF-kappa B-mediated repression of growth arrest- and DNA-damage-inducible proteins 45alpha and gamma is essential for cancer cell survival. *Proc Natl Acad Sci U S A*, **101**, 13618-13623.

127. Shaulian, E. and Karin, M. (1999) Stress-induced JNK activation is independent of Gadd45 induction. *J Biol Chem*, **274**, 29595-29598.

128. Wang, X., Gorospe, M. and Holbrook, N.J. (1999) gadd45 is not required for activation of c-Jun N-terminal kinase or p38 during acute stress. *J Biol Chem*, **274**, 29599-29602.

129. Smith, M.L., Kontny, H.U., Zhan, Q., Sreenath, A., O'Connor, P.M. and Fornace, A.J., Jr. (1996) Antisense GADD45 expression results in decreased DNA repair and sensitizes cells to u.v.-irradiation or cisplatin. *Oncogene*, **13**, 2255-2263.

130. Hollander, M.C., Sheikh, M.S., Bulavin, D.V., Lundgren, K., Augeri-Henmueller, L., Shehee, R., Molinaro, T.A., Kim, K.E., Tolosa, E., Ashwell, J.D. *et al.* (1999) Genomic instability in Gadd45a-deficient mice. *Nat Genet*, **23**, 176-184.

131. Hollander, M.C., Kovalsky, O., Salvador, J.M., Kim, K.E., Patterson, A.D., Haines, D.C. and Fornace, A.J., Jr. (2001) Dimethylbenzanthracene carcinogenesis in Gadd45a-null mice is associated with decreased DNA repair and increased mutation frequency. *Cancer Res*, **61**, 2487-2491.

132. Barreto, G., Schafer, A., Marhold, J., Stach, D., Swaminathan, S.K., Handa, V., Doderlein, G., Maltry, N., Wu, W., Lyko, F. *et al.* (2007) Gadd45a promotes epigenetic gene activation by repair-mediated DNA demethylation. *Nature*, **445**, 671-675.

133. Jin, S.G., Guo, C. and Pfeifer, G.P. (2008) GADD45A does not promote DNA demethylation. *PLoS Genet*, **4**, e1000013.

134. Agius, F., Kapoor, A. and Zhu, J.K. (2006) Role of the Arabidopsis DNA glycosylase/lyase ROS1 in active DNA demethylation. *Proc Natl Acad Sci U S A*, **103**, 11796-11801.

135. Gehring, M., Huh, J.H., Hsieh, T.F., Penterman, J., Choi, Y., Harada, J.J., Goldberg, R.B. and Fischer, R.L. (2006) DEMETER DNA glycosylase establishes MEDEA polycomb gene self-imprinting by allele-specific demethylation. *Cell*, **124**, 495-506.

136. Arnaud, P. and Feil, R. (2006) MEDEA takes control of its own imprinting. *Cell*, **124**, 468-470.

137. Grondin, B., Bazinet, M. and Aubry, M. (1996) The KRAB zinc finger gene ZNF74 encodes an RNA-binding protein tightly associated with the nuclear matrix. *J Biol Chem*, **271**, 15458-15467.

138. Dodson, M.L., Michaels, M.L. and Lloyd, R.S. (1994) Unified catalytic mechanism for DNA glycosylases. *J Biol Chem*, **269**, 32709-32712.

139. Sun, B., Latham, K.A., Dodson, M.L. and Lloyd, R.S. (1995) Studies on the catalytic mechanism of five DNA glycosylases. Probing for enzyme-DNA imino intermediates. *J Biol Chem*, **270**, 19501-19508.

140. Koonin, E.V. (1997) Cell cycle and apoptosis: possible roles of Gadd45 and MyD118 proteins inferred from their homology to ribosomal proteins. *J Mol Med*, **75**, 236-238.

141. Chandra Sanyal, S. and Liljas, A. (2000) The end of the beginning: structural studies of ribosomal proteins. *Curr Opin Struct Biol*, **10**, 633-636.

142. Hakes, D.J. and Berezney, R. (1991) DNA binding properties of the nuclear matrix and individual nuclear matrix proteins. Evidence for salt-resistant DNA binding sites. *J Biol Chem*, **266**, 11131-11140.

143. Berrios, M., Osheroff, N. and Fisher, P.A. (1985) In situ localization of DNA topoisomerase II, a major polypeptide component of the Drosophila nuclear matrix fraction. *Proc Natl Acad Sci U S A*, **82**, 4142-4146.

144. Schuck, P. (1997) Use of surface plasmon resonance to probe the equilibrium and dynamic aspects of interactions between biological macromolecules. *Annu Rev Biophys Biomol Struct*, **26**, 541-566.

145. Kovalsky, O., Lung, F.D., Roller, P.P. and Fornace, A.J., Jr. (2001) Oligomerization of human Gadd45a protein. *J Biol Chem*, **276**, 39330-39339.

146. Schrag, J.D., Jiralerspong, S., Banville, M., Jaramillo, M.L. and O'Connor-McCourt, M.D. (2008) The crystal structure and dimerization interface of GADD45gamma. *Proc Natl Acad Sci U S A*, **105**, 6566-6571.

147. Zhan, Q., Lord, K.A., Alamo, I., Jr., Hollander, M.C., Carrier, F., Ron, D., Kohn, K.W., Hoffman, B., Liebermann, D.A. and Fornace, A.J., Jr. (1994) The gadd and MyD genes define a novel set of mammalian genes encoding acidic proteins that synergistically suppress cell growth. *Mol Cell Biol*, **14**, 2361-2371.

148. Santi, D.V., Garrett, C.E. and Barr, P.J. (1983) On the mechanism of inhibition of DNA-cytosine methyltransferases by cytosine analogs. *Cell*, **33**, 9-10.

149. Chen, L., MacMillan, A.M., Chang, W., Ezaz-Nikpay, K., Lane, W.S. and Verdine, G.L. (1991) Direct identification of the active-site nucleophile in a DNA (cytosine-5)-methyltransferase. *Biochemistry*, **30**, 11018-11025.

150. Verger, A., Perdomo, J. and Crossley, M. (2003) Modification with SUMO. A role in transcriptional regulation. *EMBO Rep*, **4**, 137-142.

151. Muller, S., Hoege, C., Pyrowolakis, G. and Jentsch, S. (2001) SUMO, ubiquitin's mysterious cousin. *Nat Rev Mol Cell Biol*, **2**, 202-210.

152. Turker, M.S., Gage, B.M., Rose, J.A., Elroy, D., Ponomareva, O.N., Stambrook, P.J. and Tischfield, J.A. (1999) A novel signature mutation for oxidative damage resembles a mutational pattern found commonly in human cancers. *Cancer Res*, **59**, 1837-1839.

153. Hermann, A., Goyal, R. and Jeltsch, A. (2004) The Dnmt1 DNA-(cytosine-C5)-methyltransferase methylates DNA processively with high preference for hemimethylated target sites. *J Biol Chem*, **279**, 48350-48359.

154. Pradhan, S., Talbot, D., Sha, M., Benner, J., Hornstra, L., Li, E., Jaenisch, R. and Roberts, R.J. (1997) Baculovirus-mediated expression and characterization of the full-length murine DNA methyltransferase. *Nucleic Acids Res*, **25**, 4666-4673.

155. Leonhardt, H., Page, A.W., Weier, H.U. and Bestor, T.H. (1992) A targeting sequence directs DNA methyltransferase to sites of DNA replication in mammalian nuclei. *Cell*, **71**, 865-873.

156. Grandjean, V., Yaman, R., Cuzin, F. and Rassoulzadegan, M. (2007) Inheritance of an epigenetic mark: the CpG DNA methyltransferase 1 is required for de novo establishment of a complex pattern of non-CpG methylation. *PLoS ONE*, **2**, e1136.

157. Sacher, M., Pfander, B., Hoege, C. and Jentsch, S. (2006) Control of Rad52 recombination activity by double-strand break-induced SUMO modification. *Nat Cell Biol*, **8**, 1284-1290.

158. Hollander, M.C., Zhan, Q., Bae, I. and Fornace, A.J., Jr. (1997) Mammalian GADD34, an apoptosis- and DNA damage-inducible gene. *J Biol Chem*, **272**, 13731-13737.

159. Rai, K., Huggins, I.J., James, S.R., Karpf, A.R., Jones, D.A. and Cairns, B.R. (2008) DNA demethylation in zebrafish involves the coupling of a deaminase, a glycosylase, and gadd45. *Cell*, **135**, 1201-1212.

160. Schmitz, K.M., Schmitt, N., Hoffmann-Rohrer, U., Schafer, A., Grummt, I. and Mayer, C. (2009) TAF12 recruits Gadd45a and the nucleotide excision repair complex to the promoter of rRNA genes leading to active DNA demethylation. *Mol Cell*, **33**, 344-353.

161. Hollander, M.C. and Fornace, A.J., Jr. (2002) Genomic instability, centrosome amplification, cell cycle checkpoints and Gadd45a. *Oncogene*, **21**, 6228-6233.